THESIS FOR THE DEGREE OF DOCTOR OF PHILOSOPHY (PHD)

Novel metabolic effects of glycogen phosphorylase inhibitors

Lilla Nikoletta Nagy

UNIVERSITY OF DEBRECEN
DOCTORAL SCHOOL OF MOLECULAR MEDICINE

DEBRECEN, 2017

THESIS FOR THE DEGREE OF DOCTOR OF PHYLOSOPHY (PhD)

Novel metabolic effects of glycogen phosphorylase inhibitors

Lilla Nikoletta Nagy

Supervisor: Dr. Péter Bay

UNIVERSITY OF DEBRECEN

DOCTORAL SCHOOL OF MOLECULAR MEDICINE

DEBRECEN, 2017

TABLE OF CONTENT

ABBREVIATIONS

ADP	- adenosine diphosphate
AGC	- aspartate-glutamate carrier
AGL	- amylo-α-1,6-glucosidase, 4-α-glucanotransferase
Akt	- protein kinase B
AMP	- adenosine monophosphate
AMPK	- AMP-stimulated protein kinase
ATCC	- American Type Culture Collection
ATP	- adenosine triphosphate
BCA	- bicinchoninic acid assay
BEVA335	- 3-ß-D-glucopyranosyl-5-(2-naphthyl)-1,2,4-triazole
BSA	- bovine serum albumin
cAMP	- cyclic adenosine monophosphate
CCD	- charge-coupled device
cDNA	- complementary DNA
CLAMS	- Comprehensive Lab Animal Monitoring System
CP-316819	- 5-chloro-N-[(1S,2R)-2-hydroxy-3-(methoxymethylamino)-3-oxo-1-(phenylmethyl)propyl]-1H-indole-2-carboxamide
C2C12	- mouse myoblast cell line
DABCO	- 1,4–diazabicyclo [2.2.2] octane
DAPI	- 4',6-diamidino-2-phenylindole
DTT	- 1,4-dithiothreitol
DMEM	- Dulbecco's modified eagle medium
DMSO	- dimethyl sulfoxide
DPBS	- Dulbecco's phosphate buffered saline
ECAR	- extracellular acidification rate
ECL	- enhanced chemiluminescence
EDTA	- ethylenediaminetetraacetic acid
EGTA	- ethylene glycol tetra acetic acid
EM	- electron microscopic
ETC	- electron transport chain
EU	- European Union
FBS	- fetal bovine serum

FFA - free fatty acid
FMN - flavin mononucleotide
FOXO1 - forkhead box protein O1
Fura-2AM - fura-2 pentakis (acetoxymethyl) ester
GDM - gestational diabetes mellitus
GK - glucokinase
GKRP - glucokinase regulatory protein
GLUT - glucose transporter
GP - glycogen phosphorylase
GPis - glycogen phosphorylase inhibitors
GSK3 - glycogen synthase kinase 3
GTP - guanosine 5'-triphosphate
GYS - glycogen synthase
G1P - glucose-1-phosphate
G6P - glucose-6-phosphate
G6Pase - glucose-6-phosphatase
HEPES - 4-(2-hydroxyethyl) piperazine-1-ethanesulfonic acid, N-(2-hydroxyethyl) piperazine-N′-(2-ethanesulfonic acid)
HepG2 - human hepatocarcinoma cell line
HFD - high-fat diet
HGP - hepatic glucose production
HK - hexokinase
IMP - inositol monophosphate
ipGTT - intraperitoneal glucose tolerance test
IR - insulin receptor
IRβ - insulin receptor β subunit
IRS - insulin receptor substrate protein
K_{ATP} - ATP-sensitive K^+ channels
KB228 - N-(3,5-dimethyl-benzoyl)-N'-(ß-D-glucopyranosyl)urea
LiRiKO - liver-specific *rictor* knockout
MIN6 - murine insulinoma cell line
MODY - maturity onset diabetes of the young
MPC - mitochondrial pyruvate carrier
mTORC1/2 - mammalian target of rapamycin complex ½

NAD^+ - nicotinamide adenine dinucleotide

NADH - nicotinamide adenine dinucleotide hydrogen

2NBDG - 2-[*N*-(7-Nitrobenz-2-oxa-1,3-diazol-4-yl)amino]-2-deoxy-D-glucose

NF-κB - nuclear factor kappa-light-chain-enhancer of activated B cells

NIH - National Institutes of Health

NV5 - N-(β-D-glucopyranosyl)-N'-(4-nitrobenzoyl) urea

NV76 - N-(β-D-glucopyranosyl)-N'-(2-naphthoyl) urea

OCR - oxygen consumption rate

OGC - 2-oxoglutarate carrier

OGTT - oral glucose tolerance test

ONPG - ortho-nitrophenyl-β-D-galactopyranoside

PBS - phosphate-buffered saline

PDK1 - 3-phosphoinositide dependent protein kinase-1

PDX1 - pancreatic and duodenal homeobox factor-1

PH - pleckstrin-homology

PhK - phosphorylase kinase

PIP_3 - phosphatidylinositol-3,4,5-triphosphate

PI3K - phosphatidylinositol-3 kinase

PKA - cAMP-dependent protein kinase

PKC - protein kinase C

PLC - phospholipase C

PLP - pyridoxal phosphate

PMSF - phenylmethylsulfonyl fluoride

PP cells - pancreatic polypeptide producing cells

PP1 - protein phosphatase 1

PTG - PP1-targeting subunit protein targeting to glycogen

PYGB - brain isozyme of glycogen phosphorylase

PYGL - liver isozyme of glycogen phosphorylase

PYGM - muscle isozyme of glycogen phosphorylase

P/S - Penicillin / Streptomycin

ROS - reactive oxygen species

RQ - respiratory quotient

RT - room temperature

RT-qPCR - reverse transcription-coupled real time quantitative polymerase chain reaction

SDS-PAGE	- sodium dodecyl sulfate - polyacrylamide gel electrophoresis
SR	- sarcoplasmic reticulum
STF-1luc	- promoter of STF-1 homeodomain protein with luciferase reporter gene
TCA cycle	- tricarboxylic acid cycle
TFAm	- mitochondrial transcription factor A
TH	- D-glucopyranosylidene spiro-thiohydantoin
TNFα	- tumor necrosis factor alfa
TRIS	- 2-amino-2-hydroxymethyl-propane-1,3-diol
T1DM	- type 1 diabetes mellitus
T2DM	- type 2 diabetes mellitus
UCP2	- uncoupling protein-2
UDP	- uridine diphosphate
VEH	- vehicle
VO_2	- oxygen consumption
WM	- wortmannin

1. INTRODUCTION

Diabetes mellitus is the most common endocrine and metabolic disorder that requires continuous medical care and support to prevent the acute and to manage the long-term complications (Shafiee et al., 2012). Type 2 diabetes mellitus is characterized by hyperglycaemia owing to a combination of insulin resistance and inadequate compensatory insulin secretion of pancreatic β cells. Insulin resistance may be provoked by genetic factors (inherited) and/or unhealthy lifestyle (sedentary lifestyle, obesity, malnutrition). Impaired insulin action leads to high blood glucose levels mainly originating from undesired hepatic glucose production (HGP) (American Diabetes Association, 2010). Glycogen breakdown catalyzed by glycogen phosphorylase (GP) has a major contribution to HGP, therefore, GP became a validated target to modulate glucose levels in type 2 diabetes and pharmacological GP inhibitors (GPis) are considered as potential antidiabetic agents (Agius, 2007; Baker et al., 2005).

Numerous studies investigated the effect of pharmacological GP inhibition using structurally different GP inhibitors. The beneficial effects of GP inhibition were reported over the years, such as lowering glucose or restoring insulin sensitivity in diabetic animal models (Docsa et al., 2011; Docsa et al., 2015; Martin et al., 1998; Somsák et al., 2003; Torres et al., 2011; Treadway et al., 2001). Although GPis were confirmed to be efficacious agents in controlling hyperglycemia, prolonged treatment with GPis may cause complications, such as various forms of glycogen storage disease (Floettmann et al., 2010) or impaired muscle function (Baker et al., 2005). Several pharmaceutical companies have placed GPis into clinical development, but clinical studies on GPi were halted after phase II without explanations, and after a while industry has slowed down on GP inhibitors design (Donnier-Marechal and Vidal, 2016; Henke, 2012). However, academic researchers are continuing investigations and have provided potential drug candidates, which may resurrect the interest in GP inhibition, including its potential for targeting cancer (Donnier-Marechal and Vidal, 2016), like bladder and other urological cancers (Lew et al., 2015) or pancreatic adenocarcinoma (Lee et al., 2004).

We started our experiments with KB228, a glucose analogue GP inhibitor, tested *in vitro* and *in vivo* under normoglycaemic and hyperglycaemic conditions. Investigations were performed on two glycogen stores, the liver and the skeletal muscle. For *in vivo* studies we used 1) lean, chow-fed and 2) high fat diet-fed (HFD), obese, diabetic C57/Bl6J mice. After the characterization of the *in vivo* applicability of the KB228 compound, we investigated its

impact on glucose metabolism *in vivo* by assessing glucose tolerance, glucose excursion and glucose consumption. During *in vitro* studies we used the HepG2 cell line for modelling hepatocytes, and the C2C12 cell line, as a model for skeletal muscle. Mitochondrial dysfunction is a major feature in insulin resistance and obesity leading to development of type 2 diabetes (Andreux et al., 2013; Sivitz and Yorek, 2010), therefore, we were curious how KB228 can influence mitochondrial function in hepatocytes. To assess further metabolic rearrangements triggered by KB228 we investigated certain signaling pathways involved in insulin action and energy homeostasis.

Pancreatic β cells are responsible for insulin secretion, which is a peptide hormone with the role of maintaining normoglycaemia through inducing cellular glucose uptake and consumption. Therefore, insulin can decrease the concentration of blood glucose and enhance the anabolic processes in order to upload the stores, such as glycogen or fat stores. Consequently, insulin resistance leads to reduced glycogen synthesis and impaired glucose tolerance. β cells increase insulin secretion to compensate hyperglycaemia, however, persistent hyperglycemia may exhaust beta cells inducing their depletion and dysfunction (Prentki et al., 2013). Our next objective was to test whether GP inhibition has an impact on insulin secretion from pancreatic β cells *in vivo* and *in vitro*.

2. THEORETICAL BACKGROUND

2.1. Glycogen metabolism

Glycogen is a highly branched polymer of D-glucose that has a dominant role in glucose storage. Glycogen forms spherical granules known as β particles that vary in diameter from 20 to 50 nm, except in the liver where the β particles aggregate to form larger molecular complexes known as α-particles or α-rosettes, with a diameter up to 200 nm. Granules contain not only glycogen but also enzymes and regulatory proteins involved in their metabolism (Bendayan et al., 2009; Shearer and Graham, 2002). The synthesis of glycogen begins close to the plasma membrane and in line with the elongation of the polysaccharide chains, the particles descend from the periphery towards the interior of the cell (Garcia-Rocha et al., 2001). Glycogen is deposited predominantly in liver cells and skeletal muscle fibers, although many other tissues are capable of glycogen synthesis too, such as pancreatic β cells (Hellman and Idahl, 1969; Roach et al., 2012).

In most mammalian cells, glucose uptake is carried out by facilitated diffusion through glucose transporters (GLUTs) (Thorens and Mueckler, 2010). This family of membrane transport proteins can provide the basal glucose transport (e.g. GLUT1 and GLUT2) in a variety of cells. At the same time insulin-induced translocation of GLUT4, another member of this family, to the plasma membrane in insulin-sensitive tissues, including skeletal muscle or adipose tissues, can enhance the efficiency of glucose uptake when it is required (Roach et al., 2012). Consequently, glucose is converted to glucose-6-phosphate (G6P) in the hexokinase- or glucokinase-catalyzed reaction providing utilizable glucose for further metabolic pathways (Ritov and Kelley, 2001).

When glucose is plentiful in the cell, it is stored as glycogen (**Fig. 1**). Glycogen is synthetized by a process called glycogenesis, which is catalyzed by glycogen synthase (GYS) enzyme. GYS has two isozymes, the widely expressed glycogen synthase 1 (GYS1) and the liver-specific isozyme, termed glycogen synthase 2 (GYS2) (Kollberg et al., 2007). GYS is the rate limiting enzyme of glycogenesis and it is responsible for the formation of the α-1, 4-glycosidic linkages of glycogen. GYS, in collaboration with the branching enzyme, which forms the α-1,6-glycosidic branch points, allows further elongation and branching of the glucose polymer (Roach et al., 2012). Addition of glucose units to the polymer is an energy consuming process. In the biochemical pathway towards glycogenesis, G6P is converted

successively into G1P by phosphoglucomutase (Ferrer et al., 2003) and glucose moieties are activated by joining glucose to uridine diphosphate (UDP) forming UDP-glucose that can be readily attached to glycogen by GYS (Dow et al., 1996).

When cells need glucose, glycogen can be converted back to glucose in the counter-process termed glycogenolysis, that is catalyzed by two enzymes, glycogen phosphorylase (GP) and the debranching enzyme [AGL (amylo-α-1,6-glucosidase, 4-α-glucanotransferase)] (Lew et al., 2015). The key enzyme in glycogenolysis is GP that has three isoforms with different physiological roles encoded by separate genes. Each isozyme is named after the tissue where it is dominantly expressed. The muscle isozyme (PYGM) supports muscle contraction by liberating glucose, the liver isotype (PYGL) plays a central role in regulation of blood glucose homeostasis, and finally the brain isoform (PYGB), expressed in adult brain and embryonic tissues, is responsible for glucose supply in case of anoxia or hypoglycemia (Agius, 2007). Nevertheless, all GP isoforms catalyze the same reaction where GP hydrolyses monosaccharide units from the non-reducing ends of glycogen by breaking the α-1,4-glycosydic bonds, which is the rate limiting step of glycogenolysis (Somsak et al., 2011). AGL breaks down the α-1,6-glycosydic bonds that are otherwise unprocessable for GP (Roach et al., 2012). Each sugar unit is released as G1P that can readily enter into catabolic pathways. G1P can be converted to G6P by phosphoglucomutase providing substrate for adenosine triphosphate (ATP) producing processes such as glycolysis. In the liver, however, glucose-6-phosphatase (G6Pase) can remove the phosphate group of G6P in order to enable the transport of glucose through cell membrane into the bloodstream to support other tissues. This process is called hepatic glucose production (HGP) (Dow et al., 1996).

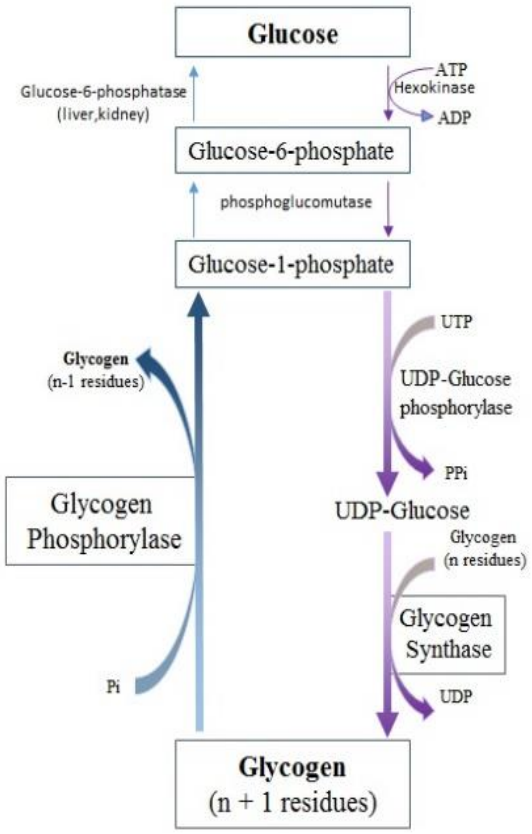

Figure 1. Glycogen metabolism
Glycogenesis is denoted by ⇨
Glycogenolysis is denoted by ⇨

GP is biologically active as a dimer of two identical subunits. The serine-14 residue of GP enzyme is the regulatory phosphorylation site that is phosphorylated by phosphorylase kinase (PhK). PhK is responsible for the activation of GP enzyme converting it to the

normally active GPa form. Conversely, protein phosphatase 1 (PP1) inactivates GP by dephosphorylation bringing about the normally inactive GPb form (Berg et al., 2002; Somsák et al., 2008b). According to protein crystallographic studies GP enzyme bears seven binding sites (**Fig. 2**):

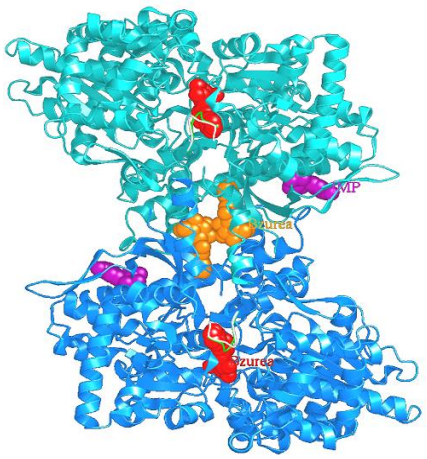

Figure 2. Structure and binding sites of the dimer glycogen phosphorylase enzyme
Glucose analog inhibitors (in red) binding to the active site. The nucleotide (AMP/IMP activatory, ATP and G6P inhibitory) binding site is marked as purple spheres. The connection surface of monomers includes the new allosteric or indole binding site marked by yellow spheres (Oikonomakos et al., 2000).

1) **The catalytic site** buried at the center of the monomers (Somsák et al., 2008b) binds glycogen and G1P. GP has an essential cofactor, pyridoxal phosphate (PLP), binding at the active site. This is a derivative of vitamin B_6 that participates in the catalysis of glycogen breakdown by transferring the phosphate group.
2) **The inhibitor site,** also known as the **caffeine binding site** or **purine nucleoside site**, is situated at the entrance to the catalytic site and binds nucleotides, nucleosides, purines, flavonoids and heterocyclic compounds.
3) **The allosteric** or the AMP/IMP activating and the G6P/ATP inhibitory sites located between the α2 helix and the cap region of the other subunit are essential in control of GP activity mainly in muscle. Caffeine and AMP can bind to inhibitor and to allosteric site as well.
4) **The glycogen storage site**, where GP is associated with glycogen particles together with other enzymes involved in glycogen regulation, exerts regulatory properties (Hayes et al., 2014; Johnson, 1992).
5) **The newly discovered allosteric** or **indole binding site** is located in the central binding cavity between the two subunits allowing regulation of GP by pharmaceutical base materials (Oikonomakos et al., 2000).
6) **The benzimidazole site** as novel binding site is located in a surface cavity (Chrysina et al., 2005).
7) **Quercetin binding site** is a shallow groove near to the active site (Morino et al., 2006).

The large number of allosteric binding sites suggest that GP is an allosteric enzyme. In line with that, GP has two conformational forms such as T (tight or tense) and R (relaxed) forms (Lehlinger et al., 2004). The T form appears to be less active having a lower affinity for its substrate, while the R form is supposed to be more active and have a greater substrate

affinity (Johnson and Barford, 1994). Both GPa and GPb exist in equilibrium between the R and T states, however, GPa exists predominantly in the R state and GPb in the T state. Equilibrium depends on the concentration of substrate, since more enzymes are found in the R state at high substrate concentrations, and in the T state at insufficient substrate amounts. Furthermore, equilibrium is also controlled by allosteric modulators, mainly in muscle (Berg et al., 2002; Lehlinger et al., 2004).

Each binding site offers potential target for allosteric GP modulation by pharmacological agents except for the glycogen storage site. High energy substrates, such as ATP, glucose and G6P are considered to be the physiological inhibitors of GP inducing stabilization of T state then GP inactivation. This is the reason why GP inhibitors mimick the action of glucose and G6P or bind to other sites, therefore, acting synergistically with glucose are expected to inhibit glycogenolysis and stimulate glycogenesis, the oppositely regulated process. Not surprisingly, there is a great deal of glucose analogue GP inhibitors. Glucose analogue inhibitors bind primarily to the catalytic site thus blocking access of the substrate to the catalytic site and promote the transition to the less active T state of GPa hence inducing dephosphorylation. These molecules were reported to bind to the allosteric site of GP, too (Agius, 2007; Somsák et al., 2008a).

N-acetyl-β-D-glucopyranosylamine was among the first efficient glucose analogue inhibitors that bind to GP (Somsák et al., 2008b). The glycogen phosphorylase inhibitors KB228, BEVA335, TH, NV50 and NV76 are glucose analogue compounds synthesized by Bálint Kónya, Éva Bokor, Veronika Nagy and Sándor Kun in the laboratory of László Somsák at the Department of Organic Chemistry, University of Debrecen.

CP-316819, belonging to the indole-2-carboxamide series of GP inhibitors, has been reported to bind to the novel allosteric site by enhancing the dephosphorylation of GPa, converting it to the inactive form (Rath et al., 2000; Torres et al., 2011). CP-316819 completed phase I in clinical trials confirming the safety of these drugs (Henke, 2012). Therefore, it was selected as a reference GP inhibitor in our studies. GPis were originally designed to be used as glucose lowering agents that trap excess glucose in the form of glycogen, mainly in the liver (Agius, 2007; Henke, 2012; Somsák et al., 2008b).

Although most inhibitors show some selectivity for the liver isoform, they inhibit all isoforms since GP isozymes show a high degree of sequence/structural homology (Agius 2007). GP inhibitors tested in our study are summarized in **Table 1.** Inhibitory constants (K_i) of the inhibitors were determined by enzyme kinetic measurements using purified rabbit muscle glycogen phosphorylase.

		NAME	STRUCTURE and NAME	Inhibitory Constant (K_i)	Ref.
GP inhibitors synthesized by László Somsák's laboratory					
Glucose analogue inhibitors	**1.**	**KB228**	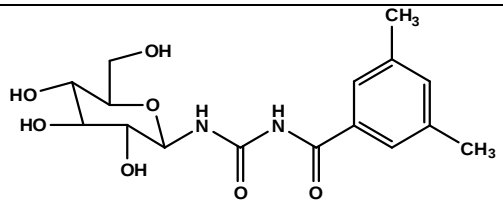 N-(3,5-dimethylbenzoyl)-N'-(b-D-glucopyranosyl)-urea	K_i = 937 nM	(Somsák et al., 2008a)
	2.	**BEVA335**	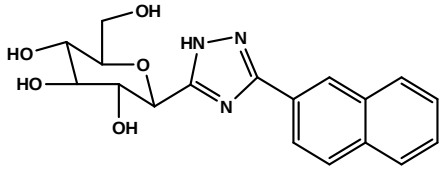 2-(β-D-glucopyranosyl)-4(5)-(2-naphthyl)-imidazole	K_i = 411 nM	(Bokor et al., 2015)
	3.	**TH**	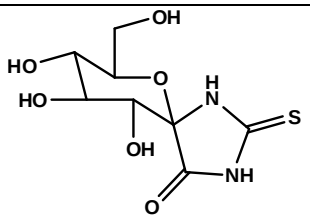 D-glucopyranosylidene spiro-thiohydantoin	K_i = 4200 nM	(Docsa et al., 2011)
	4.	**NV50**	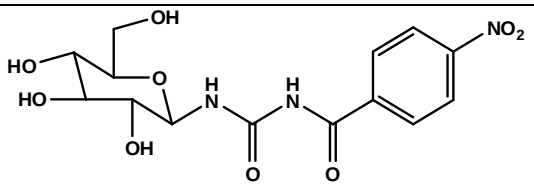 N-(β-D-glucopyranosyl)-N'-(4-nitrobenzoyl) urea	K_i = 3000 nM	(Nagy et al., 2012)
	5.	**NV76**	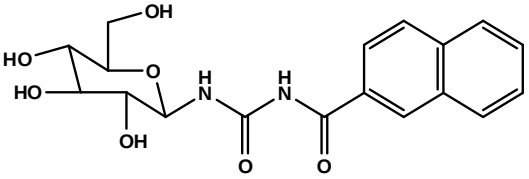 N-(β-D-glucopyranosyl)-N'-(2-naphthoyl) urea	K_i = 474,6 nM	(Oikonomakos and Somsak, 2008; Somsák et al., 2008b)
GP inhibitor under clinical trial					
New allosteric site	**6.**	**CP-316819**	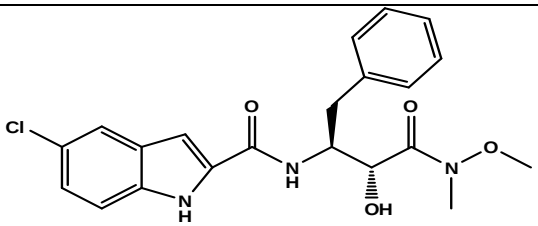 5-Chloro-N-[(1S,2R)-2-hydroxy-3-(methoxymethylamino)-3-oxo-1-(phenylmethyl) propyl]-1H-indole-2-carboxamide	K_i = 220 nM	(Sickmann et al., 2009; Torres et al., 2011)

Table 1. Glycogen phosphorylase inhibitors applied in our studies

GP and GYS, the two rate-limiting enzymes of glycogen metabolism are regulated reciprocally in response to changing physiological conditions by hormones and metabolic signals, mainly through posttranslational modifications like phosphorylation and dephosphorylation, but also by action of allosteric effectors. These regulatory interactions ensure that carbohydrate metabolism responds appropriately to glucose overload and glucose deprivation, as the synthesis and degradation of glycogen does not occur simultaneously (Lew et al., 2015; Newgard et al., 2000).

GYS is also regulated either by allosteric regulators or by phosphorylation. G6P and its substrate UDP-glucose activates GYS, whilst glycogen stores of the tissue serve as a strong negative feedback. GYS phosphorylation in response to hormonal signal is implemented on nine regulatory serine residues by several kinases, among them PhK, resulting in progressive inactivation of GYS, thereby obstructing glycogenesis under catabolic states such as fasting or stress. In turn, PhK phosphorylates and activates GP, resulting in stimulation of glycogenolysis. As for the reverse pathway, the direct dephosphorylation and subsequent activation of GYS is attributed to the serine-threonine phosphatase protein phosphatase 1 (PP1) (Newgard et al., 2000; Stipanuk and Caudill, 2013.). The reciprocal control between GP and GYS is mainly accomplished by PP1 which activates GYS and simultaneously inactivates GP contributing to stimulation of glycogen deposition.

PP1 forms a variety of distinct multimeric holoenzymes with the highly conserved catalytic subunit creating a complex with different regulatory and targeting subunits (Zhang et al., 2014). These regulatory subunits play important role in orienting PP1 to particular subcellular locations (nucleus, plasma membrane, neuronal dendrites, myosin filaments, or glycogen particles) as well as to specific substrates (Adeva-Andany et al., 2016). There are seven glycogen-targeting subunits that have distinct tissue expression patterns and control glycogen metabolism in different organs (Newgard et al., 2000; Zhang et al., 2014) including PP1-targeting subunit protein targeting to glycogen (PTG). PTG, as a molecular scaffold, localizes PP1 to the glycogen particles and directly binds to glycogen synthase and phosphorylase thereby juxtaposing the PP1 enzyme with its substrates (Crosson et al., 2003; Greenberg et al., 2006). Besides PP1, a population of proteins involved in glycogen metabolism associate with glycogen particles in order to maintain their structure and regulate their size, number and cellular location. These macromolecular complexes, also called glycosomes, as morphologically distinct cellular organelles enable the efficient regulation of glycogen metabolism (Rybicka, 1996). Furthermore, microscopic studies provided evidence for the association of glycosomes with different cellular structures, as the endoplasmic

reticulum and mitochondria or, especially in muscle, other spherical structures including sarcoplasmic reticulum (SR), β-actin, α-actinin, and smooth muscle tropomyosin (Prats et al., 2005; Rybicka, 1996). Consequently, glycogen particles as sub-cellular compartments are capable of responding to metabolic and synthetic requirements of the cell in a spatially and temporally regulated way (Stapleton et al., 2010).

2.2. Liver and muscle glycogen metabolism

Glucose can be stored as glycogen in almost all cells, however, skeletal muscle and liver are the two major glycogen reserves in mammals. The liver contains glycogen in higher concentration (10% versus 2%) than muscle, but overall the muscle glycogen deposition is larger due to the much greater total mass of skeletal muscle tissues across the body (Berg et al., 2002; Stapleton et al., 2010). Dynamic changes of glycogen stores are regulated by several hormones in both hepatocytes and muscle cells. Insulin promotes glycogenesis and the counteracting hormones (glucagon, adrenaline, cortisol and growth hormone) have glycogenolytic effects (Babata et al., 2014).

Insulin mediates its biological effects via activation of insulin receptor (IR) (see chapter **2.3**). Activated IR phosphorylates several downstream substrates and docking proteins, initiating multiple and complex intracellular signaling networks. In our context, the prominent substrates are insulin receptor substrate (IRS) proteins, which can transmit the metabolic actions of insulin by switching on the phosphatidylinositol-3 kinase (PI3K) and protein kinase B (Akt) pathway. PI3K increases the level of phosphatidylinositol-3,4,5-triphosphate (PIP_3) causing localization of Akt and (3-phosphoinositide dependent protein kinase-1) PDK1 to the cell membrane.

Akt is a serine/threonine protein kinase possessing a pleckstrin-homology (PH) domain which allows interaction with PIP_3 and recruitment to the cell membrane. Among its three isoforms, encoded by different genes, Akt2 plays a key role in mediating insulin action on metabolism in insulin sensitive tissues. Along the same line, PDK1, also possessing a PH-domain, can dock to the plasma membrane in a similar way, where it activates Akt2 phosphorylation on the threonin-308 residue (Boucher et al., 2014; Lodish, 2000; Saltiel and Kahn, 2001). Other key residue in activation of Akt2 is serine-473 which is considered as an mTORC2-specific phosphorylation site. The mammalian target of rapamycin (mTOR) is a conversed serine/threonine protein kinase functioning as a master regulator of metabolism. mTOR signaling is regulated by nutrients, growth factors and cellular energy status, and mTOR activation stimulates anabolic processes contributing to the cellular metabolic adaptation to environmental conditions. It exists in two distinct complexes: a raptor-containing, rapamycin-sensitive complex 1 (mTORC1) and a rictor-containing, questionably rapamycin-insensitive complex 2 (mTORC2) (Laplante and Sabatini, 2012; Sarbassov et al., 2005). Numerous authors suggest that mTORC2 is localized to the plasma membrane by its

PH-domain and activated upon binding to PIP_3 (Gan et al., 2011; Gaubitz et al., 2016). mTORC2 seems to be insensitive to nutrient levels, but it is activated in response to insulin receptor and insulin-like growth factor receptor activation (Laplante and Sabatini, 2012). Activation of mTORC2 induces nutrient storage (glycogen and fatty acid synthesis) and glycolysis through its downstream targets, including Akt (Hagiwara et al., 2012; Zoncu et al., 2011). Complete Akt activation requires phosphorylation of both Thr-308 and Ser-473, allowing Akt to be released into the cytosol mediating several effects of insulin (Boucher et al., 2014; Jensen et al., 2011; Lodish, 2000). The key glycogenesis-stimulating step of insulin signaling is the inhibition of GSK3 by activated Akt, therefore aborting the inhibition of GYS and leading to stimulation of glycogen synthesis (Frame and Cohen, 2001). Furthermore, activated Akt phosphorylates FOXO1 that results in its nuclear exclusion and cytoplasmic retention, inhibiting transcription of key factors in hepatic gluconeogenesis (Matsuzaki et al., 2003).

Glucagon and adrenaline induce glycogen breakdown via a signal transduction cascade, where hormones binding to their respective plasma membrane receptor inducing PhK activation, therefore GP activation (Berg et al., 2002; Cohen, 1979; Jensen et al., 2011; Stipanuk and Caudill, 2013.).

Since liver and skeletal muscle have different roles in sustaining bodily functions, there are several differences in the character of their glycogen metabolism as well. The cardinal differences are listed in the following points.

Hormonal regulation:

- Hepatocytes have **glucagon receptors and α_1-adrenergic receptors,** therefore liver can respond to glucagon and adrenalin by degradation of glycogen in order to release glucose into the bloodstream (HPG) (Stipanuk and Caudill, 2013.).
- Muscle cells lack glucagon receptors, but have **β_2-adrenergic receptor** that can bind epinephrine (adrenalin) inducing glycogen breakdown (Berg et al., 2002)

Glucose transport:

- **GLUT2** highly expressed in liver fulfils the major glucose transport role in hepatocytes. The bidirectional GLUT2 has high-capacity and low affinity (Karim et al., 2012).
- **GLUT4** is a high-affinity and low-capacity glucose transporter sequestered in intracellular vesicles and translocated to the plasma membrane in response to insulin

in muscle. In insulin signaling, Akt can contribute to GLUT4 mobilization to plasma membrane (Chang et al., 2004).

Spatial organization: the regulation of glycogen metabolism includes movement of relevant enzymes and regulatory factors within cells, and the assembly/disassembly of protein complexes that mediate glycogen synthesis and breakdown.

- Glycogen particles is synthesized from the periphery towards the center of the cell in a defined ordered way, and degraded from the interior towards the exterior in a reverse process in hepatocytes. The subcellular presence of glycogen particle (in line with GYS2) is the highest near the plasma membrane and the lowest near the center of the cell. (Berman et al., 1998; Doherty et al., 1995; Ferrer et al., 2003; Kelsall et al., 2007)
- In muscle cells, glycogen particles and PYGM are associated with SR. GYS1 and glycogenin are associated with actin cytoskeleton. Glycogen-protein complexes binding to these spherical structures suggest communication between the sarcomeric machinery and the regulation of skeletal muscle metabolism (Prats et al., 2005).

Glycogen synthesis:

- Liver-specific GYS2 is present in cytosol at low glucose, then as a consequence of increased glucose uptake followed by G6P production GYS2 accumulates at the periphery of the hepatocyte, at the cellular cortex (Ferrer et al., 2003).
- The widely expressed muscle isoform GYS1 concentrates in the nucleus under glucose deprivation, then translocates to the cytosol in case of glucose abundance. At rest, GYS1 is mainly found associated with glycogen particles and myofibrils (Prats et al., 2005).

Function:

- Liver glycogen provides energy for liver cells, but its primary role is supplying the other tissues with glucose. This function is permitted by large amount of G6Pase which allows the release of free glucose from hepatocytes (Berg et al., 2002).
- Muscle lacks G6Pase, therefore glucose is forced to remain inside the cells. Consequently, muscle glycogen is not generally available to other tissues, but dedicated as a local energy supply instead. However, muscle glycogen through glycolysis can be broken down to lactate and its transport to the liver contribute to HGP through gluconeogenesis (Cori cycle) (Jensen et al., 2011).

Glycogen breakdown:

- PYGL is more tightly controlled by phosphorylation than by allosteric regulation. Glucose is a negative regulator of GPa, shifting it from the R to the T state, therefore

obstructing glycogen degradation. PYGL is insensitive to regulation by AMP as there are no such dramatic energy changes in hepatocytes as in contracting muscle cells.

- ATP and G6P compete with AMP for binding to nucleotide binding site of PYGM in order to allosterically regulate GPb according to the energy charge of muscle cells. When ATP is used during muscular contraction, increased AMP induces and stabilizes the fully active R conformation of GPb therefore stimulates glycogen degradation. ATP and G6P, as a sign of sufficient energy state, act as negative allosteric effector of GPb, favoring the T (inactive) state. Exercise also results in hormone-induced phosphorylation of GPb generating GPa. In contrast, GPa is fully active regardless of the levels of allosteric effectors. Allosteric modification is faster (milliseconds) than hormonal (seconds to minutes) and generally, these two mechanisms function in an ordered sequence (Berg et al., 2002; Stipanuk and Caudill, 2013.).

2.3. The physiology of pancreatic β cell

Pancreatic β cells are specifically evolved to synthesize, store and secrete large amounts of insulin in order to respond to the nutritional status of the body (Wiederkehr and Wollheim, 2012). β cells are one of the five types of cells present in the islets of Langerhans, the endocrine part of the pancreas.

The signaling pathways regulating β cell development include the hedgehog system, the pancreatic and duodenal homeobox factor-1 (PDX1) and notch signaling pathways (Pandol, 2010). PDX1 transcription factor, also known as IDX-1/STF-1/IPF1, plays a crucial role in all aspects of β cell structure and function. PDX1 expression is maintained in precursor cells during pancreatic development but becomes restricted to β cells in the mature pancreas. In mature β cells, PDX1 transactivates genes involved in glucose sensing and metabolism, including GLUT2, glucokinase (GK), mitochondrial respiratory chain complex I, mitochondrial transcription factor A (TFAm) and insulin secretion. Furthermore, it has been reported that the insulin enhancer element A-box is a PDX1 binding site, which is very important for the transcription of the insulin gene. Based on these facts, PDX1 worthily attained the title of master regulator of β cell survival and function (Humphrey et al., 2010; Johnson et al., 2006; Kaneto and Matsuoka, 2015). In addition, insulin stimulates DNA-binding activity of PDX1 in human islets, therefore, a reciprocal linkage is supposed to exist between insulin and PDX1 in β cells (Johnson et al. 2006).

Insulin is an anabolic peptide hormone playing central role in maintaining normal blood glucose levels by facilitating cellular glucose uptake, regulating carbohydrate, lipid and protein metabolism as well as promoting cell division and growth through its mitogenic effects. Insulin gene encodes preproinsulin, which goes through a series of processes to reach the mature form. The mature insulin hormone is stored in secretory granules of β cells until exocytosis. Glucose activates insulin gene transcription, enhances insulin mRNA stability and stimulates its translation (Weiss M, 2014).

Glucose is the main stimulus for β cells to secrete insulin, enabling β cells to serve as a glucose sensor or glucostat. β cells also respond to other nutrients (amino or fatty acids, and ketone bodies) or to neurohormonal stimulation (acetylcholine, glucagon-like peptide-1, and glucagon) but in an absolutely glucose-dependent manner (Prentki et al., 2013). Glucose transport into β cells is not limited, which results in rapid equalization of extra- and intracellular glucose levels by transporters GLUT1 in human or GLUT2 in mice (De Vos et al., 1995; McCulloch et al., 2011). Similarly to hepatocytes, glucose is phosphorylated via

high glucose-affinity GK with lacking any form of feedback control from downstream metabolites (Prentki et al., 2013).

On the course of β cell maturation several genes belonging to metabolically unfavorable pathways for insulin secretion (e.g. lactate production or pentose-phosphate pathway) are repressed early in life, therefore, a specific gene expression pattern characterizes β cells (Wiederkehr and Wollheim, 2012). Glucose degradation generates two products supporting mitochondrial activity: pyruvate and nicotinamide adenine dinucleotide hydrogen (NADH). In most tissues, NADH re-oxidation to nicotinamide adenine dinucleotide (NAD^+) is ensured by cytosolic conversion of pyruvate to lactate, but not in β cells. In β cells lactate production is an unfavorable pathway, thus mitochondrial NAD^+/NADH shuttles take over cytosolic NADH regeneration, transferring glycolysis-derived electrons to mitochondria in β cells. In addition, β cells favor transferring glucose-derived pyruvate into mitochondria over lactate production. This task is performed by mitochondrial pyruvate carrier (MPC) contributing to generation of acetyl-CoA and supporting tricarbon acid (TCA) cycle then ATP production in mitochondria. These processes assure tight coupling between glycolysis and mitochondrial metabolism essential for glucose sensing. Increased substrate feed into the TCA cycle induces the electron transport chain resulting in the hyperpolarization of the mitochondrial membrane, increasing in O_2 consumption and ATP generation (or increasing in ATP/ADP ratio). In fact, mitochondria translate increased glucose levels into ATP signals (Brun and Maechler, 2016; Wiederkehr and Wollheim, 2012). Intracellular ATP binding to Kir6.2 subunit of ATP-sensitive K^+ channels (K_{ATP}) closes the channel and consequently depolarizes the plasma membrane which triggers the opening of voltage-gated Ca^{2+} channels. Ca^{2+} influx increases cytosolic free Ca^{2+} triggering exocytosis of insulin secretory granules (Gembal et al., 1992; Henquin, 2004) **(Fig. 3)**.

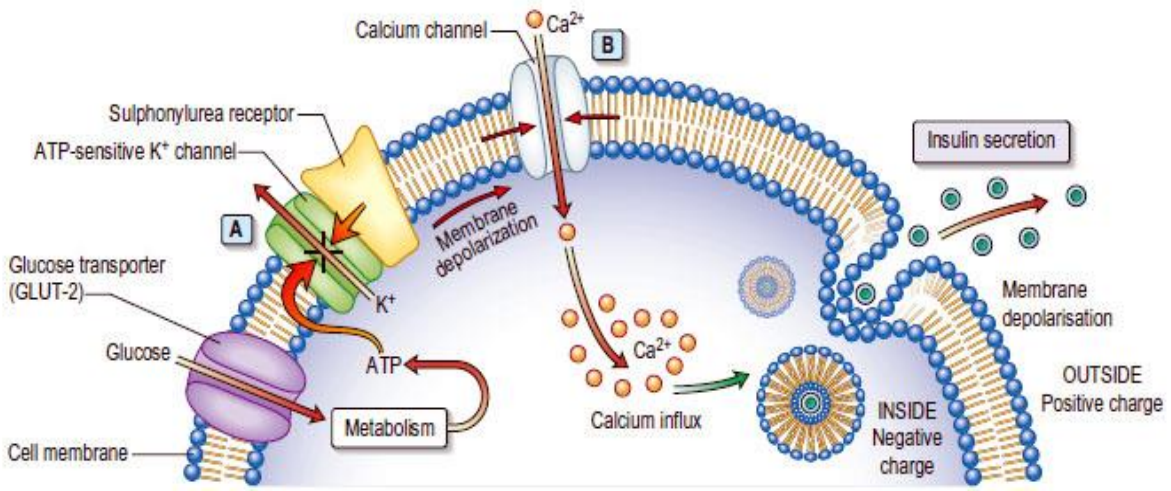

Figure 3. Glucose-stimulated insulin secretion, the triggering pathway
Adapted from www.medicinehack.com

The classical ATP/K_{ATP}/Ca^{2+}-signaling, also called triggering pathway, is complemented by amplifying signals and pathways (Henquin, 2004; Prentki et al., 2013). It was observed by Gembal et al. (1992) that there is a non-identified mechanism by which glucose can control insulin release independently of the triggering pathway. The triggering signal alone is barely effective, but amplifying signals augment its efficacy (Nenquin et al., 2004). Henquin et al. (2003) ascertained that insulin secretion is determined by the triggering pathway, and the amplifying pathway contributes to the optimization of this secretory response induced by the triggering signal (the increase of Ca^{2+} concentration). The nature of metabolic signals and molecular mechanisms involved in mediating the amplifying pathway are still poorly understood (Wiederkehr and Wollheim, 2012).

Insulin secretion from pancreatic β cells is biphasic, consisting of an initial rapid first phase that occurs within 1 minute (peaking at 3-5 minutes), representing the secretion of insulin already synthesized and stored in secretory granules. The second phase lasts about 10 minutes when both stored and newly synthesized insulin is released (Wilcox, 2005). Considering that the insulin receptor (IR) is expressed in pancreatic β cells as well, insulin has been proposed to serve as an autocrine regulator on β cells, as well (Leibiger et al., 2008) . From the 1940s (Best and Haist, 1941), the precise definition of autocrine feedback on β cell function by secreted insulin was prominent, debated and incomplete. Despite that insulin has been historically suggested to have negative effect on β cells, an increasing number of data provide evidence for a positive role of insulin in transcription, translation, ion flux, insulin secretion and β cell survival (Aikin et al., 2006; Aspinwall et al., 1999; Johnson et al., 2006; Leibiger et al., 2008). But the presence of insulin receptors (IRs) in β cells is generally

accepted (Rhodes et al., 2013), furthermore it is evidenced that mice lacking IRs in β cells have increased apoptosis, decreased proliferation and reduced β cell mass (Johnson and Alejandro, 2008).

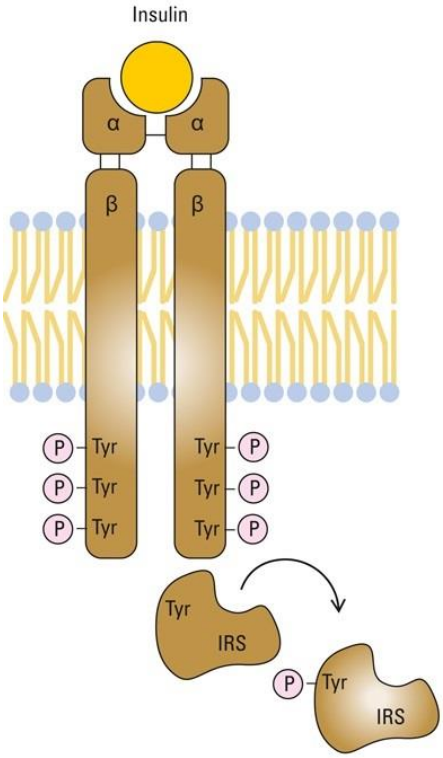

Figure 4. The structure and function of insulin receptor
Adapted from
www.medi-learn.de/bc5-18
MEDI-LEARN Script Biochemie 5,
Fig.18, page 19.

IR, a hormone-activated protein tyrosine kinase, consists of two extracellular regulatory α-subunits and two transmembrane catalytic β-subunits with tyrosine kinase activity localized in the cytosol. 2α and 2β subunits are linked by disulphide bonds into a tetramer but functionally a dimeric protein complex (αβ-αβ) (**Fig.4**). Insulin binding to α-subunits induces conformational change and rapid intracellular autophosphorylation of multiple tyrosine residues on the β-subunits. This causes the recruitment and tyrosine residue phosphorylation of a variety of docking proteins, especially IRS proteins (IRS1-6). Among them, IRS2 is essential in β cells (Boucher et al., 2014; Saltiel and Kahn, 2001). Insulin signaling cascade activates the master regulator Akt (as detailing above in chapter **2.2.**) resulting in the stabilization of PDX1 master regulator. Akt can inhibit glycogen synthase kinase 3 (GSK3), which is responsible for the phosphorylation-dependent degradation of PDX1, furthermore Akt relieves FOXO1-mediated Pdx1 gene repression. Accordingly, insulin-IR-Akt signaling is required for normal functioning of the β cell (Elghazi and Bernal-Mizrachi, 2009; Rhodes et al., 2013).

Long-term exposure to insulin, as a negative feedback, causes insulin-insulin receptor internalization through clathrin-dependent endocytosis. IR signal transduction continues from the internalized receptor until phosphatase-mediated termination. Insulin-IR complexes are delivered to endosomes where dissociation of insulin molecules from IR is accomplished by acidic pH. IRs are then sorted in endosomes for recycling back to the cell surface or in late endosomes and lysosomes for degradation, just like insulin itself (Bergeron et al., 2016; Sorkin and Fortian, 2015).

2.4. Type 2 diabetes mellitus and its metabolic consequences

Diabetes mellitus is the most common endocrine and metabolic disorder with an escalating prevalence. This chronic disease may arise due to inherited or acquired deficiency in insulin secretion, or by ineffective insulin response of the target tissues. The two major types of diabetes are type 1 and type 2 diabetes mellitus (Piero et al., 2015). Type 1 diabetes mellitus (T1DM) stems from genetic predisposition and environmental factors leading to cell-mediated autoimmune destruction of the β cells with consequent absolute insulin deficiency. T1DM accounts for 5–10% of all diabetes cases (American Diabetes Association, 2010). However, in our context type 2 diabetes mellitus (T2DM) is more important to discuss.

T2DM is responsible for 90–95% of diabetes cases worldwide. This multifactorial disorder results from an interaction between genetic and environmental conditions (sedentary lifestyle and obesity) and characterized by a peripheral insulin resistance, hyperglycaemia and β cell dysfunction (American Diabetes Association, 2010). Obesity-associated chronic inflammation is responsible for the development of insulin resistance, which is a complicated condition in the primary metabolic tissues that are sensitive to insulin: skeletal muscle, liver and white adipose tissue. During obesity the expansion of adipose tissue may lead to hypoxia and stress in adipocytes, which is followed by the release of pro-inflammatory signals, e.g. tumor necrosis factor-α (TNFα) or interleukin 6, exacerbating inflammation. TNFα stimulation leads to serine phosphorylation of IRS1 trough NFκB pathway, thereby obstructing insulin signaling and sensitivity (de Luca and Olefsky, 2008; Pandey et al., 2015). Glucose uptake of adipocytes through GLUT4 transporters is insulin-dependent, therefore, in insulin resistant state adipocytes are blocked from glucose uptake and produce little glycerol-3-phosphate beside of accelerated lipolysis. Basically, insulin suppresses lipolysis and restrains the release of free fatty acids (FFAs) from adipocytes, but the consequence of insulin resistance is increased fatty acids released attending to increase ketone synthesis and ketosis. Ketone bodies, as carboxylic acids lower blood pH lead to acidosis. Moreover, ketone bodies are excreted in the urine inducing water and electrolyte loss (Dow et al., 1996; Joslin and Kahn, 2005). Furthermore, chronic elevation in the plasma FFA is also involved in the etiology of obesity-associated insulin resistance. Among major human FFAs, palmitate markedly inhibits insulin-stimulated phosphorylation of key insulin signaling molecules (e.g.IR, IRS1, Akt), moreover, palmitate facilitates their ubiquitination and subsequently elicits their proteasomal degradation (Ishii et al., 2015).

In skeletal muscle, raising plasma FFA reduces insulin stimulated glucose uptake thereby induces starving state and usage of the final reserve, the proteins. Alanine and glutamine are the principal amino acids released into the circulation to serve as gluconeogenic substrates owing to high degree of energy deprivation in tissues under diabetic conditions (Joslin and Kahn, 2005). Furthermore, in skeletal muscle intramyofibrillar lipid metabolites play a pivotal role in triggering insulin resistance that is associated with decreased mitochondrial oxidative phosphorylation. Since fatty acid β-oxidation takes place in the mitochondria, impaired fat oxidation refers to the presence of a mitochondrial defect that contributes to the impaired muscle fat oxidation and intramyocellular lipid accumulation (Abdul-Ghani and DeFronzo, 2010; Morino et al., 2006). Mitochondrial dysfunction is associated with insulin resistance in liver and skeletal muscle, which can be attributable to FFA and glucose overload (Sivitz and Yorek, 2010).

Uncoupling protein-2 (**UCP2**) is a mitochondrial intermembrane ion transporter protein that induces proton leak uncoupling respiration from ATP production (Baffy et al., 2002). UCP2 enables transport non-esterified fatty acid anions out of the matrix in a process called fatty acid cycling and protons into the mitochondrial matrix (Ruiz-Ramírez et al. 2016). UCP2 senses and negatively regulates superoxide production – derived from excess glucose influx or enhanced hepatic fatty acid accumulation and catabolism – exerting its cytoprotective effect (Fülöp et al., 2006; Horimoto et al., 2004). Normally, plasma FFAs regulate positively both the expression and the activity of UCP2 (Ruiz-Ramírez et al. 2016). UCP2 may compensate the elevated FFA levels by switching the cell metabolism from glucose to fatty acid oxidation (Bouillaud, 2009; Ruiz-Ramírez et al., 2016). In line with these, increased UCP2 expression in white adipose tissue and skeletal muscle is associated with a reduced risk of developing obesity, which is the most important risk factor for the development of T2DM (Schrauwen and Hesselink, 2002).

In obesity, hepatic inflammation could be the result of steatosis and/or increased stress pathway responses, inducing Kupffer cells (liver-resident macrophage-like cells), which further exacerbates inflammation and hepatic insulin resistance. In addition, overnutrition and obesity are often accompanied by elevations FFA concentrations, and saturated FFAs can directly activate pro-inflammatory responses and attenuate insulin signaling. Nevertheless, physiological elevations of FFA inhibit insulin suppression of HGP, including glycogenolysis and gluconeogenesis, therefore contribute to fasting hyperglycemia (de Luca and Olefsky, 2008). In various animal models of insulin resistance and T2DM, elevated glycogenolysis has

been detected, accordingly GP inhibition may improve glucose tolerance and supply to suppress HGP (Agius, 2007; Levinthal and Tavill, 1999).

Insulin deficiency or insulin resistance coexists with increased secretion of glucagon, even when blood glucose concentration is high because tissues do not take up glucose. Despite that insulin resistance is well established early in the emergence of T2DM, glucose tolerance remains normal because of a compensatory increase in insulin secretion of β cells. The process of β cell compensation is a combination of β cell mass expansion and an increase of acute glucose-stimulated insulin secretion. Moreover, the process is associated with an improved capacity of the secretory machinery to support increased insulin production.

When this adaptive response unable to offset the progressive deterioration in glucose homeostasis, insulin concentration declines precipitously and HGP begins to rise. Hyperinsulinemia is a strong predictor of the development of impaired glucose tolerance and T2DM. In contrast to these, chronic β cell exposure to high glucose and FFA levels can inhibit insulin secretion, impair β cell function and finally induce β cell apoptosis. The progressive β cell failure ultimately determines the rate of T2DM (American Diabetes Association, 2010; Cerf, 2013).

To diagnose T2DM in humans oral glucose tolerance test (OGTT) is considered as the gold standard method. In animal research, oral or intraperitoneal glucose tolerance (ipGTT) test is used to assess the degree of diabetes and also to test the desired effects of insulin or other drugs. An early marker for T2DM is decreased **oxygen consumption (**VO_{2max}). VO_{2max} is a measure of aerobic fitness expressed in ml of oxygen/kg/minute absorbed by the body from the blood. Exercise capacity (VO_{2max}) strongly correlates with insulin resistance (Leite et al., 2009). A simple test for evaluating the amount of energy derived from carbohydrate as opposed to fat metabolism is the **respiratory quotient** (RQ). RQ is the ratio of CO_2 produced to the volume of O_2 consumed while food is being metabolized. The ratio of RQ ranges from 0.7 to 1.0 and averages around 0.8. The RQ varies with the fuel source used. For carbohydrates it is 1.0, for lipids 0.7, for proteins 0.8 and with overfeeding (lipogenesis) 1.0-0.3 (Nakaya et al., 1998).

3. AIM OF THE STUDY

GP inhibition has been shown to be a potential target for influencing blood glucose levels in T2DM. We set out to investigate the metabolic effects of GP inhibition in different models. In our experiments, we used an apparently potent glucose analog GP inhibitor, namely KB228 compound. On one hand, we utilized normal and high-fat diet-fed murine models in order to obtain evidences for KB228 applicability and efficiency. On the other hand, we used hepatic and muscle myoblast cells, as models of investigated metabolic organs (liver and skeletal muscle). To imitate the normal and diabetes-induced hyperglycemic conditions, experiments were implemented under normoglycaemic (5.5 mM) and hyperglycemic (25 mM) conditions.

1. **Our aims were the following:**

- to set out to find an appropriate dose and administration of KB228 for *in vivo* studies,
- to characterize the impact of KB228 on *in vivo* glucose metabolism including glucose tolerance, excursion and consumption,
- to explore the effects of KB228 on glucose metabolism in HepG2 cells,
- gene expression profiling of HepG2 cells to evaluate the effects of KB228 on key marker genes of major metabolic pathways,
- to investigate the activity of protein kinases involved in energy homeostasis.

Furthermore, taken in consideration that the pancreatic β cells are in the center of the diabetes research, β cells became our next model to investigate the effects of GP inhibition in details. MIN6 insulinoma cell, as a well-established model for β cells, was in the focus of the next chapter of our study. KB228 was further investigated in *in vivo* experiments and three structurally different GPis (KB228, BEVA335 and CP-3016819) were tested in *in vitro* experiments.

2. **Our goals were the following:**

- to assess glycogen metabolism and the localization of glycogen particles in MIN6 cells,
- to explore the glycogen-associated proteins by *in silico* screening,
- To evaluate the impact of GP inhibition on proliferation and on classical insulin secretion pathways in MIN6 cells and in mice.

4. MATERIALS AND METHODS

4.1. Chemicals

Unless otherwise stated, all chemicals were from Sigma-Aldrich (St. Louis, MO, USA).

The applied inhibitors in our study are summarized in **Table 2.**

Name	Inhibitor type	Applied concentration	Applied for experiments
Synthesized in the Laboratory of László Somsák at Department of Organic Chemistry, University of Debrecen			
KB228	GP inhibitor	3 μM	*In vivo, in vitro*
BEVA335	GP inhibitor	1.5 μM	*in vitro*
TH	GP inhibitor	20 μM	*in vitro*
NV50	GP inhibitor	25 μM	*in vitro*
NV76	GP inhibitor	2 μM	*in vitro*
From Sigma Aldrich			
CP-316819	GP inhibitor	0.5 μM	*in vitro*
wortmannin (WM)	PI3K inhibitor	1 μM	*in vitro*

Table 2. Inhibitors used in the study

Structure, name and inhibitory constant of the GP inhibitors used by us are summarized in **Table 1.** (see chapter **2.1.** Glycogen metabolism)

4.2. Animal studies

Animal experiments were authorized by the Institutional Animal Care and Use Committee at University of Debrecen (7/2010 DE MÁB) and were carried out according to the NIH guideline "Guide for the care and use of laboratory animals", the ARRIVE 4 guidelines and the applicable national laws. C57/Bl6J male mice were purchased from Charles River Laboratories (Wilmington, MA, USA) and had *ad libitum* access to water and food, and were kept under a 12/12 h dark-light cycle (light 7 a.m. – 7 p.m., night 7 p.m. – 7 a.m.). Mice were kept on chow (10 kcal% of fat) (SAFE, Augy, France) or on high-fat diet (HFD, hypercaloric diet, 60% fat content, Research Diets, Inc., New Brunswick, NJ, USA). GP inhibition in mice was implemented by using KB228 inhibitor. Mice were randomly incorporated into the vehicle or KB228-treated group. Mice were administrated with vehicle (physiological saline + 1% DMSO) or with 90 mg/kg bodyweight of KB228 (diluted in 1% DMSO-containing physiological saline) as a single intraperitoneal (i.p.) bolus once a week for

5 weeks before sacrifice. All measurements were carried out on mice of 6 months of age and took place 2 hours after injection and tissues were collected and processed as specified. After mice were sacrificed by cervical dislocation, the indicated organs (liver, gastrocnemius muscle and pancreas) were removed and further investigated.

4.2.1. Intraperitoneal glucose tolerance test

Animals were fasted for 8 hours prior to the experiment. Before glucose challenge a drop of peripheral blood was drawn from each animal by cutting their tail and starting blood glucose levels were determined using a handheld Accu-Chek (Roche Molecular Systems Inc., CA, USA) device. Next each animal received an intraperitoneal glucose (20% m/m) injection (10 μL/body weight g) using a 1 mL tuberculin syringe with an attached 26 G needle. Subsequently, blood-glucose levels were monitored at regular intervals (time points) for each animal the same way the initial values were determined.

4.2.3. Indirect calorimetry

Indirect calorimetry experiments were performed in a CLAMS system (Comprehensive Lab Animal Monitoring System, Columbus Instruments, Columbus, OH, USA). Mice were habituated to the new environment of the cages for 24 hours. At 8 a.m. mice received a bolus i.p. injection of KB228 (90 mg/kg) or vehicle then were returned to the measurement cages. Oxygen consumption and carbon dioxide release was recorded for the following six hours.

4.2.4. Glucose uptake assay

Under isoflurane anesthesia mice were injected with 120 μCi/kg ^{14}C-2-deoxyglucose and 20 U/kg insulin through the jugular vein then the incision above the vein was closed with a suture. Blood glucose levels were monitored at the time of the suture, 15 and 30 minutes post intervention. The mice were sacrificed by cervical dislocation 30 minutes post intervention and the liver, skeletal muscle, pancreas, white adipose tissue and heart were removed. Carefully weighed pieces of these tissues were lysed in 0.5 mL 1 M NaOH at 70 ^{o}C

for 60 mins. Lysates were mixed with Aqualight HIBEX (Perkin Elmer Life Sciences, The Netherlands) scintillation liquid and were measured in a Wallac scintillation counter (Perkin Elmer, Waltham, MA, USA).

4.2.5. Histochemical assessment of glycogen content in the pancreas

Glycogen content of pancreatic tissue was determined by Periodic Acid Schiff (PAS) staining. Formalin fixed, dehydrated samples were embedded into paraffin, then 5 μm sections were prepared by using Leica (Leica Biosystem, Germany). Deparaffinization was followed by hydration with water and oxidation of the 5 μm sections in 0.5% periodic acid solution for 20 minutes. After rinsing in distilled water, sections were placed in Schiff reagent for 15 minutes. Sections were washed in lukewarm tap water for 5 minutes, then counterstained in hematoxylin for 2-3 minutes. After extensive washing with tap water, sections were dehydrated and covered. Microscopic images were acquired with a Zeiss Axioscope 20 microscope (Carl Zeiss Technika Kft., Hungary) using Plan NEOFLUOR 40x objective at 25°C. Images were processed using Leica Application Suite V4.8 software (Leica Microsystems, Germany). Glycogen content was determined by measuring the intensity with Image J software, where more intensive PAS staining correlates with higher glycogen content.

4.2.6. Insulin immunohistochemistry and islet size determination

Embedding tissue into paraffin blocks, then deparaffinization of slides, endogenous peroxidase activity was blocked (3% hydrogen peroxide in methanol on 5 μm paraffin sections for 15 minutes at RT), and then the slides were rinsed briefly with PBS. Non-specific binding was blocked by incubating the slides for 1 hour in 1% BSA diluted in PBS. To detect insulin, guinea pig polyclonal insulin antibody (DAKO, Glostrup, Denmark; 1:100) was applied overnight at 4 °C in 1% BSA diluted in PBS. After extensive washing with PBS, slides were stained with Envision one-step polymer HRP (BioGenex Fremont CA, USA) for 90 minutes. Color reaction was developed for 2 minutes using nickel 3,3'-diaminobenzidine tetrachloride (Ni-DAB) as a substrate for antibody-coupled HRP (1.6 mM DAB, 140 mM NaCl, 90 mM $NiSO_4$, 100 mM Na-acetate, 3 mM H_2O_2, pH 6.6). After rinsing sections in 50 mM Tris-HCl (pH 7.4), the color was enhanced by incubating the sections for 2 minutes in

2% cobalt chloride (in 50 mM Tris-HCl, pH 7.2). Sections were then rinsed in distilled water and counterstained with 1% methyl green solution. A negative immunohistochemical control was included in each run. Microscopic images were acquired with a Zeiss Axioscope 20 microscope (Carl Zeiss Technika Kft., Hungary) using Plan NEOFLUOR 40x objective at 25°C. Images were processed using Leica Application Suite V4.8 software (Leica Microsystems, Germany). Islet size was determined in μm^2 by using Image J software.

4.3. Cell culture

HepG2 human hepatocarcinoma and C2C12 mouse myoblast cell lines were obtained from ATCC (Manassas, VA, USA) and were cultured in DMEM, 10% fetal calf serum, 1% L-glutamine, 1% penicillin-streptomycin. HepG2 cells were cultured in DMEM containing 5.5 mM glucose, while C2C12 cells were maintained in DMEM containing 25 mM glucose. C2C12 cells were differentiated in DMEM, 2% horse serum for 4 days. The length of KB228 treatments are described in the corresponding figure legends. Normoglycaemic condition was provided by using 5.5 mM glucose-containing medium, while hyperglycaemic conditions was provided by using 25 mM glucose-containing medium during the treatments. Control group, which is marked in black as vehicle in the figures, was treated with 0.01 % DMSO in DMEM.

MIN6 mouse insulinoma cell line (Miyazaki et al., 1990) was a generous gift from Dr. J. Miyazaki (Osaka University Medical School, Japan) and was provided to us by Dr. P. Halban (Faculty of Medicine, University of Geneva, Switzerland). MIN6 cells were cultured in DMEM, 15% fetal calf serum, 1% L-glutamine, 1% penicillin-streptomycin, 50 μM 2-mercapto-ethanol and 25 mM glucose. MIN6 cellular treatments and measurements took place in DMEM containing 5.5 mM glucose. The measurements took place 1 and 2 days after the addition of inhibitors, including KB228, BEVA335 and CP-316819, as indicated. Wortmannin was used in the last 1 hour of the GPi treatment. Control group, which is marked in black as CTL in the figures, was treated with 0.01 % DMSO in DMEM.

4.4. Biochemical glycogen determination

KOH-ethanol glycogen extraction method was used for extraction of the glycogen. $10x10^5$ of cells were seeded in 10 cm^3 petri dish in medium. After treatment, cells were scraped and collected into Eppendorf tubes. During *in vivo* experiments murine livers were removed for measurement 2 hours post-treatment. 200 μL of 30% KOH solution was added to

the cell pellet or 2500 µL to 1 gram of murine liver. Samples were boiled at 100 °C for 15-30 minutes, shaken continuously until the complete dissolution of the tissue or pellet, then the tubes were cooled down on ice. After 10 minutes incubation on ice 2x volume of 96% ethanol was added to the solution and tubes were centrifuged at 4°C for 30 minutes at 21 500 g. After second ethanol wash the supernatant was evaporated using SpeedVac and the glycogen pellets were resuspended in distilled water. Phenol-sulfuric acid assay was applied for determination of glycogen content. We added 3x volume of concentrated H_2SO_4 to the glycogen suspension and incubated it for 10 minutes at RT with shaking. Then a tenth of volume of 5% phenol was added to each tube and shaken for additional 10 minutes at 90°C. The samples were measured within 10 to 30 min in a microplate reader set at 450 nm. Readings were normalized to protein content or wet weight of the liver piece.

4.5. Total RNA isolation, reverse transcription and RT-qPCR

Total RNA was prepared using TRIzol (Invitrogen, Carlsbad, CA, USA) reagent following the manufacturer's instructions. Concentrations and quality of RNA was assessed using NanoDrop spectrophotometer (NanoDrop Technologies, Wilmington, DE, USA). 2 µg of RNA was used for reverse transcription (RT) (High Capacity cDNA Reverse Transcription Kit, Applied Biosystems, Foster City, CA, USA). Reverse transcription was carried out in a PCR machine (Applied Biosystems Veriti 96-Well Thermal Cycler). 10x diluted cDNA samples were used for real-time quantitative PCR (qPCR) reactions which were performed using qPCR Supermix (qPCRBIO SyGreen Mix, Nucleotest Bio Kft., Hungary) with the primers summarized in **Table 3** and carried out in the Light-Cycler 480 II instrument (Roche Applied Science, Penzberg, Germany). Expression was normalized to the geometric mean of three control genes (β-actin, cyclophilin, 36B4 or/and GAPDH).

Gene		**Forward primer**	**Reverse primer**
β-actin	Human	5'-GACCCAGATCATGTTTGAGACC-3'	5'-CATCACGATGCCAGTGGTAC-3'
β-actin	Murine	5'-TGGAGAGCACCAAGACAGACA-3'	5'-TGCCGGAGTCGACAATGAT-3'
Cyclophilin	Human	5'-GTCTCCTTTGAGCTGTTTGCAGAC-3'	5'-CTTGCCACCAGTGCCATTATG-3'
Cyclophilin	Murine	5'-CAAGGTCATCCATGACAACTTTG-3'	5'GGCCATCCACAGTCTTCTGG-3'
Gapdh	Murine	5'-CAAGGTCATCCATGACAACTTTG-3'	5'-GGCCATCCACAGTCTTCTGG-3'
36B4	Human	5'-CCATTGAAATCCTGAGTGATGTG-3'	5'-GTCGAACACCTGCTGGATGAC-3'
36B4	Murine	5'-AGATTCGGGATATGCTGTTGG-3'	5'-AAAGCCTGGAAGAAGGAGGTC-3'
UCP2	Human	5'-CTACAAGACCATTGCCCGGAG-3'	5'-ACAATGGCATTACGAGCAACA-3'
Ucp2	Murine	5'-TGGCAGGTAGCACCACAGG-3'	5'-CATCTGGTCTTGCAGCAACTCT-3'

Gys1	Murine	5'-AACAAGGTGGGTGGCATCTAC -3'	5'-TACAACCCTTGCTGTTCATGG -3'
Gys2	Murine	5'-TAAAGGAGGTGACAGACCACG -3'	5'- GTCGAACTTGTCAAGCTGGTTGTAG-3'
PYGL	Human	5'-GTGCCCCAAGAGGGTATATTAC-3'	5'-AAGAAGCAGGCAGCAAGTCTC-3'
Pygl	Murine	5'-CCCCGTGCCTGGATATATGA-3'	5'-TGTTTCAGCCGCAACTCCTT-3'
PYGM	Human	5'-GGACCCCAAGAGGATCTACTACC-3'	5'-CCTCGTCACAGGCATTCTCTA-3'
Pygm	Murine	5'-CCCAAGAGGATCTACTACCTGTC-3'	5'-ACTCATAGCGGATCCCATAGC-3'
PYGB	Human	5'-AGCCATCTATCAGTTGGGGTTAG-3'	5'-TGCCAGCCATTGACAATCTTC-3'
Pygb	Murine	5'-CACTTATCAGTTGGGGTTGGAC-3'	5'-GCCAGTCATCAGCTTCTTCAAC-3'
Insulin	Murine	5'-GTGGGGAGCGTGGCTTCTTCTA-3'	5'-ACTGATCCACAATGCCACGCTTCT-3'
Pdx1	Murine	5'-AATCCACCAAAGCTCACGCGTGGAA-3'	5'-TGATGTGTCTCTCGGTCAAGTTCAA-3'

Table 3. Primers used in RT-qPCR reactions

4.6. Protein extraction and Western blotting

HepG2 cells and murine liver homogenates were lysed in RIPA lysis buffer (50 mM Tris pH 8.0, 150 mM NaCl, 0.1 % SDS, 0.5 % Sodium deoxycholate, 1 % NP-40, 1 mM NaF, 1 mM Na_3VO_4, PMSF, protease inhibitors) then homogenized using a 22 G then a 26 G needle. Lysates were cleared by centrifugation.

MIN6 cells were lysed in a homogenizing lysis buffer (250 mM saccharose, 20 mM Hepes, 1 mM EDTA, 1 mM EGTA, 0.5 % Nonidet P-40). Cells were incubated on ice in the buffer then homogenized using a 26 G needle. Lysates were cleared by centrifugation. Supernatant contained the cytoplasmic fraction and the pellet contained the nuclear fraction. Pellet was further extracted using buffer "A" (350 mM saccharose, 10 mM pH 7.9 Hepes, 3.3 mM $MgCl_2$, 10 mM KCl) followed by buffer "B" (the same as "A" except 250 mM saccharose). Sonicated samples were cleared by centrifugation.

Proteins were separated by SDS-PAGE and transferred onto nitrocellulose membranes. Blots were probed with antibodies summarized in **Table 4.** Signals were developed using SuperSignal™ WestPico Enhanced Chemiluminescent (ECL) Substrate (Pierce Biotechnology Inc., Rockford IL) and captured by a Fluorchem FC2 gel documentation system (Alpha Innotech, San Leandro, CA, USA). Densitometry was performed using the Image J software.

Primary antibodies:			
UCP2 (Abcam, Cambridge, UK)	mouse	polyclonal	1:1000
Akt (Sigma Aldrich, MO, USA)	rabbit	monoclonal	1:1000
Phospho-Akt (Ser-473) (Cell Signaling, The Netherlands)	rabbit	monoclonal	1:2000
Insulin (DAKO, Glostrup, Denmark)	guinea pig	polyclonal	1:1000
Insulin Receptor (Cell signaling, The Netherlands)	rabbit	monoclonal	1:1000
Phospho-Insulin Receptor β (Tyr-1345) (Cell signaling, Netherlands)	rabbit	monoclonal	1:500
p70S6K (Cell Signaling)	rabbit	polyclonal	1:1000
Phospho-p70S6K (Thr-389) (Cell Signaling)	rabbit	polyclonal	1:1000
PDX1 (Abcam, Cambridge, UK) /cytoplasmic fraction/	rabbit	polyclonal	1:2000
PDX1 (Cell signaling, Netherlands) /nuclear fraction/	rabbit	monoclonal	1:1000
LaminB1 (Cell signaling, Netherlands)	rabbit	monoclonal	1:1000
β-Actin−Peroxidase (Sigma Aldrich, MO, USA)	mouse	polyclonal	1:25000
Secondary antibodies:			
HRP-linked anti-rabbit IgG (Cell Signaling, Netherlands)	goat	polyclonal	1:2500
Peroxidase conjugated anti-mouse IgG (Sigma Aldrich, MO, USA)	rabbit	polyclonal	1:10000
Peroxidase conjugated anti-guinea pig IgG (Sigma Aldrich, MO, USA)	goat	polyclonal	1:2000

Table 4. Antibodies used in Western blot analysis

4.7. Determination of oxygen consumption and extracellular acidification rate

Oxygen consumption rate (OCR, reflecting mitochondrial oxidation) of HepG2 cells were measured using an XF96 oximeter (Agilent Technologies, Santa Carla, California, USA). Briefly, HepG2 cells (5000 cells/well) were seeded in a XF96 Cell Culture Microplate. After recording the baseline OCR, cells received a single bolus dose of 3 μM KB228. Then, OCR was recorded at every hour to follow the effects of GPis. Final reading took place at 8 hours post-treatment. Data were normalized to protein content and normalized readings were used for calculations. For protein determination we used 1 M NaOH, 10 times volume of BCA reagent (Pierce^{TM} BCA Protein Assay Kit, Thermofisher, Walthman, MA, USA) and plate reader. OCR values expressed as pmol O_2/mg protein x minutes.

OCR and changes in pH, termed extracellular acidification rate (ECAR, reflecting glycolysis) of MIN6 cells were assessed by using the mentioned XF96 oximeter, when MIN6 cells were seeded in XF96 Cell Culture Microplate and were treated with GP inhibitors for 1 and 2 days. After recording the baseline, OCR and ECAR were recorded every 3 minutes up to 60 minutes to follow the effects of GPis. Antimycin (10 μM) was used for distinguishing the mitochondrial from non-mitochondrial oxygen consumption. The antimycin-resistant respiration gives information on the leakage through the inner membrane of the mitochondria (*proton leak*). Final reading took place at 1 hour. OCR values obtained pmol O_2 / 10^5 MIN6 cells / minutes. ECAR values obtained mpH/ 10^5 MIN6 cells x minutes.

4.8. Confocal microscopy

MIN6 cells were grown on glass coverslips for one day then starved overnight in glucose-free medium (XF Assay Medium Modified DMEM containing 0 mM glucose, 1% P/S, 1% L-glutamine, 10% FBS, Agilent Technologies) overnight. Next morning, cells were charged with 500 μM fluorescent D-glucose analogue (2-[N-(7-nitrobenz-2-oxa-1,3-diazol-4-yl) amino]-2-deoxy-D-glucose (2-NBDG), Cayman Chemicals Company, Ann Arbor, Michigan, USA) in uptake buffer pH 7.4 (138 mM NaCl, 5.5 mM D-glucose, 5 mM KCl, 1 mM $MgCl_2$, 1.5 mM $CaCl_2$, 10 mM Hepes) for 3 hours, then incubated in 5.5 mM glucose-containing DMEM for one more day. Next day, cells were fixed with 100 % methanol for 20 min at -20°C, then rinsed three times with 1x PBS. The cells were permeabilized with 1 % Triton X-100 in PBS for 5 min, blocked in 1 % BSA in PBS for 1 hour, and incubated with primary monoclonal rabbit antibody (insulin receptor β (IRβ, Cell signaling, 1:50) in moist chamber overnight at 4°C. The next day, samples were extensively washed and the secondary antibody (Alexa Fluor ® 647 donkey anti-rabbit IgG (H+L), Life Technologies, 1:1000), diluted in blocking solution, was added for 1 hour at room temperature. Coverslips were rinsed three times with 1x PBS then cell nuclei were stained with DAPI special formation (NucBlue® Fixed cell Stain ReadyProbes™ reagent, Life Technologies, Carlsbad, CA, USA) and rinsed in PBS again. The coverslips were fixed on the microscope slide by using Moviol® mounting medium containing 2.5 % DABCO to prevent dehydration and photobleaching of the samples. Confocal images were acquired with a Leica TCS SP8 confocal microscope using HC PL APO CS2 63x/1.40 OIL immersion objective on a DMI6000 CS microscope at 25°C. The following lasers were used for the measurements: OPSL 488 for 2NDBG, Diode 638 for Alexa Fluor 647 and 405 visible for DAPI. Images were processed using LAS X

2.0.1.14392 software (Leica Microsystems, Germany). Nonspecific binding of secondary antibodies were checked in control experiments.

4.9. Electron microscopy

Pellets of cells, after GP inhibitor or vehicle treatment were processed for electron microscopic investigation according to the ferrocyanide-reduced osmium method. Cells were fixed in 3% glutaraldehyde dissolved in 0.1 M cacodylate buffer (pH: 7.4) containing 5% sucrose for 1 hour at room temperature. After washing several times in cacodylate buffer (pH: 7.4), cells were post-fixed in ferrocyanide-reduced osmium (2% osmium tetroxide and 3% potassium ferrocyanide dissolved in 0.1 M cacodylate buffer, pH: 7.4) for 2 hours at room temperature. Following several washes in cacodylate buffer (pH: 7.4), cells were dehydrated and embedded into Durcupan ACM resin. Ultrathin sections were cut, collected on Formvar-coated single-slot grids, and counterstained with uranyl acetate and lead citrate. Sections were investigated with a JEOL 1010 transmission electron microscope and photographed at a magnification of 6000-10000x with an Olympus Veleta CCD camera. Digitalized images were processed with Adobe Photoshop CS5 software. Morphometric assessment was done using the Image J software. To control the specificity of the staining, a group of cells – marked as negative control - underwent the same EM staining protocol without the addition of potassium ferrocyanide to osmium tetroxide.

4.10. Measurement of changes in intracellular Ca^{2+} concentrations

MIN6 cells had been seeded on glass coverslips (25 mm diameter and 1 mm thickness; Thermo Fisher (Thermo Fisher Scientific Gerhard Menzel B.V. & Co. KG, Braunschweig, Germany) and treated with GP inhibitors for 1 or 2 days before the experiments. Cells were loaded with 5 μM of Fura-2AM fluorescent Ca^{2+} indicator dye (Molecular Probes) for 90-120 minutes. Then coverslips were placed into a tissue chamber suitable for fluorescence microscopy. The tissue chamber was filled with DPBS (Invitrogen, containing calcium and magnesium) and was placed on the stage of an InCyte IM2 system (Intracellular Imaging Inc., Cincinnati, OH, USA). Cells were illuminated alternately at 340 and 380 nm of light (excitation) and pictures were recorded detecting the fluorescent emission with a 510 nm long pass filter (emission). 20 cells were selected in each regions of interest and changes in

intracellular Ca^{2+} concentration were recorded as changes in the ratio (340/380 nm). After reaching a stable baseline (min. 60 seconds) cells were induced with 20 mM glucose.

4.11. Insulin release in MIN6 cells

MIN6 cells were plated in 6-well plates at a concentration of $2x10^5$ cells per well. Cells were pre-incubated in DMEM for 1 day with or without inhibitors. Before measurement the medium was changed in each well to 1 mL of 5.5 mM glucose-containing DMEM medium and after 2 minutes 10 µl sample was taken and diluted to 50x in medium. Insulin production of MIN6 cells was measured using a Mouse Insulin ELISA Kit (Mercodia, Winston Salem, NC, USA) following the manufacturer's instructions. After the assay, 1 M NaOH was added to adhered MIN6 cells in 6-well plates and the total protein content was determined using BCA reagent (Pierce™ BCA Protein Assay Kit, Thermofisher, Walthman, MA, USA). Insulin secretion was normalized for protein content.

4.12. Glucose-induced insulin release in MIN6 cells

Glucose-induced insulin release from MIN6 cells was determined using a static incubation protocol as described previously (Johnson et al., 2007). MIN6 cells were cultured in 96-well plates until ~80% confluency, and the medium (containing 25 mM glucose) was changed in every 48 h. On the day of the experiment, growth medium was removed, and the cells were washed twice with glucose-free KRBH (HEPES-balanced Krebs-Ringer phosphate buffer, composed of 111 mM NaCl, 25 mM $NaHCO_3$ (pH 7.4), 4.8 mM KCl, 1.2 mM KH_2PO_4, 1.2 mM $MgSO_4$, 10 mM HEPES, 2.3 mM $CaCl_2$ and 0.1% BSA). Cells were preincubated for 1 h in 5% CO_2 at 37°C in KRBH (1 mM glucose). The pre-incubation medium was removed, and the cells were washed once in glucose-free KRBH. The cells were then incubated for 1 h in 20 mM glucose-containing KRBH in the absence (control, CTL) or presence of inhibitors (KB228, BEVA335, CP-316819 and/or Wortmannin). At the same time, a set of control cells were incubated for 1 h in 1 mM glucose-containing KRBH for determination of insulin baseline. For all experiments, incubation medium was collected, spun at 1500 g for 5 min 4°C, and then diluted 20x. Insulin concentration in diluted samples was determined using a Mouse Insulin ELISA Kit (Mercodia, Winston Salem, NC, USA). After the assay, 1 M NaOH was added to adhered MIN6 cells and the total protein content was determined using BCA reagent (Pierce™ BCA Protein Assay Kit, Thermofisher, Walthman, MA, USA). Insulin secretion was normalized to protein content.

4.13. Total insulin protein in MIN6 cells

MIN6 cells were seeded in 24-well plates in 5.5 mM glucose-containing DMEM medium. After 1 day-treatment, cells were scraped and collected. Cells were extracted by using acid-ethanol extraction where 150 µL 70% ethanol containing 1.5% HCl was added to each cell pellet then samples were incubated overnight at -20°C. Next day samples were centrifuged at 2000 g at 4°C for 15 minutes. Aqueous solution was divided into two parts. 100 µL aqueous solution was neutralize with 100 µL 1 M Tris pH 7.5 then further diluted 500x in Insulin ELISA calibrator 0 solution and measured using Mouse Insulin ELISA Kit (Mercodia, Winston Salem, NC, USA) following the manufacturer's instructions. The remaining aqueous solution was neutralized with Na_3BO_4 in order to measure protein concentration by using BCA reagent (Pierce™ BCA Protein Assay Kit, Thermofisher, Walthman, MA, USA). Insulin content was normalized for protein content where ng insulin / mg protein values were transformed to fold change compared to the controls.

4.14. Transfection and luciferase assay

1,5 x 10^5 MIN6 cells were seeded in 6-well plates and were transfected with 5 µg of the corresponding PDX1 promoter construct [-6500STF-1luc plasmid, a generous gift from Marc Montminy (Salk Institute, La Jolla, CA, USA) (Sharma et al., 1996)] and 1 µg of β-galactosidase expression plasmid in Pei (Polyethylenimine) transfection reagent in 200 µl/well 150 mM NaCl solution. The promoter insert ($^{+}$68 - $^{-}$6500 bp) is of rat origin. To assess its applicability for the construct harboring the murine sequence we performed a sequence alignment of the promoter sequence and found 82% identity between rat and murine promoter (**Figure 5.**):

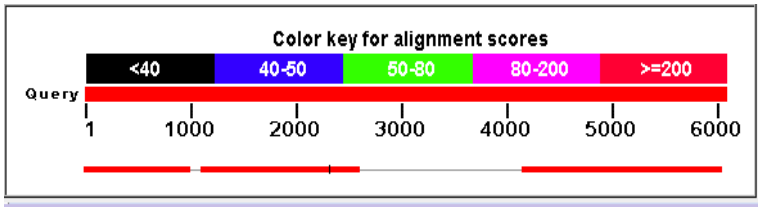

Max score	Total score	Query cover	E value	Ident	Accession
1513	3640	72%	0.0	82%	Query_110531

Figure 5. Sequence alignment of the PDX1 promoter sequence

Query: Rat
Subject: Mouse

48-hour post transfection cells were washed with PBS, collected into Eppendorf tubes by scraping in luciferase lysis buffer (25 mM Tris-phosphate pH 7.8, 2 mM EDTA, 1 mM DTT, 10% glycerol, 1% Triton-X 100). Samples were disrupted by 3 freeze-thaw cycles using 37°C

waterbath and liquid N_2. Lysates were cleared by centrifugation at 4°C, 21 500 g for 30 minutes then divided into two parts for determination of luciferase and β-galactosidase activity. For β-galactosidase activity we mixed 20 μL of lysate, 30 μL of ortho-nitrophenyl-β-D-galactopyranoside (ONPG) substrate and 150 μL of Z-buffer (60 mM Na_2HPO_4, 40 mM NaH_2PO_4, 10 mM KCl, 1 mM Mg_2SO_4, 50 mM β-mercapto-ethanol). Samples were incubated for 20-50 minutes in CO_2-free thermostat then absorbance was determined at 405 nm. For the determination of luciferase activity 100 μL of lysate, 50 μL of luciferase lysis buffer and 50 μL of luciferase assay mix (470 μM Luciferin, 530 μM ATP, 270 μM Coenzyme A and 20 mM Tris-phosphate pH 7.8, 1.07 mM $MgCl_2$, 2.7 mM $MgSO_4$, 100 μM EDTA and 33.3 mM DTT) were used. Luciferase activity was measured in a Victor Luminescence Reader (PerkinElmer, Waltham, MA, USA). The reaction was started by adding luciferase assay mix. Luciferase activity was expressed as luciferase activity/β-galactosidase activity transformed to fold change with respect to the control.

4.15. *In silico* screening for glycogen-binding proteins

The database containing a list of proteins with potential association with glycogen was assembled form multiple queries using the UniProt database (http://www.uniprot.org). The resulting list was manually revised and redundancies in the list were removed manually.

4.16. Statistical analysis

We determined the statistical significance between two groups regarding control/vehicle versus KB228 by using Student's *t*-test (unpaired, two-tailed) unless otherwise stated. Statistical significance of 3-5 group-designed measurements was determined using one-way ANOVA with Tukey HSD.

Error bars represent ± standard error of the mean (SEM) unless otherwise stated.
*, ** and *** indicate statistically significant difference between vehicle and treated groups at $p<0.05$, $p<0.01$ or $p<0.001$, respectively.

5. RESULTS

5.1. Characterization of the *in vivo* applicability of GP inhibitor KB228

KB228 displayed mixed type inhibition on purified rabbit muscle glycogen phosphorylase. The K_i of this inhibitor was 937 nM. We set out to find an appropriate dose and administration for KB228 during *in vivo* studies. KB228 was administered to C57/Bl6J mice as a single i.p. injection in a 90 mg/kg dose (lower doses were ineffective – data not shown). KB228 treatment reduced blood glucose levels 30 minutes post treatment and the effect remained for 6 hours after KB228 administration (**Fig. 6A**) that coincided with an increment in hepatic glycogen content (**Fig. 6B**) with unaltered change or rather decreasing tendency in the expression of GP isoforms (*Pygl*, *Pygm*, *Pygb*) (**Fig. 6C**).

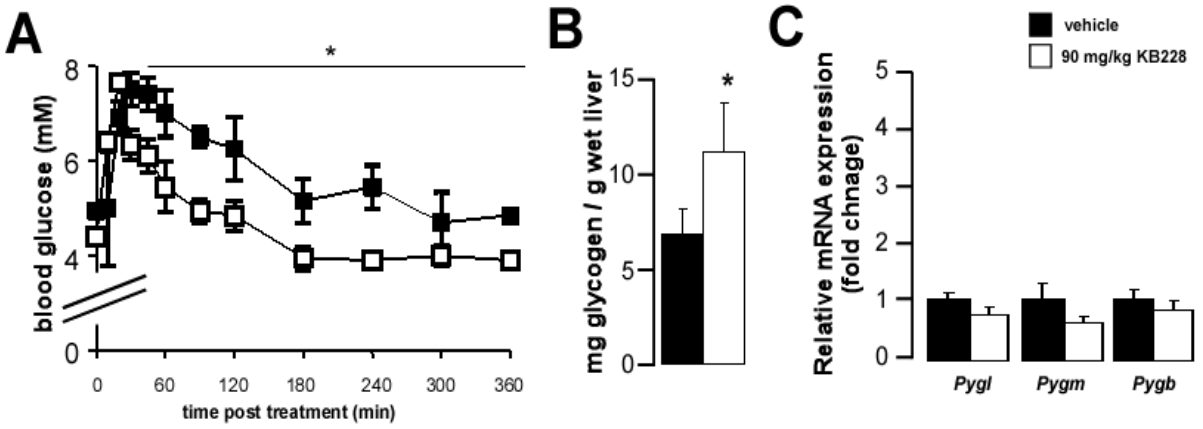

Figure 6. Characterization of the *in vivo* applicability of KB228

(A) Blood glucose levels of C57/Bl6J male mice (n=3/3, 3 months of age).

In chow-fed C57/Bl6J male mice (n=7/7, 6 months of age) **(B)** glycogen content and **(C)** mRNA expression of the liver, brain and muscle isoforms of GP (*Pygl*, *Pygm* and *Pygb*, respectively) were determined.

After 3 months of HFD, mice received 1 injections of KB228 weekly on 5 consecutive weeks. KB228 treatment increased hepatic glycogen content (**Fig. 7A**). Furthermore, we observed the induction of brain isotype GP (*Pygb*) in contrast to chow-fed mice (**Fig. 7B**).

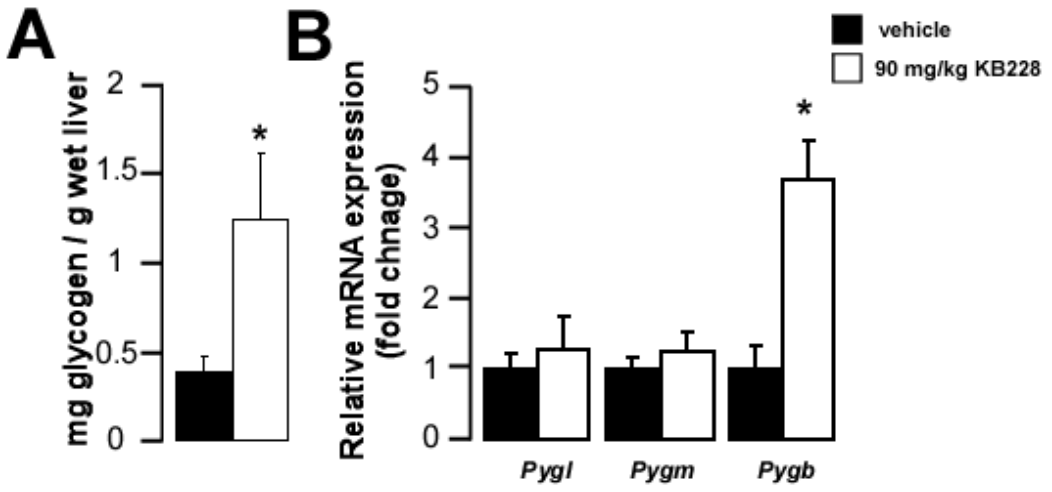

Figure 7. Characterization of the applicability of KB228 in HFD-fed mice

(A) Glycogen content and **(B)** expression of GP isoforms were determined in HFD-fed (n = 9/9) C57/Bl6J male mice (6 months of age).

5.2. Effect of KB228 on energy balance

We performed indirect calorimetry experiments on chow- and HFD-fed C57/Bl6J mice. Surprisingly, KB228 treatment enhanced oxygen consumption both in chow and HFD-fed mice (**Fig. 8A**). Moreover, KB228 slightly induced the RQ in chow-fed mice, too (**Fig. 8B**).

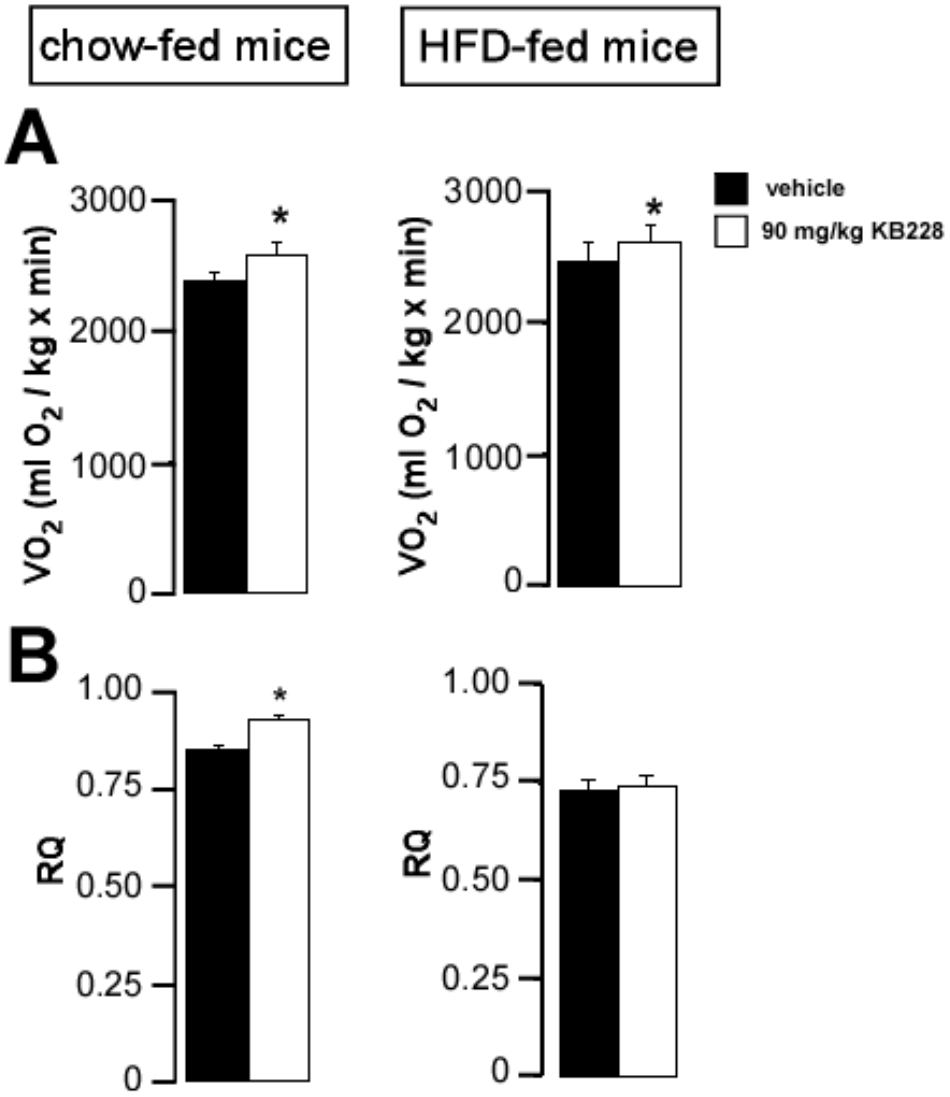

Figure 8. The impact of KB228 on *in vivo* glucose metabolism

Impact of KB228 on VO_2 **(A)** and RQ **(B)** in chow-fed (n = 7/7) and HFD-fed mice (n = 9/9), 6 months of age.

In line with these data, KB228-treatment improved glucose tolerance both in chow- and HFD-fed mice (**Fig. 9A, B**). However, the improvement of glucose disposal was less pronounced in HFD-fed mice as compared to the chow-fed animals and increases in RQ was abrogated in HFD-fed mice suggesting a lower potency of KB228 in hyperglycaemic mice.

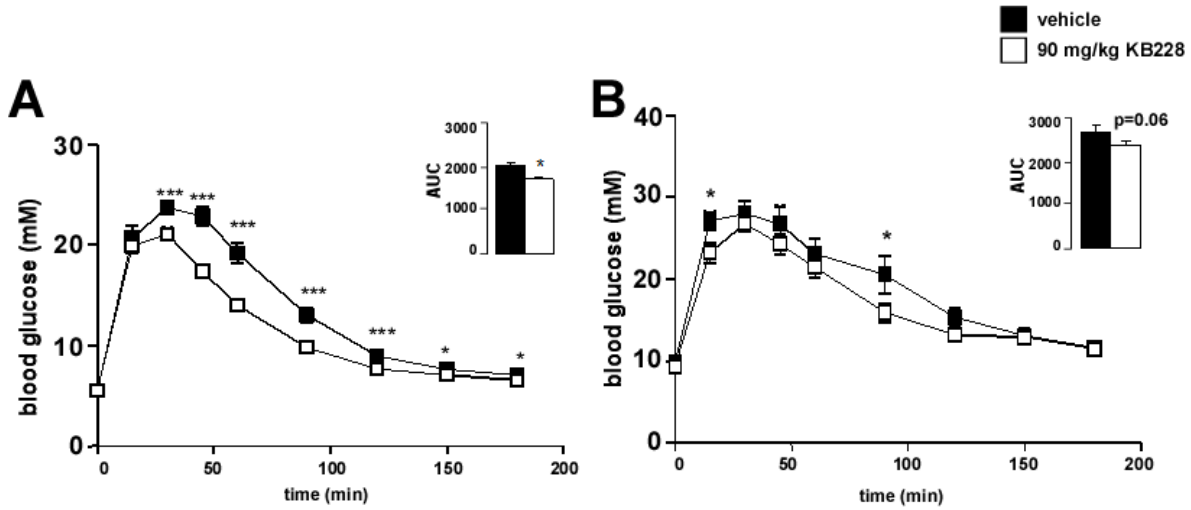

Figure 9. The effect of KB228 on glucose tolerance *in vivo*

(A) Chow-fed (n = 7/7) and **(B)** HFD-fed (n = 9/9) C57/Bl6J male mice (6 months of age) underwent vehicle or KB228 treatment, then they were subjected to ipGTT. The adjacent bar graph represents the average area under the curve (AUC).

In glucose uptake assays, liver was the only organ out of those assessed in which glucose excursion was significantly enhanced by KB228 (**Fig. 10**).

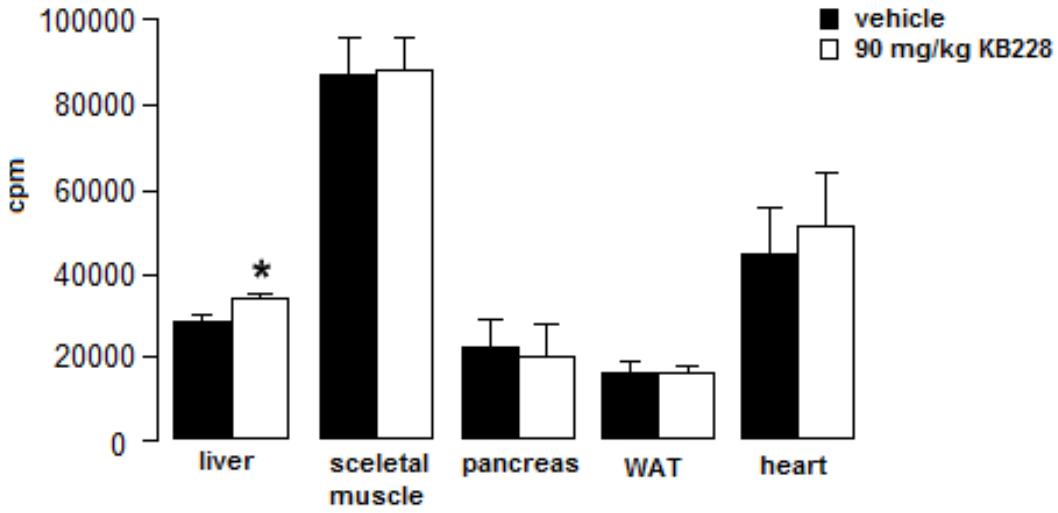

Figure 10. The effect of KB228 on glucose excursion *in vivo*

Chow-fed C57/Bl6J male mice (n = 4/4, 6 months of age) were subjected to a glucose uptake assay.

In vivo data suggested the characteristic involvement of liver during KB228 treatment. Therefore, we performed a set of experiments on HepG2 cells under normoglycaemic and hyperglycaemic conditions (5.5 mM vs. 25 mM glucose in the medium, respectively). The expression of GP isoforms were unaltered or tended to decrease **(Fig. 11A)**. Glycogen build-up was induced upon KB228 treatment in both under normo- and hyperglycemia **(Fig. 11B)**.

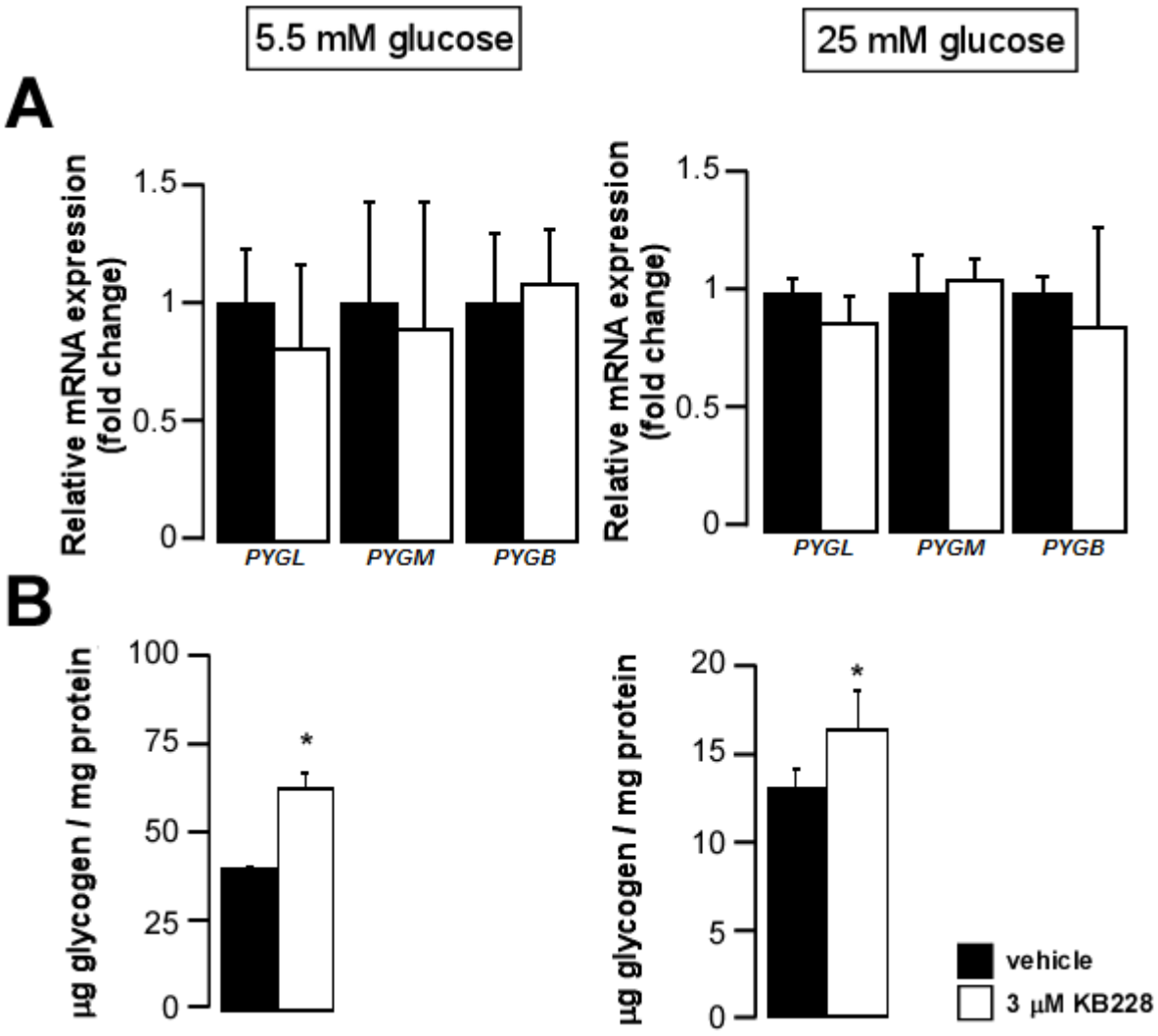

Figure 11. KB228 as an effective GP inhibitor in HepG2 cells

(A) Expression of GP isoforms (*Pygl*, *Pygm* and *Pygb*, respectively) and **(B)** glycogen content of HepG2 cells in normoglycemic and hyperglycemic conditions.

The administration of KB228 to HepG2 cells enhanced mitochondrial oxidation under normoglycaemia (**Fig. 12A**). Treatments under hyperglycaemia exerted negligible effects on mitochondrial oxidation (**Fig. 12B**) similarly to the *in vivo* experiments.

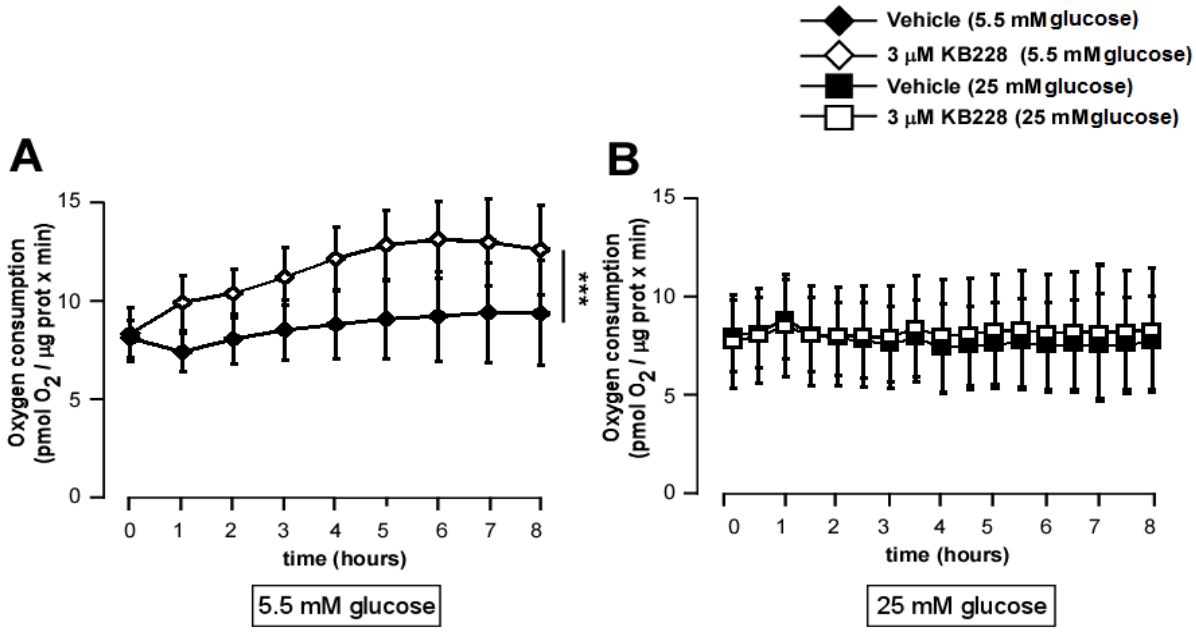

Figure 12. Effect of KB228 treatment on *in vitro* mitochondrial oxidation

OCR in HepG2 cells (n = 47/47) under normoglycemic **(A)** and hyperglycemic conditions **(B)**. Error is given as ± SD.

5.3. KB228 treatment induces UCP2 expression

Upon assessing the gene expression profile of HepG2 cells, among more than 105 genes only the expression of uncoupling protein-2 (UCP2) was induced. UCP2 mRNA and protein levels were induced by KB228 treatment in a time-dependent manner (**Fig. 13**). The induction of UCP2 mRNA and protein levels were not as pronounced in hyperglycaemic conditions as in normoglycaemia.

Following the time-dependent studies in HepG2 cells, 8-hour KB228 treatment was performed for *in vitro* studies hereinafter.

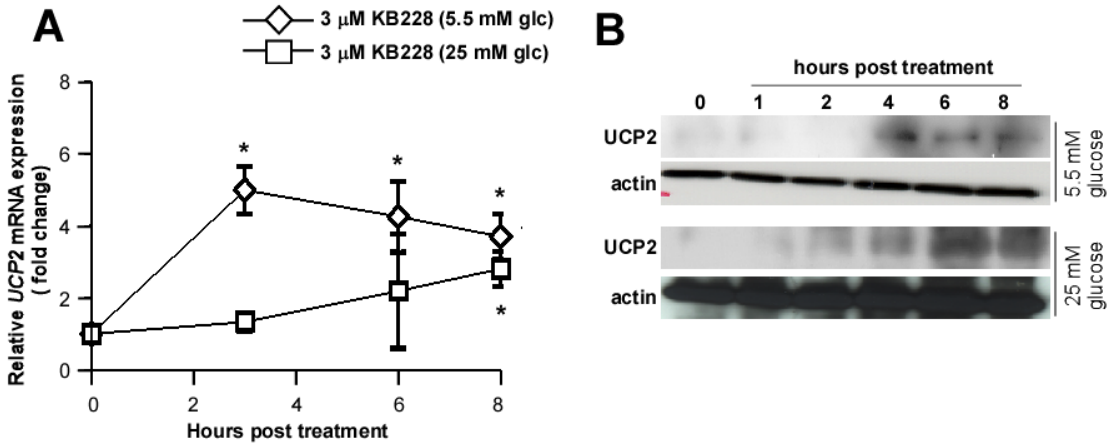

Figure 13. *In vitro* UCP2 induction by KB228 in HepG2 cells

UCP2 mRNA **(A)** and protein expression **(B)** in HepG2 cells (n = 4/4) under normoglycaemic hyperglycaemic conditions. Values were normalized to the vehicle group, which was considered 1.00 under both conditions. Error is given as ± SD.

Similarly to our findings in cellular models, KB228 induced expression of UCP2 at both mRNA and protein levels in livers of chow and HFD- fed mice (**Fig. 14**).

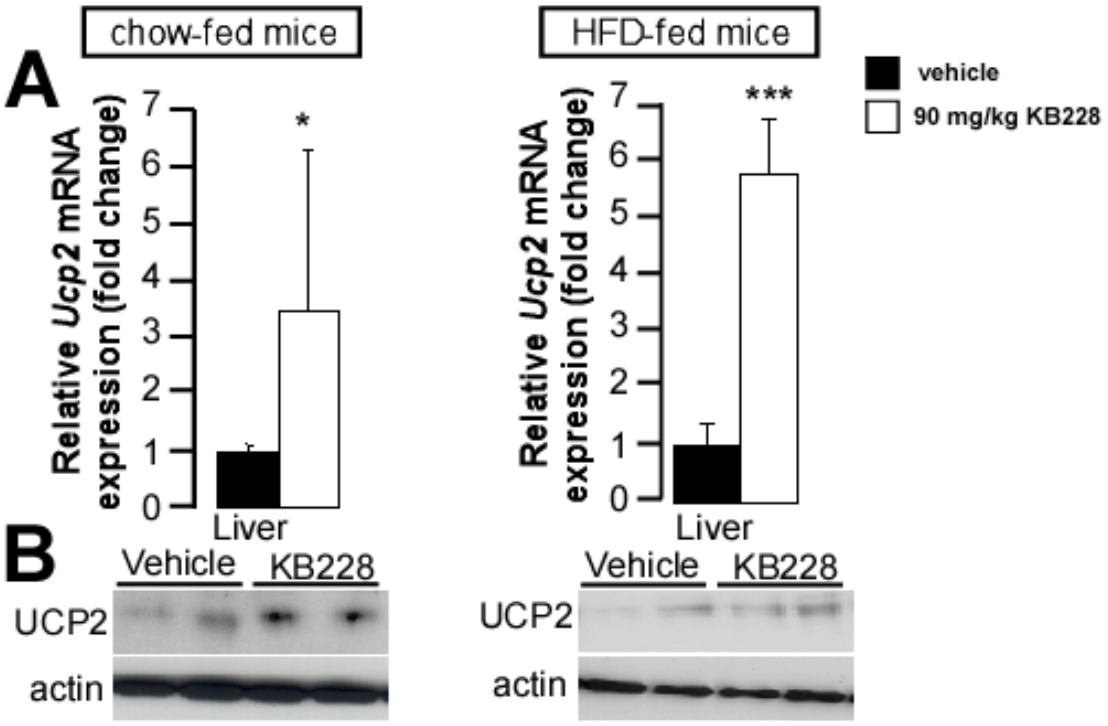

Figure 14. *In vivo* hepatic UCP2 induction by KB228

Ucp2 mRNA expression (**A**) in the livers of chow-fed (n = 7/7) and HFD-fed (n = 9/9) mice (6 months of age). Representative western blots show UCP2 protein levels (**B**) in liver homogenates of chow- and HFD-fed (n = 2/2) mice (6 months of age).

We assessed the expression of UCP2 in murine skeletal muscle samples and C2C12 cells. Although, we did not detect changes in UCP2 expression in chow-fed mice, we have observed a 2-fold induction of mRNA levels of UCP2 in HFD-fed mice (**Fig. 15A, B**). Interestingly, a much larger (6-fold) enhancement of UCP2 expression was observed in C2C 12 myoblasts (**Fig. 15C**).

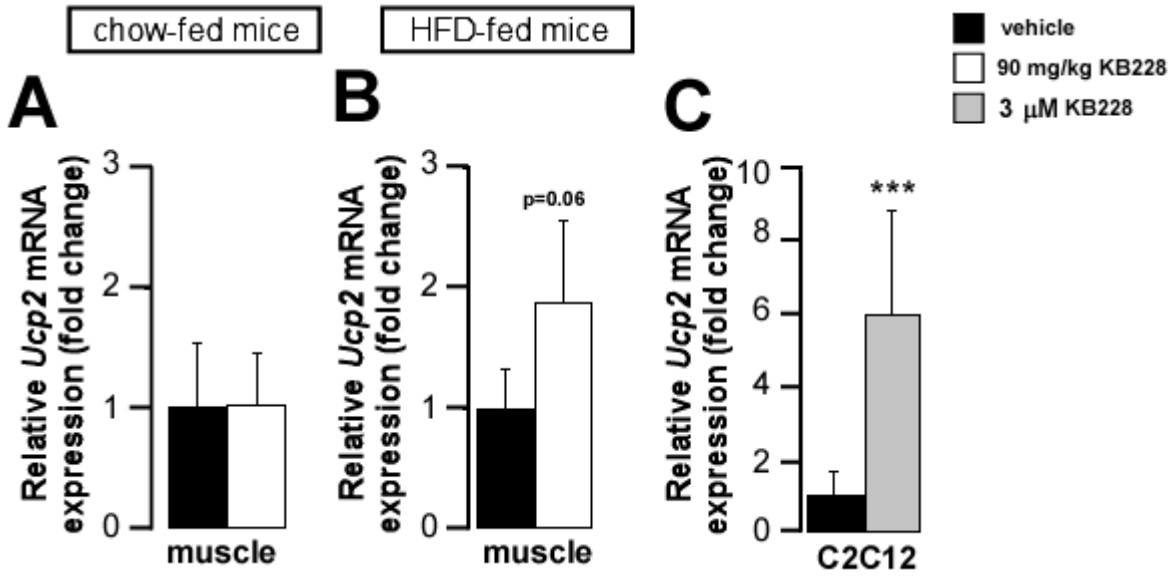

Figure 15. UCP2 induction by KB228 in striated muscle model *in vivo* and *in vitro*

Ucp2 mRNA expression were measured in gastrocnemius muscle homogenates from chow-fed (n = 7/7) **(A)** and HFD-fed (n = 9/9) mice **(B)** (6 months of age).

(C) *Ucp2* expression was determined in 8-hour KB228-treated differentiated C2C12 myoblasts.

We tested other potent GPis (TH, K_i=5.1 μM, NV50, K_i=3 μM and NV76, K_i=0.47 μM) on HepG2 cells cultured under normoglycaemic conditions (**Fig. 16**). These GPis efficiently inhibited GP activity as demonstrated by increases in the cellular glycogen content. Furthermore, the treatment of cells with these GPis led to a ~2 fold induction of UCP2 expression, similarly to KB228. These data demonstrate that the induction of UCP2 is not limited to KB228 only but can be elicited by other GP inhibitors, too. Furthermore, potency of the drugs to induce UCP2 expression correlated with their respective K_i's.

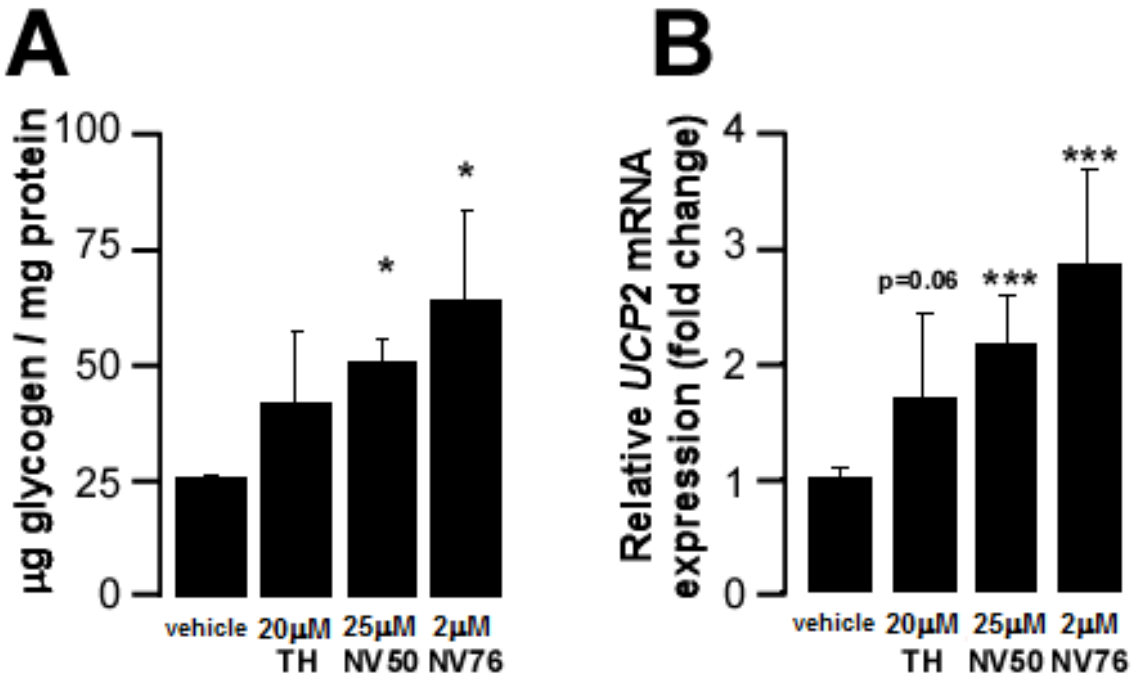

Figure 16. UCP2 induction by other GP inhibitors *in vitro*

(**A**) Glycogen content and (**B**) *UCP2* mRNA expression of HepG2 cells upon TH, NV50 and NV76 treatment for 8 hours under normoglycemic conditions. Error is given as SD throghout the figure.

5.4. KB228 treatment also induces mTORC2 activity

To assess further metabolic rearrangements triggered by KB228, we examined the activity of certain protein kinases involved in energy homeostasis, such as mTORC2 in liver. Akt2 phosphorylation on serine-473 was enhanced upon KB228 treatment both in chow-fed and HFD-fed mice despite its lowering effects on the Akt2 protein content highlighting marked activation of mTORC2 (**Fig. 17**).

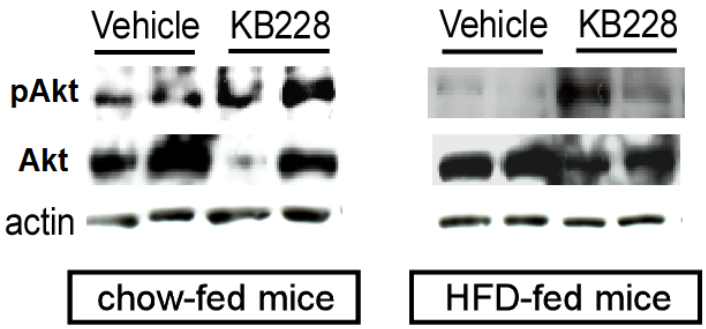

Figure 17. KB228 induced mTORC2 in mice

Akt and phospho-Akt (Ser^{473}) protein levels in liver homogenates of chow- and HFD-fed (n = 2/2) mice (6 months of age).

5.5. The presence of glycogen in pancreatic β cells

To get insight into the relevance of glycogen metabolism in β cells we investigated murine pancreas and MIN6 insulinoma cells. To confirm the existence of active glycogen metabolism and to assess the presence of glycogen granules in MIN6 cells we used confocal microscopy. Living MIN6 cells were charged with fluorescent labelled derivative of D-glucose (2NBDG) in order to incorporate it into glycogen. 2NBDG fluorescence appeared in MIN6 cells and displayed a punctate pattern in various sizes in the cytosol (**Fig. 18**).

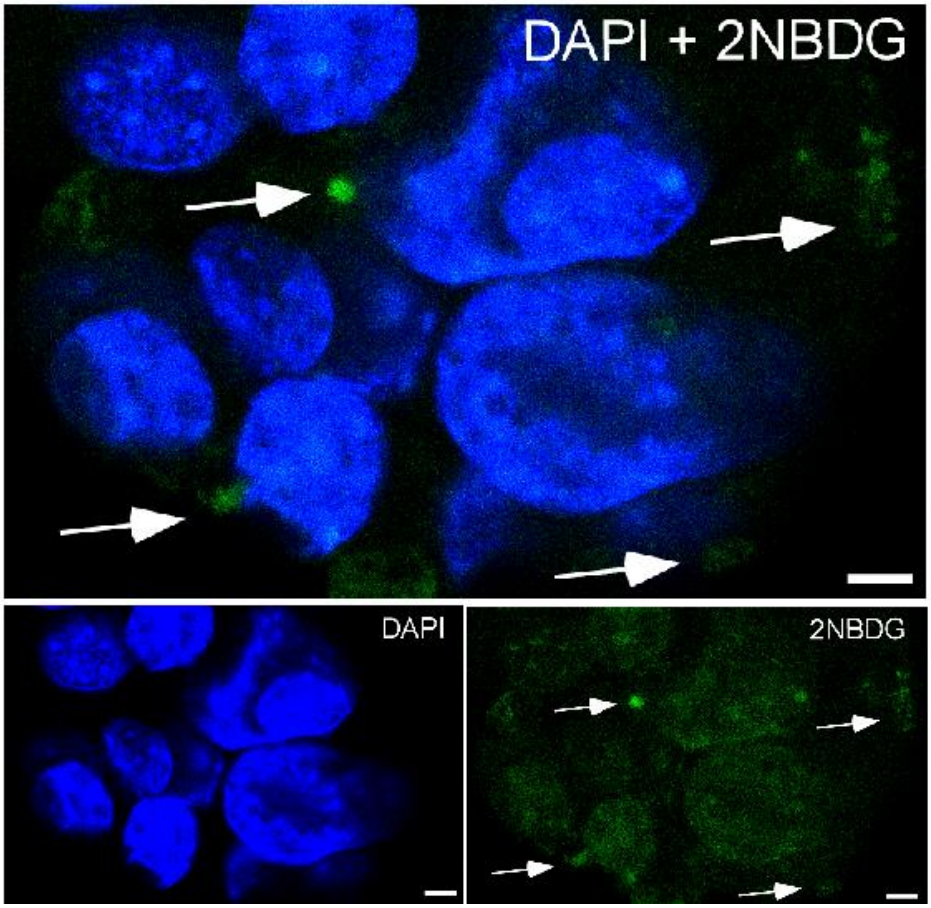

Figure 18. Detection of glycogen particles in MIN6 cells

Visualization of glycogen particles (green) in MIN6 cells. Nuclei of the cells are blue. White arrows point at representative glycogen particles in cytoplasm. Bars represent 5 μm.

MIN6 cell were treated with structurally unrelated GP inhibitors, such as glucose-based inhibitors (KB228, BEVA335) and a heterocyclic derivative (CP-316819) in concentrations close to their K_i to ensure pharmacological specificity (**Table 1.**). We assessed total glycogen content using biochemical methods. All GPis enhanced cellular glycogen content, supporting an active glycogen metabolism in MIN6 cells (**Fig. 19**).

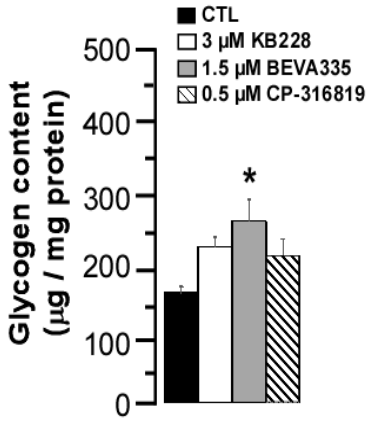

Figure 19. GP inhibition increases the glycogen content in MIN6 cells
Glycogen content of MIN6 cells (n=6) after 1 day treatment.

We investigated the effects of the KB228 administration in mice kept either on chow diet or HFD. PAS staining showed elevated glycogen content in Langerhans-islets upon KB228 treatment under both feeding regimens **(Fig. 20)**.

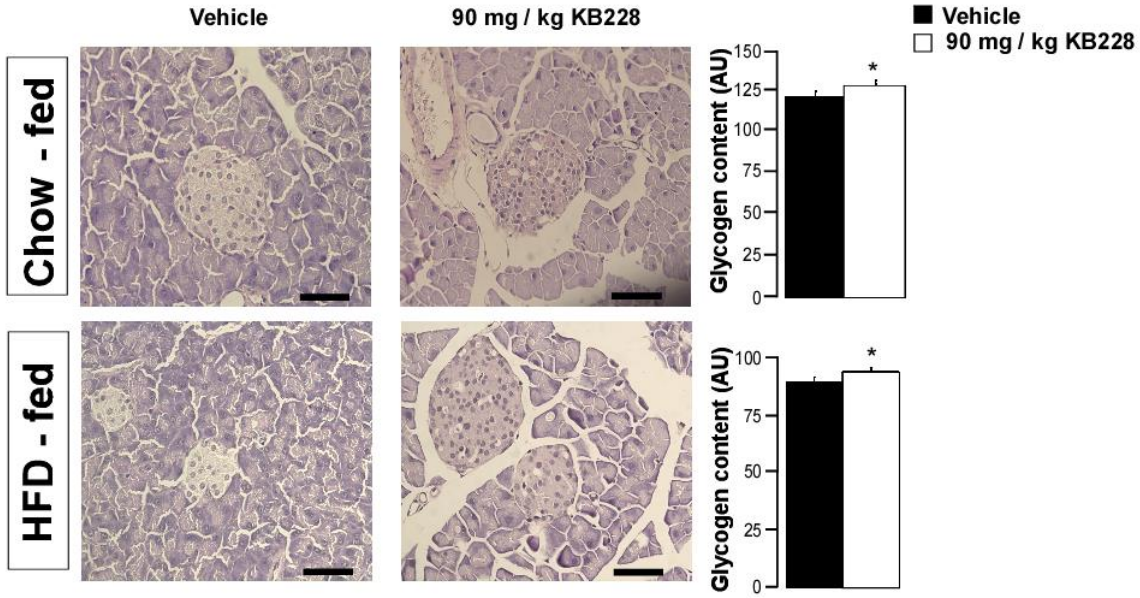

Figure 20. Effect of KB228 treatment on glycogen content in vivo
Glycogen content in the Langerhans-islets of chow- and HFD-fed C57/Bl6J mice (n = 6/6, 6 months of age). Representative images are presented (scale bar = 50µm).

We further investigated and confirmed the presence of the glycogen particles in MIN6 cells by electron microscopy (**Fig. 21**).

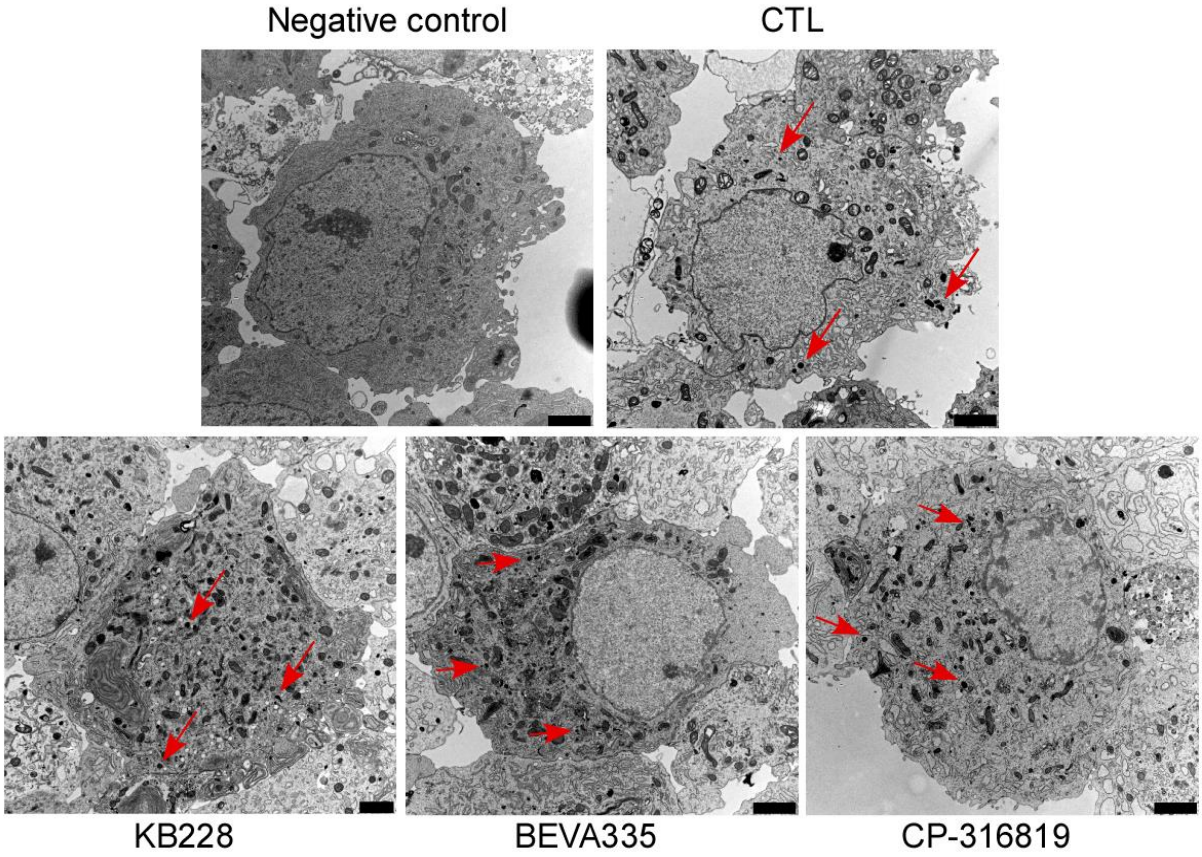

Figure 21. Glycogen particles in MIN6 cells

Glycogen particles were visualized in EM experiments. The representative EM sections are presented according to the treatment, respectively. Red arrows point to representative glycogen granules (calibration bars = 2 μm).

As a next step, we evaluated glycogen content in MIN6 cells by image analysis of electron microscopic sections. This way we were able to quantify glycogen content in cells and to approximate the size of glycogen particles. We have observed an increase in cellular glycogen content upon GP inhibition (**Fig. 22A**). In a similar fashion, the circumference of glycogen particles also increased in the presence of KB228, BEVA335 and CP-316819 (**Fig. 22B**). Taken together, the application of GPis increases cellular glycogen content and the circumference of the glycogen particles.

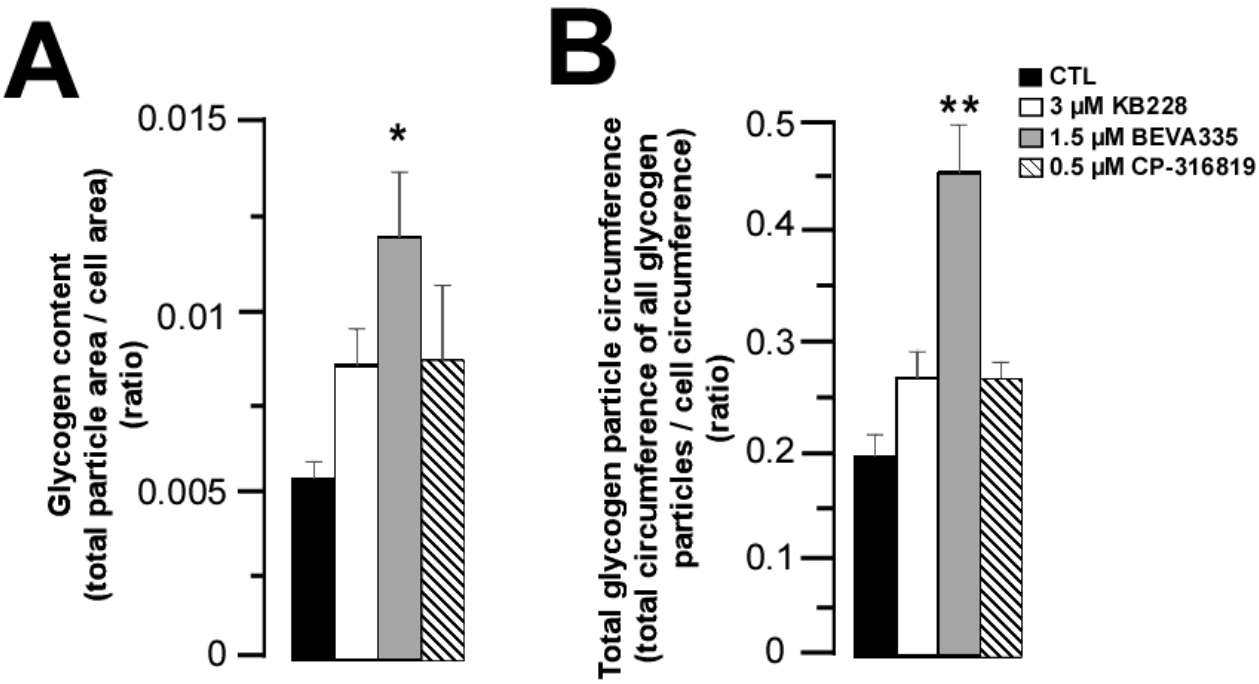

Figure 22. GP inhibition increases the glycogen content and the size of glycogen particles in MIN6 cells

Glycogen was assessed by morphometric analysis of ultrasections of ferrocyanide-reduced osmium-stained MIN6 cells after 1-day treatment. (**A**) Quantification of glycogen content in cells (n=5) and (**B**) the circumference of the total glycogen particle (total circumference of all glycogen particles / cell circumference (ratio) a proxy for particle surface) in cells (n=5) were determined on EM sections.

5.6. Assessment of the role of glycogen in MIN6 cells

To explain these data, we hypothesized that increases in glycogen content and size of glycogen granules may provide additional surface area for binding and interaction with proteins involved in the regulation of β cell function. We performed an *in silico* screen and identified more than 100 potential glycogen bound proteins (**Table 5**). Importantly, the list was dominated by members of the IR signaling pathway, mTOR and Akt were found among the bound proteins.

	All genes are human!	
PATHWAY/CATEGORY	**GENE**	**PROTEIN NAME(S)**
GLYCOGEN METABOLISM	SLC2A2	Solute carrier family 2, facilitated glucose transporter member 2 (Glucose transporter type 2, liver) (GLUT-2)
	GYG2	Glycogenin-2 (GN-2) (GN2) (EC 2.4.1.186)
	GYG1	Glycogenin-1 (GN-1) (GN1) (EC 2.4.1.186)
	TRIM7	Tripartite motif-containing protein 7 (Glycogenin-interacting protein) (RING finger protein 90)
	UGP1	UTP--glucose-1-phosphate uridylyltransferase (EC 2.7.7.9)
	GYS1	Glycogen [starch] synthase, muscle (EC 2.4.1.11)
	GYS2	Glycogen [starch] synthase, liver (EC 2.4.1.11)
	GBE1	1,4-alpha-glucan-branching enzyme (EC 2.4.1.18) (Brancher enzyme)
	PYGL	Alpha-1,4 glucan phosphorylase (EC 2.4.1.1)
	PYGB	Alpha-1,4 glucan phosphorylase (EC 2.4.1.1) (Fragment)
	PYGM	Glycogen phosphorylase, muscle form (EC 2.4.1.1) (Myophosphorylase)
	SI	Sucrase-isomaltase, intestinal [Cleaved into: Sucrase (EC 3.2.1.48)
	GAA	Lysosomal alpha-glucosidase (EC 3.2.1.20)
	AGL	Glycogen debranching enzyme (Glycogen debrancher)
	PHKA1	Phosphorylase b kinase regulatory subunit alpha, skeletal muscle isoform (Phosphorylase kinase alpha M subunit)
	PHKA2	Phosphorylase b kinase regulatory subunit alpha, liver isoform (Phosphorylase kinase alpha L subunit)
	PHKB	Phosphorylase b kinase regulatory subunit beta (Phosphorylase kinase subunit beta)
	PHKG1	Phosphorylase b kinase gamma catalytic chain, skeletal muscle/heart isoform
	PHKG2	Phosphorylase b kinase gamma catalytic chain, liver/testis isoform (PHK-gamma-LT) (PHK-gamma-T) (EC 2.7.11.19)
INSULIN RECEPTOR SIGNALING	INSR	Insulin receptor (IR) (EC 2.7.10.1)
	INS	Insulin
	IAPP	Islet amyloid polypeptide (Amylin) (Diabetes-associated peptide) (DAP) (Insulinoma amyloid peptide)
	IRS1	Insulin receptor substrate 1 (IRS-1)
	IRS2	Insulin receptor substrate 2 (IRS-2)
	PIK3R1	Phosphatidylinositol 3-kinase regulatory subunit alpha (PI3-kinase regulatory subunit alpha)
	INPP5K	Inositol polyphosphate 5-phosphatase K (EC 3.1.3.56)
	GSK3A	Glycogen synthase kinase-3 alpha (GSK-3 alpha) (EC 2.7.11.26)
	GSK3B	Glycogen synthase kinase-3 beta (GSK-3 beta) (EC 2.7.11.26)
	NIN	Ninein (hNinein) (Glycogen synthase kinase 3 beta-interacting protein) (GSK3B-interacting protein)
	AKT2	Protein kinase B beta (EC 2.7.11.1)
	GRB10	Growth factor receptor-bound protein 10 (GRB10 adapter protein) (Insulin receptor-binding protein Grb-IR)
	IGF1	Insulin-like growth factor I (IGF-I) (Mechano growth factor) (MGF) (Somatomedin-C)
	IGF2	Insulin-like growth factor II (IGF-II) (Somatomedin-A)
mTOR AND AMPK PATHWAY	MTOR	Serine/threonine-protein kinase mTOR (EC 2.7.11.1)
	RPS6KA3	Ribosomal protein S6 kinase alpha-3 (S6K-alpha-3) (EC 2.7.11.1)
	PRKAB1	5'-AMP-activated protein kinase subunit beta-1 (AMPK subunit beta-1) (AMPKb)
	PRKAG2	5'-AMP-activated protein kinase subunit gamma-2 (AMPK gamma2) (AMPK subunit gamma-2) (H91620p)
	PRKAG3	5'-AMP-activated protein kinase subunit gamma-3 (AMPK gamma3) (AMPK subunit gamma-3)
HORMONES, HORMONAL SIGNALING	PTH	Parathyroid hormone (PTH) (Parathormone) (Parathyrin)
	ADIPOQ	Adiponectin
	POMC	Pro-opiomelanocortin (POMC)
	GCGR	Glucagon receptor (GL-R)
	ADRA1B	Alpha-1B adrenergic receptor (Alpha-1B adrenoreceptor) (Alpha-1B adrenoceptor)
INFLAMMATORY SIGNALING	NFATC1	Nuclear factor of activated T-cells, cytoplasmic 1 (NF-ATc1)
	NFKB1	Nuclear factor NF-kappa-B p105 subunit (DNA-binding factor KBF1)
	GLI3	Transcriptional activator GLI3 (GLI3 form of 190 kDa)
	IL6ST	Interleukin-6 receptor subunit beta
	RELA	Transcription factor p65 (Nuclear factor NF-kappa-B p65 subunit)

OTHER SIGNALING	CALM1	Calmodulin (CaM)
	DUSP13	Dual specificity protein phosphatase 13 isoform A (DUSP13A) (EC 3.1.3.16)
	DYRK1A	Dual specificity tyrosine-phosphorylation-regulated kinase 1A (EC 2.7.12.1)
	DYRK1B	Dual specificity tyrosine-phosphorylation-regulated kinase 1B (EC 2.7.12.1) (Minibrain-related kinase) (Mirk protein kinase)
	DYRK2	Dual specificity tyrosine-phosphorylation-regulated kinase 2 (EC 2.7.12.1)
	PTPRE	Receptor-type tyrosine-protein phosphatase epsilon (EC 3.1.3.48)
	PRUNE	Protein prune homolog (hPrune) (EC 3.6.1.1)
	SGK3	Serine/threonine-protein kinase Sgk3 (EC 2.7.11.1)
	SORBS1	Sorbin and SH3 domain-containing protein 1 (Ponsin) (SH3P12) (c-Cbl-associated protein) (CAP)
	STK40	SINK-homologous serine/threonine-protein kinase (Sugen kinase 495) (SgK495)
	TBK1	Serine/threonine-protein kinase TBK1 (EC 2.7.11.1)
	PPP1CA	Serine/threonine-protein phosphatase PP1-alpha catalytic subunit (PP-1A) (EC 3.1.3.16)
	PPP1R2P1	Putative protein phosphatase inhibitor 2-like protein 1 (Protein phosphatase 1, regulatory subunit 2 pseudogene 1)
	PPP1R2P3	Protein phosphatase inhibitor 2-like protein 3 (Protein phosphatase 1, regulatory subunit 2 pseudogene 3)
	PPP1R2 IPP2	Protein phosphatase inhibitor 2 (IPP-2)
	AKT1	Protein kinase B (PKB) (Protein kinase B alpha) (PKB alpha)
	PASK	PAS domain-containing serine/threonine-protein kinase (PAS-kinase) (PASKIN) (hPASK) (EC 2.7.11.1)
	AXIN1	Axin-1 (Axis inhibition protein 1) (hAxin)
	AXIN2	Axin-2 (Axin-like protein) (Axil) (Axis inhibition protein 2) (Conductin)
	PER2	Period circadian protein homolog 2 (hPER2) (Circadian clock protein PERIOD 2)
OTHER SUGAR METABOLISM	GCK	Glucokinase (EC 2.7.1.2)
	PFKM	ATP-dependent 6-phosphofructokinase, muscle type (ATP-PFK) (PFK-M) (EC 2.7.1.11)
	PGM1	Phosphoglucomutase-1 (PGM 1) (EC 5.4.2.2)
	PGM2	Phosphoglucomutase-2 (PGM 2) (EC 5.4.2.2)
	PGAM2	Phosphoglycerate mutase 2 (EC 3.1.3.13)
	PGK1	Phosphoglycerate kinase 1 (EC 2.7.2.3)
	ALDOA	Fructose-bisphosphate aldolase A (EC 4.1.2.13)
	LDHA	L-lactate dehydrogenase A chain (LDH-A) (EC 1.1.1.27)
	LDHB	L-lactate dehydrogenase B chain (LDH-B) (EC 1.1.1.27)
	ENO3	Beta-enolase (EC 4.2.1.11)
	KHK	Ketohexokinase (EC 2.7.1.3) (Hepatic fructokinase)
	G6PC3	Glucose-6-phosphatase 3 (G-6-Pase 3) (G6Pase 3) (EC 3.1.3.9)
	FBP2	Fructose-1,6-bisphosphatase isozyme 2 (FBPase 2) (EC 3.1.3.11)
	HNF1A	Hepatocyte nuclear factor 1-alpha (HNF-1-alpha) (HNF-1A)
	SLC37A4	Glucose-6-phosphate translocase (Glucose-5-phosphate transporter)
LIPID METABOLISM	APOA5	Apolipoprotein A-V (Apo-AV)
	THEM4	Acyl-coenzyme A thioesterase THEM4 (Acyl-CoA thioesterase THEM4) (EC 3.1.2.2)
	ACADM	Medium-chain specific acyl-CoA dehydrogenase, mitochondrial (MCAD) (EC 1.3.8.7)
	FASN	Fatty acid synthase (EC 2.3.1.85)
	PTGES3	Prostaglandin E synthase 3 (EC 5.3.99.3)
UREA CYCLE	CPS1	Carbamoyl-phosphate synthase [ammonia], mitochondrial (EC 6.3.4.16) (Carbamoyl-phosphate synthetase I) (CPSase I)
TRANSCRIPTION AND TRANSLATION	TCF7L2	Transcription factor 7-like 2 (HMG box transcription factor 4) (T-cell-specific transcription factor 4) (T-cell factor 4) (TCF-4) (hTCF-4)
	NR1D1	Nuclear receptor subfamily 1 group D member 1 (Rev-erbA-alpha) (V-erbA-related protein 1) (EAR-1)
	EIF2B5	Translation initiation factor eIF-2B subunit epsilon (eIF-2B GDP-GTP exchange factor subunit epsilon)
	TCF7L2	TCF7L2 protein (Transcription factor 7-like 2 (T-cell specific, HMG-box), isoform CRA_e)
PROTEIN DEGRADATION	BTRC	F-box/WD repeat-containing protein 1A (E3RSIkappaB)
	NHLRC1	E3 ubiquitin-protein ligase NHLRC1 (EC 6.3.2.-) (Malin) (NHL repeat-containing protein 1)
	UBA52	Ubiquitin-60S ribosomal protein L40 (CEP52)
	RPS27A	Ubiquitin-40S ribosomal protein S27a (Ubiquitin carboxyl extension protein 80)
	UBB	Polyubiquitin-B [Cleaved into: Ubiquitin]
	UBC	Polyubiquitin-C [Cleaved into: Ubiquitin]
CELL ADHESION, EXTRACELLULAR MATRIX	ILK	Integrin-linked protein kinase (EC 2.7.11.1)
	PCDH12	Protocadherin-12 (Vascular cadherin-2)
	LAMP2	Lysosome-associated membrane glycoprotein 2 (LAMP-2)
	MMP2	72 kDa type IV collagenase (EC 3.4.24.24) (72 kDa gelatinase) (Gelatinase A) (Matrix metalloproteinase-2)
	DPYSL3	Dihydropyrimidinase-related protein 3 (DRP-3) (Collapsin response mediator protein 4)
	MAPT	Microtubule-associated protein tau (Neurofibrillary tangle protein) (Paired helical filament-tau) (PHF-tau)
	PCDH12	Protocadherin-12 (Fragment)
	EPM2AIP1	EPM2A-interacting protein 1 (Laforin-interacting protein)
	GFPT1	Glutamine--fructose-6-phosphate aminotransferase [isomerizing] 1 (EC 2.6.1.16)
	GNMT	Glycine N-methyltransferase (EC 2.1.1.20)
	EPM2A	Laforin (EC 3.1.3.-) (EC 3.1.3.16)
	PCYT1A	Choline-phosphate cytidylyltransferase A (EC 2.7.7.15)
	HEL-S-182mP	Glycine N-methyltransferase (EC 2.1.1.20)

TUMORIGENESIS RELATED	MCL1	Induced myeloid leukemia cell differentiation protein Mcl-1 (Bcl-2-like protein 3)
	MUC1	Mucin-1 (MUC-1) (Breast carcinoma-associated antigen DF3)
	SPAG5	Sperm-associated antigen 5 (Astrin) (Deepest) (Mitotic spindle-associated protein p126) (MAP126)
OTHER	VIMP	Selenoprotein S (SelS) (VCP-interacting membrane protein)
	DKFZp686D0638	Putative uncharacterized protein DKFZp686D0638 (Fragment)
	C1QTNF2	Complement C1q tumor necrosis factor-related protein 2
	DCAF7	DDB1- and CUL4-associated factor 7 (WD repeat-containing protein 68) (WD repeat-containing protein An11 homolog)
	DNM1L	Dynamin-1-like protein (EC 3.6.5.5)
	DAB2IP	Disabled homolog 2-interacting protein (DAB2 interaction protein)
	PHLDA2	Pleckstrin homology-like domain family A member 2
	TWIST2	Twist-related protein 2 (Class A basic helix-loop-helix protein 39) (bHLHa39) (Dermis-expressed protein 1) (Dermo-1)
	GRB10	Putative uncharacterized protein GRB10 (Fragment)
	ENPP1	Ectonucleotide pyrophosphatase/phosphodiesterase family member 1 (E-NPP 1)
	SLC17A3	Sodium-dependent phosphate transport protein 4 (Na(+)/PI cotransporter 4)

Table 5. *In silico* screening for glycogen-binding proteins

The members of insulin receptor signaling pathway are highlighted by red framing.

The overrepresentation of the IR signaling pathway among the glycogen-bound proteins prompted us to assess the expression and localization of IR in MIN6 cells. We tested the localization of IRβ in untreated, intact MIN6 cells by immunofluorescence microscopy that displayed a punctate pattern, similarly to other reports of non-stimulated MIN6 cells (Shang et al., 2009; Zhang et al., 2001) (**Fig. 23**). It is also important to note that the IRβ staining was completely lost when the primary antibody was omitted during immunostaining.

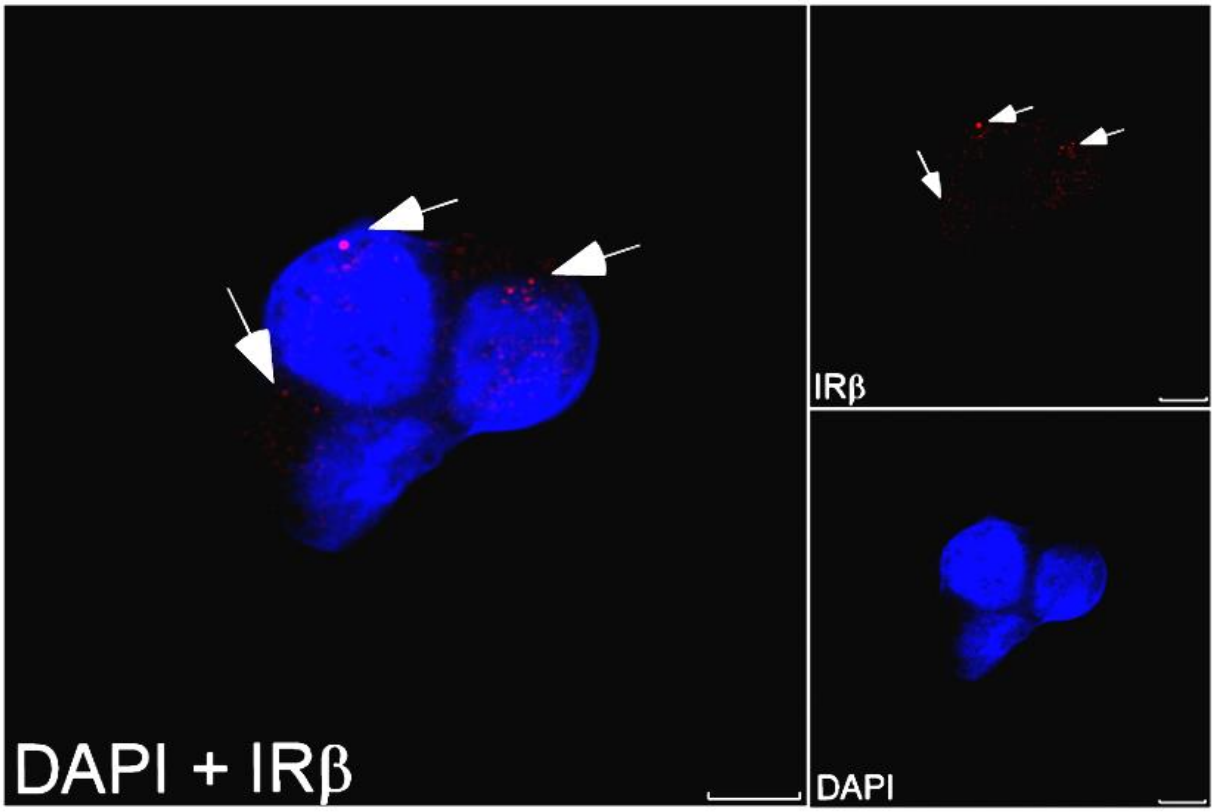

Figure 23. Detection of β subunit of insulin receptor in MIN6 cells

Nuclei of the MIN6 cells were stained using DAPI (blue). For IRβ localization IRβ primary antibody was combined with Alexa Fluor® 647 (A647) donkey anti-rabbit secondary antibody (red). In the inlay on the area marked by the arrow brightness and contrast was adjusted for the better visibility of the IRβ positive spots; the scale was not modified. Bars represent 5 μm.

We also aimed to test whether the *in silico*-detected interaction between the glycogen particles and the IR exists in cells. We found that the β subunit of the IR (IRβ) showed a colocalization with glycogen particles at the cell membrane (**Fig. 24**).

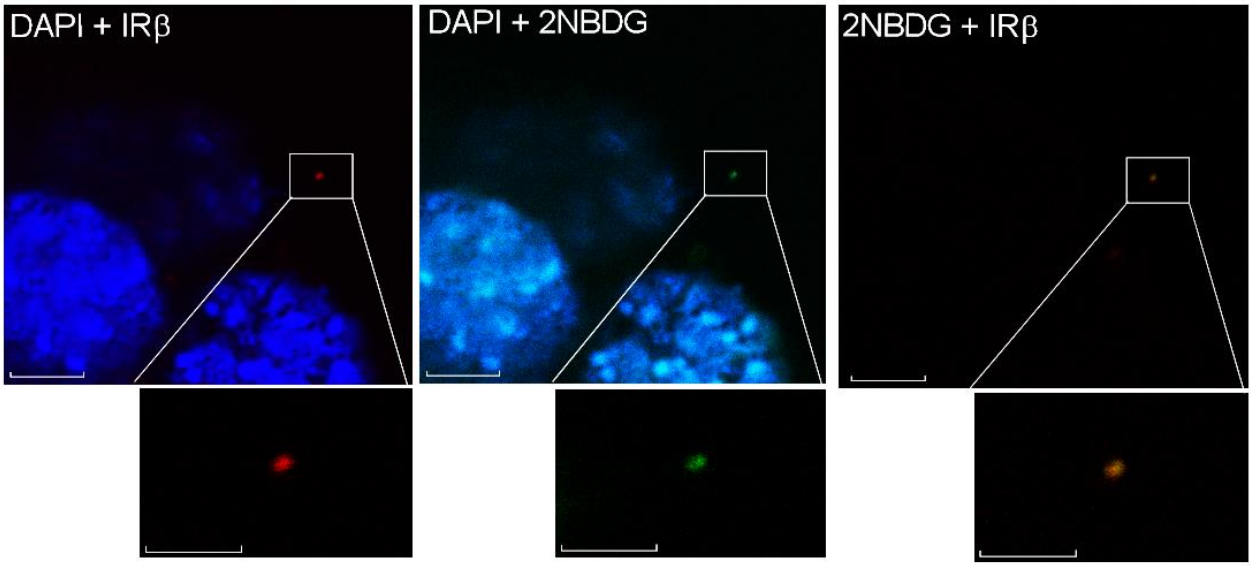

Figure 24. Colocalization of glycogen particels with β subunit of Insulin receptor
The magnified squares represent the area of interest. Glycogen was charged with a fluorescent glucose analogue (2NBDG, green), IRβ was immunostained using IRβ-specific antibody combined with Alexa Fluor 647 secondary antibody (red). Nuclei of the cells were stained using DAPI (blue). Contrast was adjusted on 2NDBG+ IRβ zoomed pictures. Bars represent 5 μm.

5.7. Glycogen phosphorylase inhibitors induce insulin receptor signaling and insulin production in MIN6 cells

In GPi-treated MIN6 cells, we have observed elevated phosphorylation of IRβ on tyrosine-1345 as compared to control cells. Downstream effectors of IRβ, such as mTORC2 and mTORC1, were also activated regarding to phosphorylation of Akt on serine-473 and of p70S6K protein on threonine-389, respectively (**Fig. 25**).

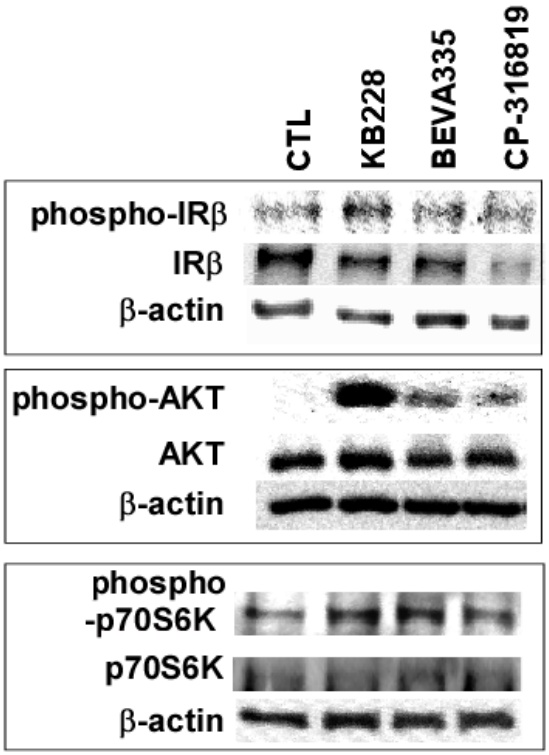

Figure 25. Phosphorylation of β subunit of insulin receptor and its downstream targets upon GPi treatment

Western blot analysis of phosphorylated and non-phosphorylated forms of proteins. MIN6 cells were treated with GPis for 1 day and the phosphorylation of IRβ on tyrosine-1345, Akt on serine-473 and p70S6K on threonine-389 were assessed.

Furthermore, we investigated the expression of PDX1, a downstream effector of IR/PI3K/Akt pathway and the master regulator of pancreatic β cell. We observed enhanced *Pdx1* promoter activity and mRNA expression upon GPi treatment that subsequently led to a large increase in PDX1 protein content both in the cytoplasmic and nuclear fraction **(Fig. 26)**.

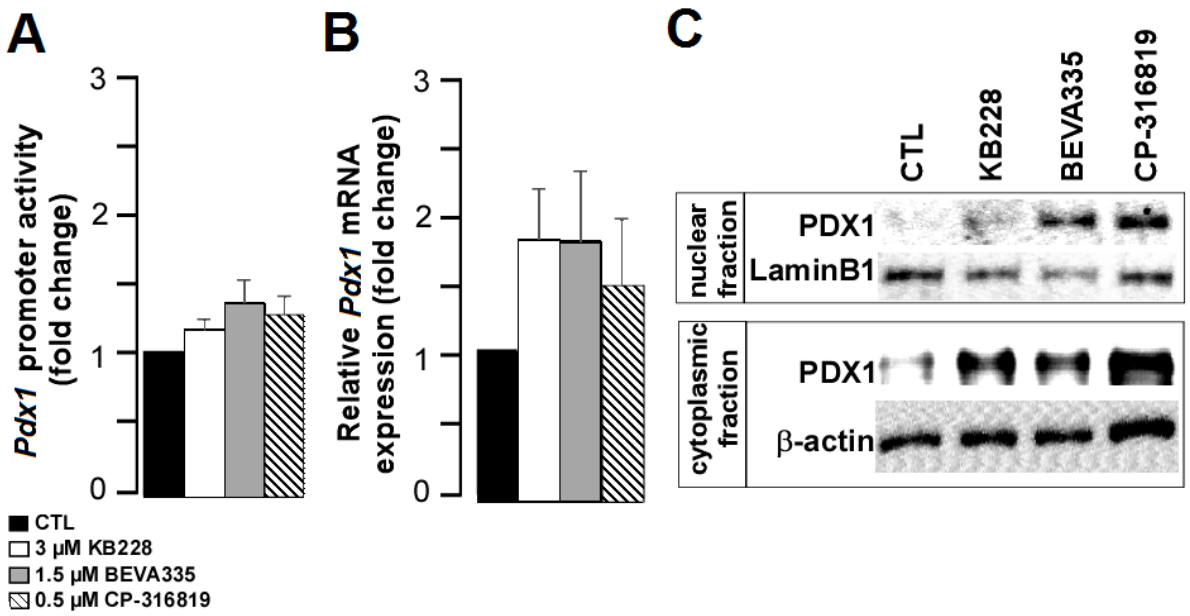

Figure 26. Inhibition of GP enzyme induce the PDX1 master regulator in MIN6 cells

In 1-day treated MIN6 cells **(A)** *Pdx1* promoter activity (n=5) and **(B)** mRNA levels (n=5) were determined. When calculating fold changes, control group was considered as 1.00. **(C)** PDX1 protein levels were determined in the nuclear and cytoplasmic fractions of MIN6 cell lysates by Western blotting.

Observing induced growth and survival signaling, we investigated the MIN6 cell proliferation and size of Langerhans islets in mice. Although the GPi treatment had no effect on MIN6 cell proliferation (data not shown), KB228 treatment resulted in a significant increase in the size of the Langerhans islets in mice kept on HFD. The size of Langerhans islet also tended to grow during KB228 treatment in chow-fed mice, however, the difference did not reach the levels of significance **(Fig. 27)**.

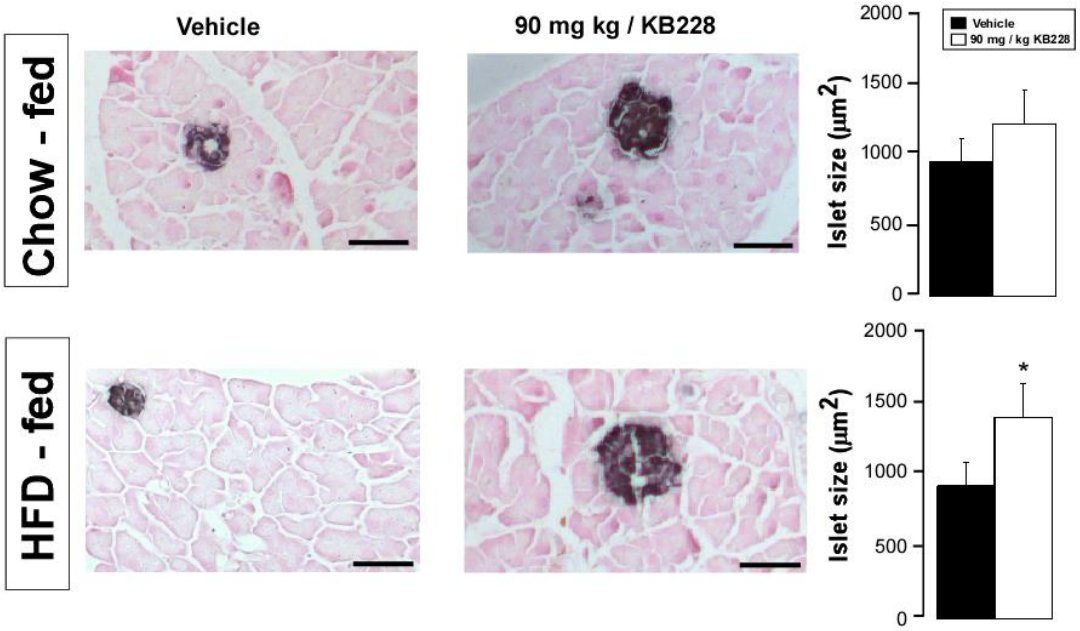

Figure 27. Change in Langerhans islet size upon KB228 treatment

The size of Langerhans islets were determined on insulin-immunostained histological sections (scale bars = 50 µm) in chow-and HFD-fed mice (n = 6/6, 6 months of age). Representative images are shown.

The next focus of our investigations was the main function of β cells, namely insulin production and secretion. Insulin expression and protein levels were enhanced upon 1-day GPi treatment (**Fig. 28A, B**). Non-stimulated insulin release also showed a tendency towards increase as well as glucose-induced insulin release in GPi-treated groups of MIN6 cells (**Fig. 28C, D**).

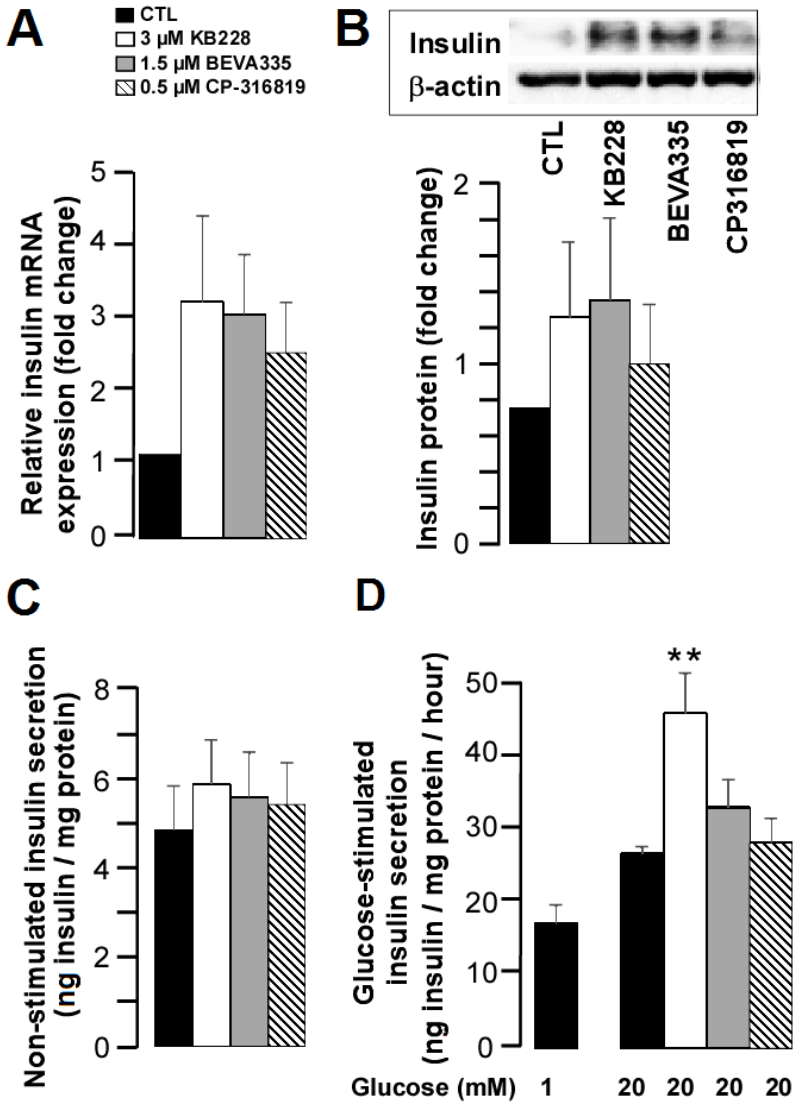

Figure 28. GP inhibition increased the expression, production and secretion of insulin in MIN6 cells

In GPi-treated MIN6 cells **(A)** insulin mRNA expression (n=5) and **(B)** the corresponding protein levels (n=5), as well as **(C)** non-glucose-stimulated (n=5) and **(D)** glucose-stimulated insulin release (n=5) were analyzed. When calculating fold changes, control group was considered as 1.00.

To verify the involvement of insulin receptor signaling in GP inhibitor-evoked biochemical changes wortmannin (WM, an inhibitor of PI3K) was used. Treatment of MIN6 cells with applying WM abolished the GPi-induced increases in mRNA and protein levels of PDX1 (**Fig. 29A, B**) and insulin (**Fig. 29C, D**), as well as insulin secretion (**Fig. 29E, F)**.

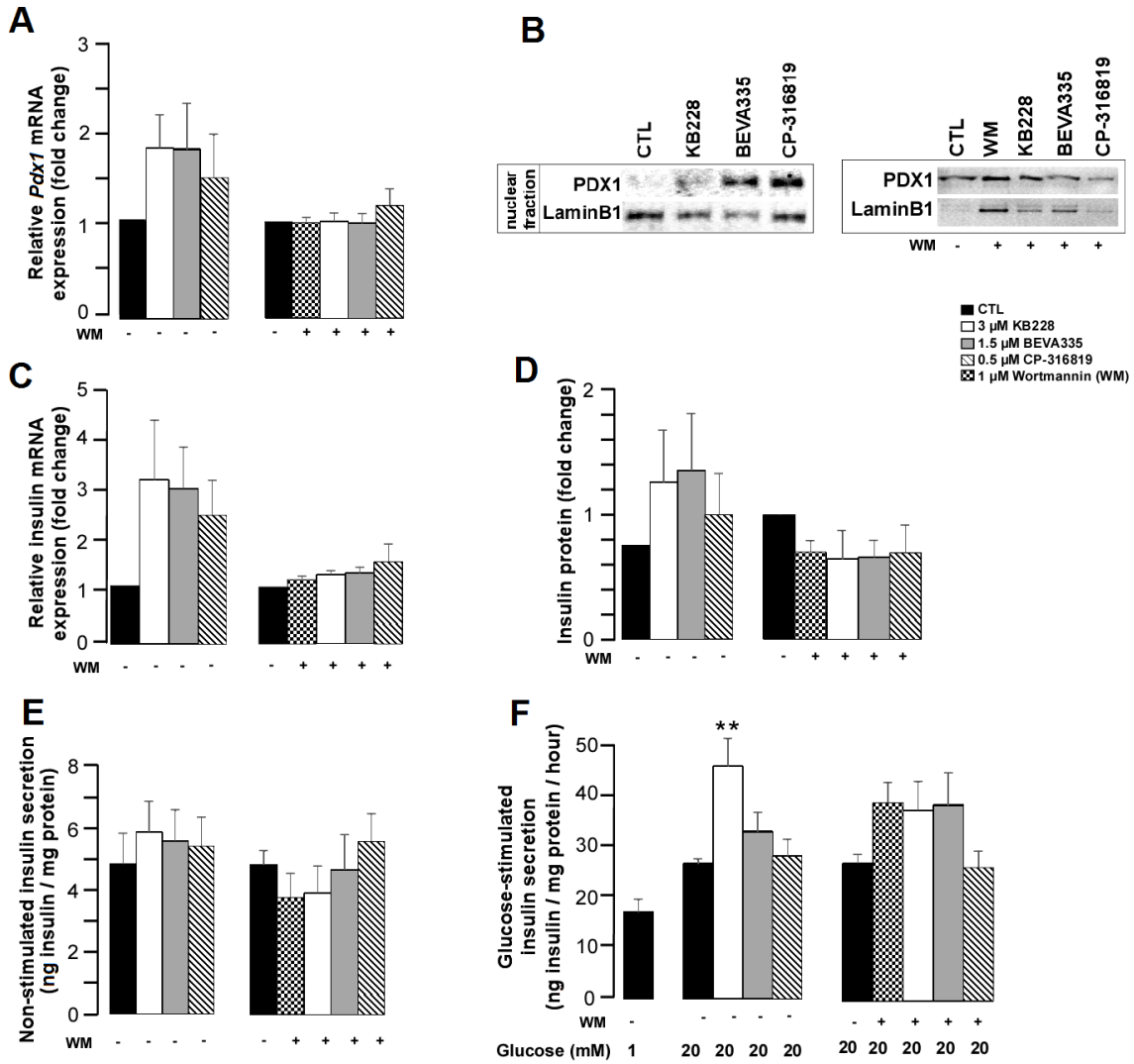

Figure 29. Inhibition of PI3K blocks GPi-induced PDX1 induction and enhancement of insulin production/secretion of MIN6 cells

MIN6 cells were treated with GP inhibitors for 1 day and a subset of these cells were treated with 1 μM WM, at last 1 hour of the GPi treatment. **(A)** *Pdx1* mRNA (n=5) and **(B)** protein (from the nuclear fractions) levels, **(C)** insulin mRNA (n=5) expression and **(D)** insulin total protein, **(E)** non-stimulated (n=5) and **(F)** glucose-stimulated insulin secretion (n=5) was assessed. When calculating fold changes, control group was considered as 1.00.

5.8. KB228 and CP-316819 improves β cell function

We next turned to investigate the effects of GP inhibition on the "classical" pathway of insulin release. Our first observation was that BEVA335 did not influence most features of the "classical" insulin secretion pathway (data not shown), therefore we omitted it from further investigations and used KB228 and CP-316819. Interestingly, the effects of KB228 and CP-316819 on the classical pathway lasted longer (2 days) than their effects on IR signaling (all experiments described in chapters **5.5. - 5.7.** were performed after 1 day of treatment). KB228 and CP-316819 GP inhibitors enhanced glycolysis (as measured by ECAR) and mitochondrial oxidation (as measured by OCR) in MIN6 cells (**Fig. 30B**).

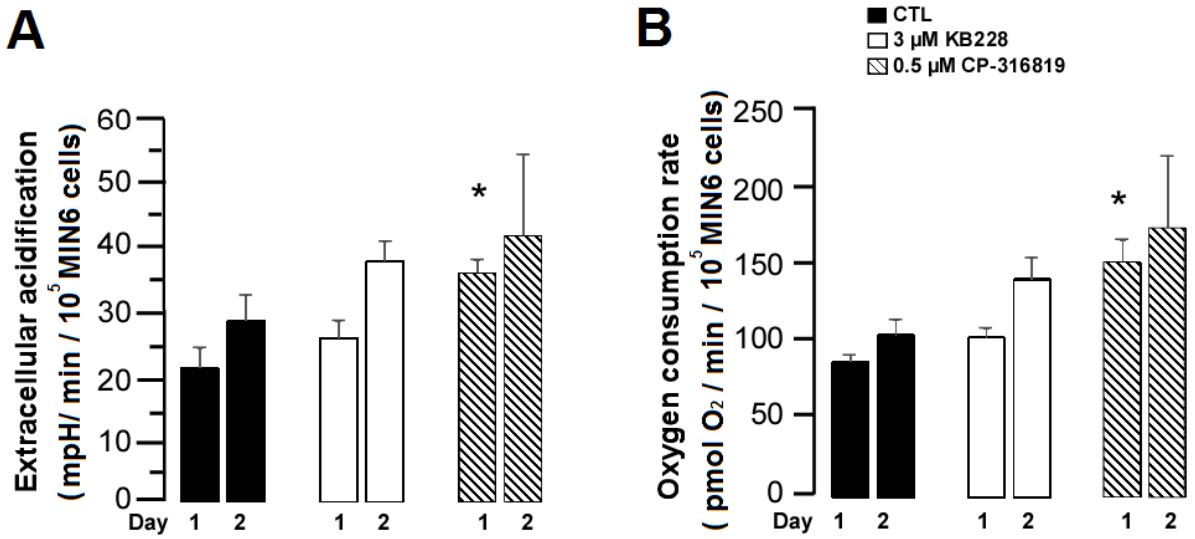

Figure 30. Enhanced glycolysis and mitochondrial oxidation in MIN6 cells upon treatment

In 1-and 2-day-treated MIN6 cells (n=7) ECAR as the result of glycolysis **(A)** and OCR as the indicator of mitochondrial respiration **(B)** were determined.

In pancreatic β cells, increased ATP levels lead to depolarization by closing the ATP-sensitive potassium channels which triggers opening of voltage-gated calcium channels. Consequently, we have observed enhanced glucose-induced calcium influx upon treatment suggesting the depolarization of MIN6 cell (**Fig. 31**).

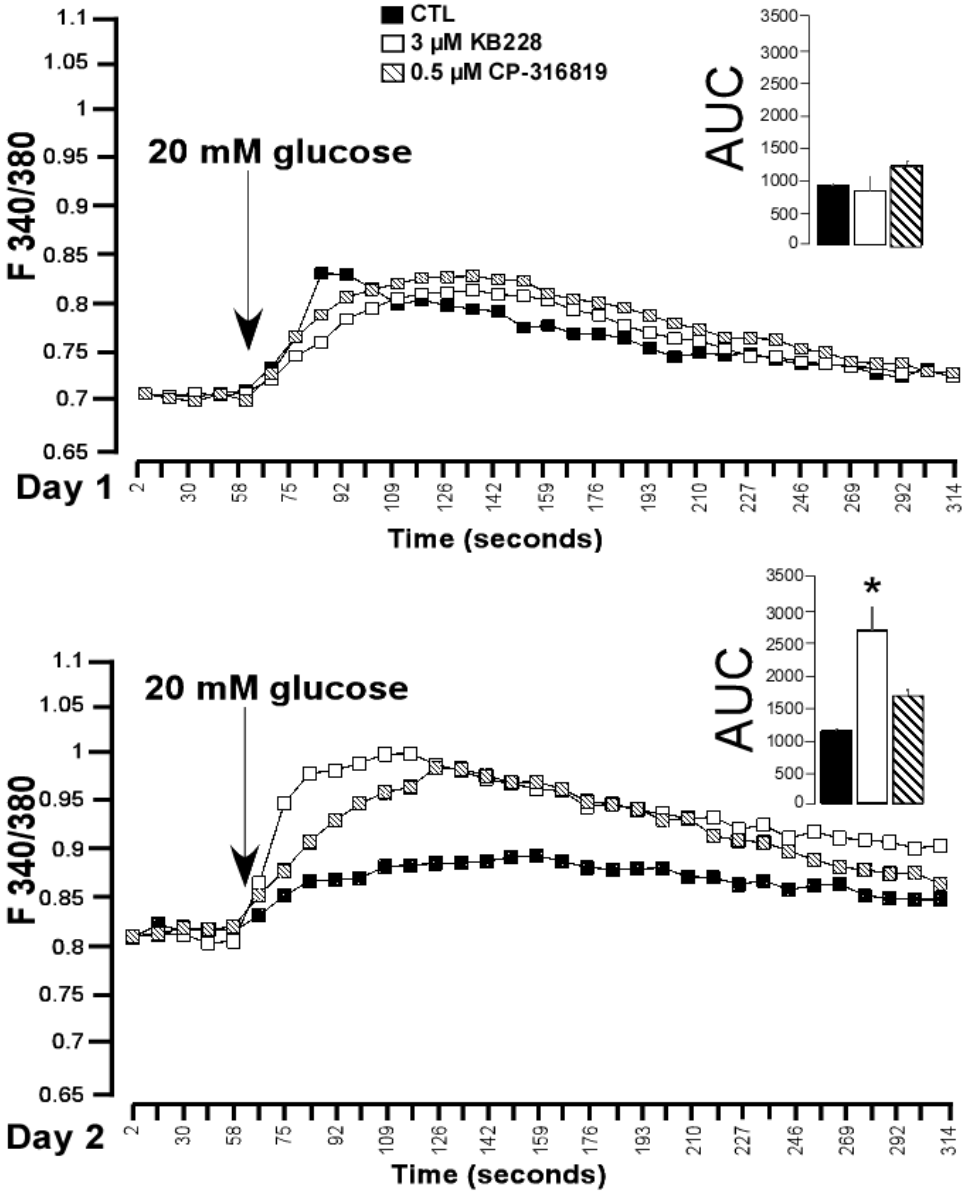

Figure 31. GP inhibition induced Ca^{2+}-influx in MIN6 cells

Calcium influx was induced by 20 mM glucose and was determined by fura-2AM staining (n=5) in MIN6 cells after **(A)** 1- and **(B)** 2-day treatment. The adjacent bar graph represents the average area under the curve (AUC).

In pancreatic β cells, Ca^{2+}-influx leads to the fusion of insulin-rich granules with the cell membrane resulting in insulin secretion. Therefore, we investigated the glucose-stimulated insulin secretion in MIN6 cells and we observed that GPi treatment enhanced insulin secretion (**Fig. 32).**

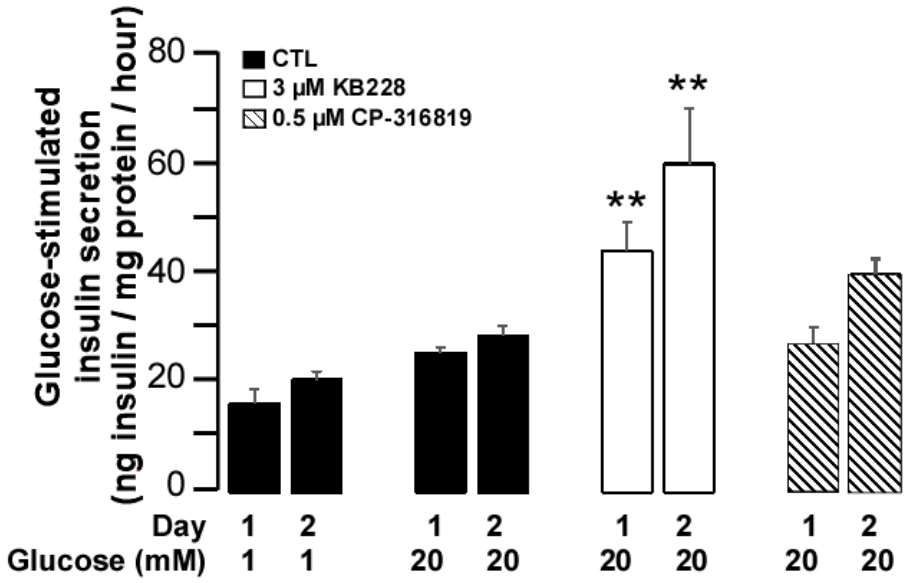

Figure 32. Increase in insulin release upon KB228- and CP-316819-treatment in MIN6 cells

Glucose-induced insulin release in MIN6 cells (n=5) after 1- and 2-day treatment.

We were curious whether the administration of KB228 has effect on insulin secretion in mice. We have observed that KB228 had a tendency to improve glucose-induced insulin release mainly in HFD-mice **(Fig. 33)**.

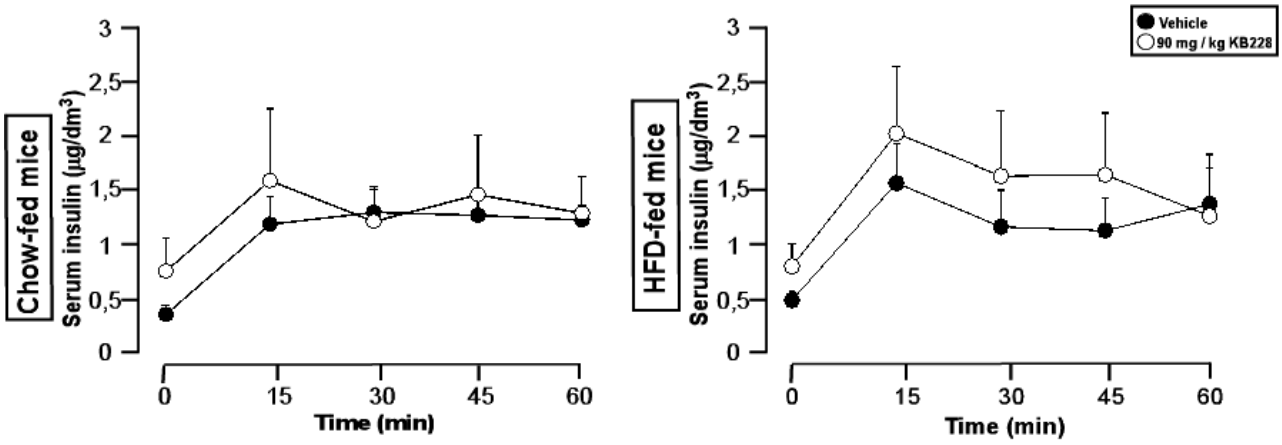

Figure 33. GPi treatment improves glucose-stimulated insulin release *in vivo*

Glucose-induced increases in serum insulin was determined in chow-and HFD-fed mice (n = 6/6, 6 months of age).

6. DISCUSSION

We characterized the metabolic effects of potent glycogen phosphorylase inhibitors. In our first study we investigated KB228, an N-(3,5-dimethyl-benzoyl)-N'-(β-D-glucopyranosyl) urea compound belonging to the efficient GP inhibitors, which displayed mixed type inhibition on purified rabbit muscle glycogen phosphorylase. Similarly to previously described observations with other GPis (Baker et al., 2006; Furukawa et al., 2005; Martin et al., 1998), KB228 increased oxygen consumption, reduced serum glucose levels and enhanced hepatic glycogen content. However, the potency of KB228 was reduced under hyperglycemic conditions. Our assumption is that KB228, which has a glucose moiety, competes with glucose for binding to the catalytic center of GP enzyme, hence high glucose levels may reduce KB228's affinity to GP. Similar observations were reported regarding other glucose analogue GPis under high glucose concentrations (Docsa et al., 2011).

Changes in the uptake of radioactive 2-deoxyglucose clearly pointed out the principle role of the liver in glucose clearance upon KB228 treatment. Nevertheless, we provided evidence for the involvement of skeletal muscle in glucose clearance that was highlighted by induction of UCP2 in murine gastrocnemius muscle and in C2C12 cells. Our data are consistent with the phenotype observed by Baker and co-workers (Baker et al., 2006), in which muscular oxygen consumption was elevated in GPi-treated rats, although the glucose uptake by muscle did not increase but decreased upon GP inhibition.

UCP2 mRNA is present in many tissues and its regulation is implemented by at both transcriptional and translational levels. UCP2 has debated evolutionary role and biological function, although the short half-life of this protein suggests its suitability for regulating rapid biologic responses (Esteves et al., 2014; Fülöp et al., 2006). Increased UCP2 expression has shown to be an adaptive response to increased fatty acid β-oxidation and ROS production that occurs during obesity (Fülöp et al., 2006; Pheiffer et al., 2016). Furthermore, evidences also suggest the beneficial role of UCP2, such as promoting mitochondrial respiration, reducing ROS production and fatty acid accumulation, that might contribute to its anti-steatotic and anti-inflammatory effects (Horimoto et al., 2004; Zhou et al., 2012). In our view, the UCP2 induction might help to understand the metabolic rearrangements generated by KB228-induced GP inhibition in mice. Under hyperglycemic conditions, excess glucose and fatty acid influx contributes to production of mitochondrial free radicals by obstructing the mitochondrial electron transport chain (ETC) (Zahr et al., 2007). UCP2 is able to mediate proton leaks across the mitochondrial inner membrane in mammalian cells and uncouples fuel

oxidation from ATP synthesis. Therefore, UCP2 keep the membrane potential sufficiently low via abolishing high proton gradients built across the inner membrane to minimize superoxide production (Baffy et al., 2002; Horimoto et al., 2004). Mitochondrial dysfunction - including reduction of fatty acid oxidation, lower expression of genes involved in oxidative activity, as well as decrease or blockade of ETC function - has been described in the development of metabolic syndrome, such as T2DM (Albert and Hall, 2015). It is presumable that the upregulated UCP2 by KB228 treatment may release the blockade of ETC by channeling excess proton load to the matrix thereby protecting cells from oxidative stress. Hence, GP inhibition not only enhanced glucose uptake and mitochondrial oxidation but it contributed to the elimination of oxidative damage through UCP2 induction.

Several GPis were designed and tested for the treatment of T2DM (Burgess, 2015; Henke, 2012; Treadway et al., 2001). Former studies demonstrated that pharmacological GP inhibition improves hyperglycaemia in animal models of diabetes, although long term application was reported to have adverse effects characterized by hepatic lipid and glycogen accumulation symptoms, characteristic of glycogen storage diseases (Burgess, 2015; Gu et al., 2011). The induction of mitochondrial oxidation or UCP2 activation may be beneficial over these adverse effects that could be exploited to counteract hepatic glycogen and lipid accumulation upon prolonged GP inhibition. We uncovered another molecular event induced by KB228, the induction of mTORC2 activity. mTOR signaling is associated with numerous metabolic disorders such as obesity, diabetes, and cancer (Albert and Hall, 2015; Malley and Pidgeon, 2016; Pópulo et al., 2012). mTORC2 functions as a key activator of protein kinases, including PKB (Akt), that act downstream of insulin and growth factor signaling. Studies with liver-specific *rictor* knockout (LiRiKO) mice demonstrated the functional importance of hepatic mTORC2 in the regulation of glucose and lipid homeostasis via insulin-induced Akt signaling (**Fig. 34**). LiRiKO mice displayed loss of Akt phosphorylation on serine-473 and reduced glucokinase activity, leading to constitutive gluconeogenesis and impaired glycolysis. These liver-specific defects consequently induced systemic hyperglycemia and hyperinsulinemia, featuring glucose intolerance and insulin resistance (Hagiwara et al., 2012; Yuan et al., 2012). Other studies revealed that chronic administration of the mTOR inhibitor rapamycin dramatically worsened the metabolic syndrome in T2DM (Deblon et al., 2012; Fraenkel et al., 2008). Long-term application of rapamycin substantially impaired glucose tolerance and insulin action by disrupting not only mTORC1 but mTORC2 as well, which in turn obstructed insulin-mediated suppression of hepatic gluconeogenesis (Lamming et al., 2012; Yin et al., 2016).

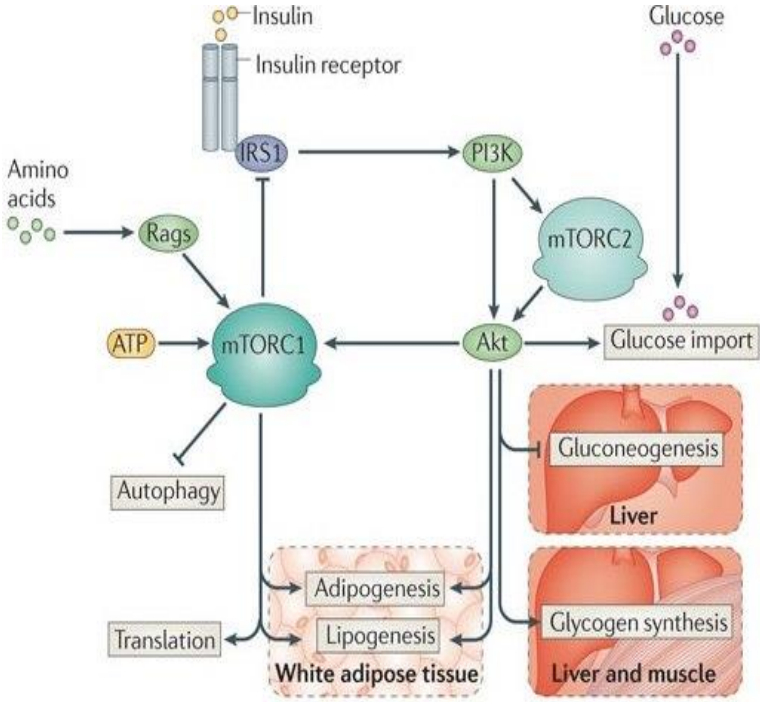

Figure 34. Physiological activation of mTOR
Activation of mTOR by insulin and growth factors is mediated by PI3K/AKT pathway, while mTORC1/ S6K signaling generates a negative-feedback loop augmenting IRS (Fraenkel et al., 2008). mTORC1 activates anabolism, such as transcription and translation, ribosome biogenesis, lipid synthesis, nucleotide biosynthesis, and nutrient uptake, while inhibiting catabolic processes such as autophagy (Albert and Hall, 2015). mTORC2 induces glucose import and promotes glycogen synthesis, but inhibits hepatic gluconeogenesis (Zoncu et al., 2011).

How KB228 treatment leads to mTORC2 activation in liver is yet unknown, but it could be explained by alterations in insulin signaling. Alternatively, glucose influx could simply rearrange mTOR signaling, whereby cells sense glucose plenitude and turn towards storage. The activation of mTORC2, or more importantly, of mTORC1 induction by GP inhibition was observed in pancreatic β cell model, MIN6 cell. KB228, BEVA335 and CP-316819 treatment induced the insulin receptor signaling, which was shown in mTORC2, Akt and mTORC1 activation. KB228 and BEVA335 proved to be more effective in this regard, however, in almost all respects, the effects of the reference inhibitor CP-316819 were far behind the KB228 or even BEVA335. Several studies confirmed the concept that mTORC1 is critical for β cell expansion, cell growth, proliferation and regeneration (Fraenkel et al., 2008; Liu et al., 2009a; Niclauss et al., 2011; Nir et al., 2007; Zahr et al., 2007), as well as for β cell adaptation to hyperglycemia and insulin resistance (Fraenkel et al., 2008). The mTORC2 pathway could be linked indirectly to β cell proliferation and insulin secretion through Akt activation (Gu et al., 2011) . In line with that, GP inhibition induced Akt and PDX1 in MIN6 cells, which are known to be survival and growth signals (Elghazi and Bernal-Mizrachi, 2009; Fujimoto and Polonsky, 2009). Enhanced growth and survival signaling may explain the increase in size of Langerhans islets in mice upon KB228 treatment.

The major goal in diabetes research is to find ways to improve the regeneration and function of insulin secreting pancreatic β cells to prevent and/or delay diabetes (Kulkarni et al., 2012). We suggest that not only the liver and skeletal muscle are targeted by GP inhibition, but pancreatic β cells, too. Our data point out the beneficial effects of mild

increases in the glycogen content of β cells and demonstrate that GP inhibitors have positive impact on β cell function. The pro-proliferative effects of GPis, however, raise safety concerns. Although confirmatory studies do not exist, there are studies that assessed the effects of GPis on cancer cell proliferation. Two studies (Favaro et al., 2012; Lee et al., 2004) showed that GPis are anti-proliferative in pancreatic adenocarcinoma cells and other tumor cells as well, suggesting that GPis may have a cytostatic effect on cancer cells. Our results demonstrate that, although KB228 increased to a small extent but significantly the size of the islets of Langerhans in mice, we were unable to detect even a little change in the proliferation of MIN6 insulinoma cells under KB228, BEVA335 and CP-316819 treatment for several days (1-14 days). It must be stated, however, that long-term carcinogenesis studies will be required if GPis enter clinical application. In our investigations, beyond the proliferative effects, insulin transcription and translation were induced by GP inhibition in β cells, which was further evidenced by elevated non-stimulated insulin secretion. Here, I have to note that the induction of PDX1 and mTORC1 greatly contribute to these processes (Albert and Hall, 2015; Kaneto and Matsuoka, 2015).

GPi-induced biochemical modifications involve several downstream targets of insulin signaling and within that, the elements of IR-PI3K cascade in MIN6 cells. GP inhibition mildly induced IR activity, furthermore, we have evidenced the involvement of PI3K by using its specific inhibitor, WM. Inhibition of PI3K blunted GPi-induced PDX1 and insulin expression, as well as non-stimulated insulin secretion.

Another hallmark of GP inhibition was the increased glucose-induced insulin secretion. Here, we showed that KB228 and CP-316819 induced glycolysis, mitochondrial oxidation and glucose-induced calcium transients. During the study CP-316819 induced significant changes only in case of glycolysis and mitochondrial activity in MIN6 cells after 1-day treatment. But the expected consequences, including enhanced Ca^{2+}-influx and glucose-induced insulin release, were absent. Surprisingly, BEVA335 did not influence most features of the "classical" insulin secretion pathway that has resulted in its exclusion from these experiments with MIN6 cells. Glucose-induced insulin release was significantly enhanced *in vitro*, while the *in vivo* experiments did not yield significant elevation of serum insulin levels, however, tendency is promising for the future. Presumably, further adjustment of KB228 formulation and dosing are indispensable in the future. We cannot explain how GPis induce glucose-stimulated insulin release in MIN6 cells, although in current study and the results of others (Baker et al., 2006) reported the induction of mitochondrial oxidation by GP inhibition. Along these lines, it would be an easy explanation that IR signaling can enhance

mitochondrial oxidation (Cheng et al., 2010; Liu et al., 2009b) and consequently glucose-induced insulin release. However, the activation of the insulin secretion cascade lasted longer (up to 2 days of treatment) than the induction of IR signaling (up to 1 day of treatment), suggesting the involvement of other, yet unknown, pathway(s). Furthermore, PI3K inhibition only modestly reduced GPi-mediated increases in glucose-induced insulin release, suggesting again additional mechanism(s).

Several studies emphasize the physiological role of glycogen in pancreatic β cells (Doherty and Malaisse, 2001; Graf and Tolken, 1984; Hellman and Idahl, 1969; Malaisse, 2016), although there are many contradictions. Earlier studies (Malaisse et al., 1993; Malaisse et al., 1977) suggest that glycogen breakdown provides glucose for glycolysis and mitochondrial oxidation in β cells under starvation and thereby facilitates insulin release. However, chronic exposure of β cells to high concentrations of glucose, as in diabetes, provokes accumulation of glycogen in islet cells by inhibiting glycogenolysis, which did not appear to adversely affect the utilization of glucose resulting in a paradoxical decrease in glycolytic rate. Therefore, under hyperglycemia, glycogen accumulation in β cells may lead to glucotoxicity (Malaisse, 2016; Malaisse et al., 1992). However, latest research by Mir-Coll et al. provided controversial results by showing that glycogen accumulation alone is not sufficient to trigger dysfunction, apoptosis and progression to diabetes in β cells, and anyway, glycogen metabolism is not required for the maintenance of β cell function (Mir-Coll et al., 2016). We cannot provide a well-established interpretation for these apparent discrepancies. Nevertheless, GPi-induced increases in glycogen is likely lower in our study than in others (Malaisse et al., 1992) that may obstruct different pathways. Similar differences in glycogen accumulation may account for the lack of glucotoxicity in our models (Malaisse et al., 1992).

Until now, glycogen was considered as a glucose reserve, while we suggest an additional structural role for glycogen, as its particles with their increased surface area may contribute to the induction of IR signaling. Either glycogen itself may induce IRβ autophosphorylation, or, more likely, glycogen may serve as a scaffold for the members of the IR signaling cascade (**Fig. 35**), as suggested by the *in silico* screen for glycogen-binding proteins. Other large cellular polymers, such as poly(ADP-ribose) (Bai, 2015; Tartier et al., 2003) or fuzzy proteins (Fuxreiter, 2012; Sharma et al., 2015), were shown to act as interactive surfaces for large protein complexes in a similar fashion as we suggest here for glycogen.

In summary, our data highlight that structurally different GPis exert more effects than a simple inhibition of catalytic activity. As for the liver, our data show that glycogen metabolism interacts with mTORC2 signaling and mitochondrial function suggesting that GP might be involved in a complex metabolic regulatory network, which could be exploited in diabetes management. With regard to pancreatic β cells, we showed that the pharmacological inhibition of GP and the consequent increase in cellular glycogen content was associated with induction of the insulin signaling pathway, β cell proliferation, and glucose-induced insulin release. These data raise the possibility of repurposing GP inhibitors from the original indication as agents to inhibit hepatic glucose output in T2DM to a new indication that is the improvement of β cell function in the context T2DM. However, GPi clinical studies were halted after phase II, though the reasons were not communicated (Henke, 2012). Our experiments suggest that infrequent or low dose-administration of the GPis can target metabolic regulatory pathways without promoting the typical adverse effects of GP inhibition, such as hypoglycemia or glycogen storage disorder. Moreover, well-designed efficacy studies are also a must to show the later onset of T2DM upon the application of GPis.

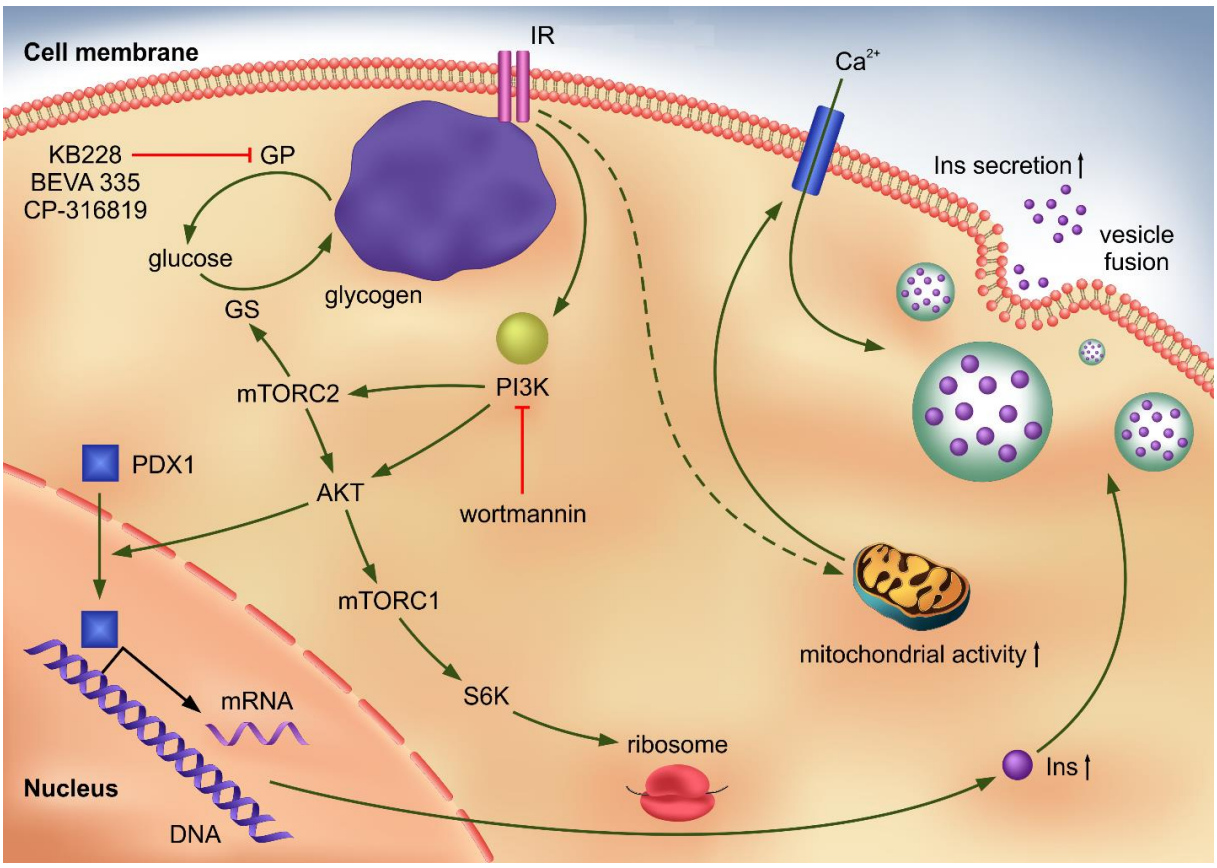

Figure 35. A possible mechanism of action of the GP inhibition in pancreatic β cells

Inhibition of glycogen phosphorylase (GP) results in an increase in size of glycogen particles, which may provide additional surface area for binding and interaction with proteins, involved in insulin receptor (IR) signaling. IR indirectly induces PI3K activation, consequently stimulating mTORC2 and mTOC1 pathways. mTORC2 can contribute to glycogen synthesis, while mTORC1 participates in the stimulation of protein translation, including insulin translation. Akt is responsible for the PDX1 translocation to nucleus thereby activating the expression of several genes, especially insulin gene. IR signaling cascade may enhance mitochondrial activity contributing to the insulin release.

7. SUMMARY

Glycogen phosphorylase, engaged in the regulation of glycogen metabolism, has a major role in hepatic glucose production. Therefore, glycogen phosphorylase has become a validated target to modulate glucose levels in type 2 diabetes mellitus and pharmacological glycogen phosphorylase inhibitors are considered as potential antidiabetic agents.

KB228, a glucose analogue glycogen phosphorylase inhibitor, was tested *in vitro* and *in vivo* under normal and hyperglycaemic conditions on two major glycogen stores, liver and skeletal muscle. KB228 enhanced hepatic glycogen content *in vivo* that coincided with significantly increased glucose excursion to the liver. KB228 affected the energy balance as well by enhancing oxygen consumption and improving glucose tolerance in mice. However, changes were smaller in high-fat diet-fed mice as compared to the chow-fed animals, probably because high glucose levels, which may reduce the potency of KB228. *In vitro* studies on HepG2 hepatocytes presented KB228-induced mitochondrial activity, which was paralleled by an increase in UCP2 mRNA and protein levels. The unexpected induction of UCP2 was detected in murine liver and skeletal muscle, as well as C2C12 cells, suggesting the involvement of skeletal muscle in increased glucose oxidation upon KB228 treatment. To further assess metabolic rearrangements triggered by KB228 we investigated certain signaling pathways involved in insulin action and energy homeostasis. We detected induced mTORC2 activity, which modulating hepatic glucose production and glycolysis, as well as inducing glycogen storage and glucose import, may improve diabetes.

We also tested whether glycogen phosphorylase inhibition affects β cells *in vivo* and *in vitro* using KB228 and another glucose-based glycogen phosphorylase inhibitor BEVA335, and the structurally different CP-316819. Increased glycogen content led to elevated surface of glycogen particles. Glycogen phosphorylase inhibition induced IR/PI3K/Akt signaling cascade. We also showed that IRβ co-localized with glycogen particles, and components of IR signaling were identified as glycogen-bound proteins. Glycogen phosphorylase inhibition also induced glucose-stimulated insulin secretion marked by enhanced glycolysis, mitochondrial oxidation, and calcium signaling. Finally, glycogen phosphorylase inhibitor treatment increased the size of the islets of Langerhans.

Taken together these data, we conclude that glycogen phosphorylase might be involved in a complex metabolic regulatory network in the liver, the skeletal muscle and even in the β cells that could be exploited in the management of diabetes.

7. ÖSSZEFOGLALÁS

A glikogén anyagcsere szabályozásában fontos glikogén foszforiláz enzimnek nagy szerepe van a máj glükóz termelésének szabályozásában, így a 2-es típusú cukorbetegség kezelésének egyik potenciális célpontja.

A KB228 jelű glükóz analóg GF inhibitor *in vivo* és *in vitro* vizsgálatát végeztük normál és hiperglikémiás körülmények között. A KB228 kezelés hatására növekedett a máj glikogén mennyisége *in vivo*, ami összefüggésben van a máj glükóz felvételének szignifikáns növekedésével. A normál és magas zsírtartalmú diétán tartott (HFD) egerek glikogén foszforiláz inhibitorral történő kezelése az oxigénfogyasztás emelkedéséhez és a glükóz tolerancia javulásához vezetett. Megjegyzendő, hogy a változás mértéke kisebb volt az elhízott egereknél, ami feltehetőleg azzal magyarázható, hogy a KB228 glükóz motívuma verseng a glükózzal a glikogén foszforiláz enzimhez való kapcsolódásért, így magasabb cukorszint esetén csökken a glikogén foszforiláz inhibitor hatékonysága. HepG2 sejtekkel végzett kísérletek során a KB228 kezelés fokozta a mitokondriális aktivitást és az UCP2 expressziót. Az UCP2 indukciója az egerek májában, sőt harántcsíkolt izomszövetében és C2C12 mioblaszt sejtekben is kimutatható volt, ami a vázizom KB228-indukált fokozott glükóz oxidációban való részvételére utal. További kutatásunk tárgya a metabolikus változások hátterében álló jelátviteli útvonalak feltérképezése volt, melynek során kimutattuk az mTORC2 aktiválódását glikogén foszforiláz gátlás hatására, mely hozzájárulhat a máj glükóz termelésének csökkentéséhez, a glükózfelvétel és a glikogén raktározás fokozásához, ezáltal javítva a diabéteszes állapoton.

Egy másik kísérletsorozatban a glikogén foszforiláz gátlás hatásait vizsgáltuk β sejteken *in vivo* és *in vitro*. A KB228 mellett egy szintén glükóz analóg BEVA335 jelű, és egy strukturálisan eltérő CP-31819 GF inhibitort is alkalmaztunk. A glikogén foszforiláz gátlása során a β sejtek modelljeként használt MIN6 sejtekben lévő glikogén mennyisége, valamint a glikogén szemcsék felszíne is növekedett. Az inhibitorok alkalmazása aktiválta az IR/PI3K/Akt jelátviteli útvonalat, amit a PI3K specifikus gátlásával is igazoltunk. Emellett észleltük az IRβ glikogén szemcsékkel való kolokalizációját, valamint azonosítottuk az IR jelátviteli útvonal résztvevőit, mint glikogén-kapcsolt fehérjéket. A glikogén foszforiláz inhibitorok növelték a glükóz-indukált inzulin felszabadulást, valamint növelték a Langerhans szigetek méretét.

Eredményeink alapján a glikogén foszforiláz enzim komplex szabályozó folyamatok részét képezi, mely a jövőben felhasználható a cukorbetegség kezelésében.

8. REFERENCES

Abdul-Ghani, M.A., and DeFronzo, R.A. (2010). Pathogenesis of insulin resistance in skeletal muscle. J. Biomed. Biotechnol. *2010*, 476279.

Adeva-Andany, M.M., Gonzalez-Lucan, M., Donapetry-Garcia, C., Fernandez-Fernandez, C., and Ameneiros-Rodriguez, E. (2016). Glycogen metabolism in humans. BBA clinical *5*, 85-100.

Agius, L. (2007). New hepatic targets for glycaemic control in diabetes. Best Pract. Res. Clin. Endocrinol. Metab. *21*, 587-605.

Aikin, R., Hanley, S., Maysinger, D., Lipsett, M., Castellarin, M., Paraskevas, S., and Rosenberg, L. (2006). Autocrine insulin action activates Akt and increases survival of isolated human islets. Diabetologia *49*, 2900-2909.

Albert, V., and Hall, M.N. (2015). mTOR signaling in cellular and organismal energetics. Curr. Opin. Cell. Biol. *33*, 55-66.

American Diabetes Association (2010). Diagnosis and Classification of Diabetes Mellitus. Diabetes Care *33*, S62-S69.

Andreux, P.A., Houtkooper, R.H., and Auwerx, J. (2013). Pharmacological approaches to restore mitochondrial function. Nat. Rev. Drug Discov. *12*, 465-483.

Aspinwall, C.A., Lakey, J.R., and Kennedy, R.T. (1999). Insulin-stimulated insulin secretion in single pancreatic beta cells. J. Biol. Chem. *274*, 6360-6365.

Babata, L.K., Pedrosa, M.M., Garcia, R.F., Peicher, M.V., and de Godoi, V.A. (2014). Sustained liver glucose release in response to adrenaline can improve hypoglycaemic episodes in rats under food restriction subjected to acute exercise. Int. J. Endocrinol. *2014*, 969137.

Baffy, G., Zhang, C.Y., Glickman, J.N., and Lowell, B.B. (2002). Obesity-related fatty liver is unchanged in mice deficient for mitochondrial uncoupling protein 2. Hepatology *35*, 753-761.

Bai, P. (2015). Biology of poly(adp-ribose) polymerases: the factotums of cell maintenance. Mol. Cell. *58*, 947-958.

Baker, D.J., Greenhaff, P.L., MacInnes, A., and Timmons, J.A. (2006). The experimental type 2 diabetes therapy glycogen phosphorylase inhibition can impair aerobic muscle function during prolonged contraction. Diabetes *55*, 1855-1861.

Baker, D.J., Timmons, J.A., and Greenhaff, P.L. (2005). Glycogen phosphorylase inhibition in type 2 diabetes therapy: a systematic evaluation of metabolic and functional effects in rat skeletal muscle. Diabetes *54*, 2453-2459.

Bendayan, M., Londono, I., Kemp, B.E., Hardie, G.D., Ruderman, N., and Prentki, M. (2009). Association of AMP-activated protein kinase subunits with glycogen particles as revealed in situ by immunoelectron microscopy. J. Histochem. Cytochem. *57*, 963-971.

Berg, J.M., Tymoczko, J.L., and Stryer, L. (2002). Biochemistry. New York, USA: W. H. Freeman and Company.

Bergeron, J.J., Di Guglielmo, G.M., Dahan, S., Dominguez, M., and Posner, B.I. (2016). Spatial and temporal regulation of receptor tyrosine kinase activation and intracellular signal transduction. Annu. Rev. Biochem. *85*, 573-597.

Berman, H.K., O'Doherty, R.M., Anderson, P., and Newgard, C.B. (1998). Overexpression of protein targeting to glycogen (PTG) in rat hepatocytes causes profound activation of glycogen synthesis independent of normal hormone- and substrate-mediated regulatory mechanisms. J. Biol. Chem. *273*, 26421-26425.

Best, C.H., and Haist, R.E. (1941). The effect of insulin administration on the insulin content of the pancreas. J. Physiol. *100*, 142-146.

Bokor, E., Kun, S., Docsa, T., Gergely, P., and Somsák, L. (2015). 4(5)-aryl-2-c-glucopyranosyl-imidazoles as new nanomolar glucose analogue inhibitors of glycogen phosphorylase. ACS Med. Chem. Lett. *6*, 1215-1219.

Boucher, J., Kleinridders, A., and Kahn, C.R. (2014). Insulin receptor signaling in normal and insulin-resistant states. Cold Spring Harb. Perspect Biol. *6*, a009191.

Bouillaud, F. (2009). UCP2, not a physiologically relevant uncoupler but a glucose sparing switch impacting ROS production and glucose sensing. Biochim. Biophys. Acta *1787*, 377-383.

Brun, T., and Maechler, P. (2016). Beta-cell mitochondrial carriers and the diabetogenic stress response. Biochim. Biophys. Acta *1863*, 2540-2549.

Burgess, S.C. (2015). Regulation of glucose metabolism in liver. In International Textbook of Diabetes Mellitus. R.A. DeFronzo, E. Ferrannini, P. Zimmet, and K. George Alberti (Ed.). New Jersey: John Wiley & Sons, Ltd.

Cerf, M.E. (2013). Beta cell dysfunction and insulin resistance. Front. Endocrinol. *4*, 37.

Chang, L., Chiang, S.H., and Saltiel, A.R. (2004). Insulin signaling and the regulation of glucose transport. Mol. Med. *10*, 65-71.

Cheng, Z., Tseng, Y., and White, M.F. (2010). Insulin signaling meets mitochondria in metabolism. Trends Endocrinol. Metab. *21*, 589-598.

Chrysina, E.D., Kosmopoulou, M.N., Tiraidis, C., Kardakaris, R., Bischler, N., Leonidas, D.D., Hadady, Z., Somsak, L., Docsa, T., Gergely, P., et al. (2005). Kinetic and crystallographic studies on 2-(beta-D-glucopyranosyl)-5-methyl-1, 3, 4-oxadiazole, -benzothiazole, and -benzimidazole, inhibitors of muscle glycogen phosphorylase b. Evidence for a new binding site. Protein Sci. *14*, 873-888.

Cohen, P. (1979). The hormonal control of glycogen metabolism in mammalian muscle by multivalent phosphorylation. Biochem. Soc. Trans. *7*, 459-480.

Crosson, S.M., Khan, A., Printen, J., Pessin, J.E., and Saltiel, A.R. (2003). PTG gene deletion causes impaired glycogen synthesis and developmental insulin resistance. J. Clin. Invest. *111*, 1423-1432.

de Luca, C., and Olefsky, J.M. (2008). Inflammation and insulin resistance. FEBS lett. *582*, 97-105.

De Vos, A., Heimberg, H., Quartier, E., Huypens, P., Bouwens, L., Pipeleers, D., and Schuit, F. (1995). Human and rat beta cells differ in glucose transporter but not in glucokinase gene expression. J. Clin. Invest. *96*, 2489-2495.

Deblon, N., Bourgoin, L., Veyrat-Durebex, C., Peyrou, M., Vinciguerra, M., Caillon, A., Maeder, C., Fournier, M., Montet, X., Rohner-Jeanrenaud, F., et al. (2012). Chronic mTOR inhibition by rapamycin induces muscle insulin resistance despite weight loss in rats. Br. J. Pharmacol. *165*, 2325-2340.

Docsa, T., Czifrak, K., Huse, C., Somsak, L., and Gergely, P. (2011). Effect of glucopyranosylidene-spiro-thiohydantoin on glycogen metabolism in liver tissues of streptozotocin-induced and obese diabetic rats. Mol. Med. Report *4*, 477-481.

Docsa, T., Marics, B., Németh, J., Hüse, C., Somsák, L., Gergely, P., and Peitl, B. (2015). Insulin sensitivity is modified by a glycogen phosphorylase inhibitor: Glucopyranosylidene-spiro-thiohydantoin in streptozotocin-induced diabetic rats. Curr. Top. Med. Chem. *15*, 2390-2394.

Doherty, M., and Malaisse, W.J. (2001). Glycogen accumulation in rat pancreatic islets: in vitro experiments. Endocrine *14*, 303-309.

Doherty, M.J., Moorhead, G., Morrice, N., Cohen, P., and Cohen, P.T. (1995). Amino acid sequence and expression of the hepatic glycogen-binding (GL)-subunit of protein phosphatase-1. FEBS Lett. *375*, 294-298.

Donnier-Marechal, M., and Vidal, S. (2016). Glycogen phosphorylase inhibitors: a patent review (2013 - 2015). Expert. Opin. Ther. Pat. *26*, 199-212.

Dow, J., Lindsay, G., and Morrison, J. (1996). Biochemistry: molecules, cells, and the body. Wokingham, UK: Addison-Wesley.

Elghazi, L., and Bernal-Mizrachi, E. (2009). Akt/PTEN: β-cell mass and pancreas plasticity. Trends Endocrinol. Metab. *20*, 243-251.

Esteves, P., Pecqueur, C., Ransy, C., Esnous, C., Lenoir, V., Bouillaud, F., Bulteau, A.L., Lombes, A., Prip-Buus, C., Ricquier, D., et al. (2014). Mitochondrial retrograde signaling mediated by UCP2 inhibits cancer cell proliferation and tumorigenesis. Cancer Res. *74*, 3971-3982.

Favaro, E., Bensaad, K., Chong, M.G., Tennant, D.A., Ferguson, D.J., Snell, C., Steers, G., Turley, H., Li, J.L., Gunther, U.L., et al. (2012). Glucose utilization via glycogen phosphorylase sustains proliferation and prevents premature senescence in cancer cells. Cell Metab. *16*, 751-764.

Ferrer, J.C., Favre, C., Gomis, R.R., Fernandez-Novell, J.M., Garcia-Rocha, M., de la Iglesia, N., Cid, E., and Guinovart, J.J. (2003). Control of glycogen deposition. FEBS Lett. *546*, 127-132.

Floettmann, E., Gregory, L., Teague, J., Myatt, J., Hammond, C., Poucher, S.M., and Jones, H.B. (2010). Prolonged inhibition of glycogen phosphorylase in livers of Zucker Diabetic Fatty rats models human glycogen storage diseases. Toxicol. Pathol. *38*, 393-401.

Fraenkel, M., Ketzinel-Gilad, M., Ariav, Y., Pappo, O., Karaca, M., Castel, J., Berthault, M.F., Magnan, C., Cerasi, E., Kaiser, N., et al. (2008). mTOR inhibition by rapamycin prevents beta-cell adaptation to hyperglycemia and exacerbates the metabolic state in type 2 diabetes. Diabetes *57*, 945-957.

Frame, S., and Cohen, P. (2001). GSK3 takes centre stage more than 20 years after its discovery. Biochem. J. *359*, 1-16.

Fujimoto, K., and Polonsky, K.S. (2009). Pdx1 and other factors that regulate pancreatic β-cell survival. Diabetes Obes. Metab. *11*, 30-37.

Furukawa, S., Murakami, K., Nishikawa, M., Nakayama, O., and Hino, M. (2005). FR258900, a novel glycogen phosphorylase inhibitor isolated from Fungus No. 138354. II. Anti-hyperglycemic effects in diabetic animal models. J. Antibiot. (Tokyo) *58*, 503-506.

Fuxreiter, M. (2012). Fuzziness: linking regulation to protein dynamics. Mol. Biosyst. *8*, 168-177.

Fülöp, P., Derdák, Z., Sheets, A., Sabo, E., Berthiaume, E.P., Resnick, M.B., Wands, J.R., Paragh, G., and Baffy, G. (2006). Lack of UCP2 reduces Fas-mediated liver injury in ob/ob mice and reveals importance of cell-specific UCP2 expression. Hepatology *44*, 592-601.

Gan, X., Wang, J., Su, B., and Wu, D. (2011). Evidence for direct activation of mTORC2 kinase activity by phosphatidylinositol 3,4,5-trisphosphate. *J.* Biol. Chem. *286*, 10998-11002.

Garcia-Rocha, M., Roca, A., De La Iglesia, N., Baba, O., Fernandez-Novell, J.M., Ferrer, J.C., and Guinovart, J.J. (2001). Intracellular distribution of glycogen synthase and glycogen in primary cultured rat hepatocytes. Biochem. J. *357*, 17-24.

Gaubitz, C., Prouteau, M., Kusmider, B., and Loewith, R. (2016). TORC2 Structure and Function. Trends Biochem. Sci. *41*, 532-545.

Gembal, M., Gilon, P., and Henquin, J.C. (1992). Evidence that glucose can control insulin release independently from its action on ATP-sensitive K^+ channels in mouse B cells. J. Clin. Invest. *89*, 1288-1295.

Graf, R., and Tolken, M. (1984). Ultrastructural distribution of glycogen in pancreatic islets of steroid diabetic rats. J. Basic Appl. Histochem. *28*, 391-397.

Greenberg, C.C., Danos, A.M., and Brady, M.J. (2006). Central role for protein targeting to glycogen in the maintenance of cellular glycogen stores in 3T3-L1 adipocytes. Mol. Cell. Biol. *26*, 334-342.

Gu, Y., Lindner, J., Kumar, A., Yuan, W., and Magnuson, M.A. (2011). Rictor/mTORC2 is essential for maintaining a balance between beta-cell proliferation and cell size. Diabetes *60*, 827-837.

Hagiwara, A., Cornu, M., Cybulski, N., Polak, P., Betz, C., Trapani, F., Terracciano, L., Heim, M.H., Ruegg, M.A., and Hall, M.N. (2012). Hepatic mTORC2 activates glycolysis and lipogenesis through Akt, glucokinase, and SREBP1c. Cell. Metab. *15*, 725-738.

Hayes, J.M., Kantsadi, A.L., and Leonidas, D.D. (2014). Natural products and their derivatives as inhibitors of glycogen phosphorylase: potential treatment for type 2 diabetes. Phytochem. Rev. *13*, 471-498.

Hellman, B., and Idahl, L.A. (1969). Presence and mobilization of glycogen in mammalian pancreatic beta cells. Endocrinology *84*, 1-8.

Henke, B.R. (2012). Inhibition of glycogen phosphorylase as a strategy for the treatment of type 2 diabetes. In New Therapeutic Strategies for Type 2 Diabetes: Small Molecule Approaches. R.M. Jones, D.E. Thurston, and D. Rotella (Ed.) RSCPublishing, pp. 324-365.

Henquin, J.C. (2004). Pathways in beta-cell stimulus-secretion coupling as targets for therapeutic insulin secretagogues. Diabetes *53 Suppl 3*, S48-58.

Horimoto, M., Fulop, P., Derdak, Z., Wands, J.R., and Baffy, G. (2004). Uncoupling protein-2 deficiency promotes oxidant stress and delays liver regeneration in mice. Hepatology *39*, 386-392.

Humphrey, R.K., Yu, S.M., Flores, L.E., and Jhala, U.S. (2010). Glucose regulates steady-state levels of PDX1 via the reciprocal actions of GSK3 and AKT kinases. J. Biol. Chem. *285*, 3406-3416.

Ishii, M., Maeda, A., Tani, S., and Akagawa, M. (2015). Palmitate induces insulin resistance in human HepG2 hepatocytes by enhancing ubiquitination and proteasomal degradation of key insulin signaling molecules. Arch. Biochem. Biophys. *566*, 26-35.

Jensen, J., Rustad, P.I., Kolnes, A.J., and Lai, Y.-C. (2011). The role of skeletal muscle glycogen breakdown for regulation of insulin sensitivity by exercise. Front. Physiol. *2*, 112.

Johnson, D., Shepherd, R.M., Gill, D., Gorman, T., Smith, D.M., and Dunne, M.J. (2007). Glucose-dependent modulation of insulin secretion and intracellular calcium ions by GKA50, a glucokinase activator. Diabetes *56*, 1694-1702.

Johnson, J.D., and Alejandro, E.U. (2008). Control of pancreatic beta-cell fate by insulin signaling: The sweet spot hypothesis. Cell Cycle *7*, 1343-1347.

Johnson, J.D., Bernal-Mizrachi, E., Alejandro, E.U., Han, Z., Kalynyak, T.B., Li, H., Beith, J.L., Gross, J., Warnock, G.L., Townsend, R.R., et al. (2006). Insulin protects islets from apoptosis via Pdx1 and specific changes in the human islet proteome. Proc. Natl. Acad. Sci. U.S.A. *103*, 19575-19580.

Johnson, L.N. (1992). Glycogen phosphorylase: control by phosphorylation and allosteric effectors. FASEB J. *6*, 2274-2282.

Johnson, L.N., and Barford, D. (1994). Electrostatic effects in the control of glycogen phosphorylase by phosphorylation. Protein. Sci. *3*, 1726-1730.

Joslin, E.P., and Kahn, R.C. (2005). Joslin's Diabetes Mellitus. Philadelphia: Lippincott Williams & Wilkins.

Kaneto, H., and Matsuoka, T.-a. (2015). Role of pancreatic transcription factors in maintenance of mature β-cell function. Int. J. Mol. Sci. *16*, 6281-6297.

Karim, S., Adams, D.H., and Lalor, P.F. (2012). Hepatic expression and cellular distribution of the glucose transporter family. World J. Gastroenterol. *18*, 6771-6781.

Kelsall, I.R., Munro, S., Hallyburton, I., Treadway, J.L., and Cohen, P.T. (2007). The hepatic PP1 glycogen-targeting subunit interaction with phosphorylase a can be blocked by C-terminal tyrosine deletion or an indole drug. FEBS Lett. *581*, 4749-4753.

Kollberg , G., Tulinius , M., Gilljam , T., Östman-Smith , I., Forsander , G., Jotorp , P., Oldfors , A., and Holme , E. (2007). Cardiomyopathy and exercise intolerance in muscle glycogen storage disease 0. N. Engl. J. Med. *357*, 1507-1514.

Kulkarni, R.N., Mizrachi, E.-B., Ocana, A.G., and Stewart, A.F. (2012). Human β-cell proliferation and intracellular signaling: driving in the dark without a road map. Diabetes *61*, 2205-2213.

Lamming, D.W., Ye, L., Katajisto, P., Goncalves, M.D., Saitoh, M., Stevens, D.M., Davis, J.G., Salmon, A.B., Richardson, A., Ahima, R.S., et al. (2012). Rapamycin-induced insulin resistance is mediated by mTORC2 loss and uncoupled from longevity. Science *335*, 1638-1643.

Laplante, M., and Sabatini, D.M. (2012). mTOR signaling in growth control and disease. Cell *149*, 274-293.

Lee, W.N.P., Guo, P., Lim, S., Bassilian, S., Lee, S.T., Boren, J., Cascante, M., Go, V.L.W., and Boros, L.G. (2004). Metabolic sensitivity of pancreatic tumour cell apoptosis to glycogen phosphorylase inhibitor treatment. Br. J. Cancer *91*, 2094-2100.

Lehlinger, A.L., Cox, M.M., and Nelson, D.L. (2004). Regulatory enzymes. Principles of Biochemistry. New York: W. H. freeman & company.

Leibiger, I.B., Leibiger, B., and Berggren, P.O. (2008). Insulin signaling in the pancreatic beta-cell. Annu. Rev. Nutr. *28*, 233-251.

Leite, S.A.O., Monk, A.M., Upham, P.A., Chacra, A.R., and Bergenstal, R.M. (2009). Low cardiorespiratory fitness in people at risk for type 2 diabetes: early marker for insulin resistance. Diabetol. Metab. Syndr. *1*, 8-8.

Levinthal, G.N., and Tavill, A.S. (1999). Liver disease and diabetes mellitus. Clin. Diabetes *17*, 2.

Lew, C.R., Guin, S., and Theodorescu, D. (2015). Targeting glycogen metabolism in bladder cancer. Nat. Rev. Urol. *12*, 383-391.

Liu, H., Remedi, M.S., Pappan, K.L., Kwon, G., Rohatgi, N., Marshall, C.A., and McDaniel, M.L. (2009a). Glycogen synthase kinase-3 and mammalian target of rapamycin pathways contribute to DNA synthesis, cell cycle progression, and proliferation in human islets. Diabetes *58*, 663-672.

Liu, S., Okada, T., Assmann, A., Soto, J., Liew, C.W., Bugger, H., Shirihai, O.S., Abel, E.D., and Kulkarni, R.N. (2009b). Insulin signaling regulates mitochondrial function in pancreatic beta-cells. PLoS One *4*, e7983.

Lodish, H., Berk, A, Zipursky, SL, (2000). Interaction and regulation of signaling pathways. In Molecular Cell Biology. New York: W. H. Freeman.

Malaisse, W.J. (2016). Role of glycogen metabolism in pancreatic islet beta cell function. Diabetologia *59*, 2489-2491.

Malaisse, W.J., Maggetto, C., Leclercq-Meyer, V., and Sener, A. (1993). Interference of glycogenolysis with glycolysis in pancreatic islets from glucose-infused rats. J. Clin. Invest. *91*, 432-436.

Malaisse, W.J., Marynissen, G., and Sener, A. (1992). Possible role of glycogen accumulation in B-cell glucotoxicity. Metabolism *41*, 814-819.

Malaisse, W.J., Sener, A., Koser, M., Ravazzola, M., and Malaisse-Lagae, F. (1977). The stimulus-secretion coupling of glucose-induced insulin release. Insulin release due to glycogenolysis in glucose-deprived islets. Biochem. J. *164*, 447-454.

Malley, C.O., and Pidgeon, G.P. (2016). The mTOR pathway in obesity driven gastrointestinal cancers: Potential targets and clinical trials. BBA clinical *5*, 29-40.

Martin, W.H., Hoover, D.J., Armento, S.J., Stock, I.A., McPherson, R.K., Danley, D.E., Stevenson, R.W., Barrett, E.J., and Treadway, J.L. (1998). Discovery of a human liver glycogen phosphorylase inhibitor that lowers blood glucose in vivo. Proc. Natl. Acad. Sci. U.S.A. *95*, 1776-1781.

Matsuzaki, H., Daitoku, H., Hatta, M., Tanaka, K., and Fukamizu, A. (2003). Insulin-induced phosphorylation of FKHR (Foxo1) targets to proteasomal degradation. Proc. Natl. Acad. Sci. U.S.A. *100*, 11285-11290.

McCulloch, L.J., van de Bunt, M., Braun, M., Frayn, K.N., Clark, A., and Gloyn, A.L. (2011). GLUT2 (SLC2A2) is not the principal glucose transporter in human pancreatic beta cells: implications for understanding genetic association signals at this locus. Mol. Genet. Metab. *104*, 648-653.

Mir-Coll, J., Duran, J., Slebe, F., Garcia-Rocha, M., Gomis, R., Gasa, R., and Guinovart, J.J. (2016). Genetic models rule out a major role of beta cell glycogen in the control of glucose homeostasis. Diabetologia *59*, 1012-1020.

Miyazaki, J., Araki, K., Yamato, E., Ikegami, H., Asano, T., Shibasaki, Y., Oka, Y., and Yamamura, K. (1990). Establishment of a pancreatic beta cell line that retains glucose-inducible insulin secretion: special reference to expression of glucose transporter isoforms. Endocrinology *127*, 126-132.

Morino, K., Petersen, K.F., and Shulman, G.I. (2006). Molecular mechanisms of insulin resistance in humans and their potential links with mitochondrial dysfunction. Diabetes *55*, S9-S15.

Nagy, V., Felföldi, N., Kónya, B., Praly, J.P., Docsa, T., Gergely, P., Chrysina, E.D., Tiraidis, C., Kosmopoulou, M.N., Alexacou, K.M., et al. (2012). N-(4-Substituted-benzoyl)-N′-(β-d-glucopyranosyl)ureas as inhibitors of glycogen phosphorylase: synthesis and evaluation by kinetic, crystallographic, and molecular modelling methods. Bioorg. Med. Chem. *20*, 1801-1816.

Nakaya, Y., Ohnaka, M., Sakamoto, S., Niwa, Y., Okada, K., Nomura, M., Hara, T., and Kusonoki, M. (1998). Respiratory quotient in patients with non-lnsulin-dependent diabetes mellitus treated with insulin and oral hypoglycemic agents. Ann. Nutr. Metab. *42*, 333-340.

Nenquin, M., Szollosi, A., Aguilar-Bryan, L., Bryan, J., and Henquin, J.C. (2004). Both triggering and amplifying pathways contribute to fuel-induced insulin secretion in the absence of sulfonylurea receptor-1 in pancreatic beta-cells. J. Biol. Chem. *279*, 32316-32324.

Newgard, C.B., Brady, M.J., O'Doherty, R.M., and Saltiel, A.R. (2000). Organizing glucose disposal: emerging roles of the glycogen targeting subunits of protein phosphatase-1. Diabetes *49*, 1967-1977.

Niclauss, N., Bosco, D., Morel, P., Giovannoni, L., Berney, T., and Parnaud, G. (2011). Rapamycin impairs proliferation of transplanted islet beta cells. Transplantation *91*, 714-722.

Nir, T., Melton, D.A., and Dor, Y. (2007). Recovery from diabetes in mice by β cell regeneration. J. Clin. Invest. *117*, 2553-2561.

Oikonomakos, N.G., Skamnaki, V.T., Tsitsanou, K.E., Gavalas, N.G., and Johnson, L.N. (2000). A new allosteric site in glycogen phosphorylase b as a target for drug interactions. Structure *8*, 575-584.

Oikonomakos, N.G., and Somsak, L. (2008). Advances in glycogen phosphorylase inhibitor design. Curr. Opin. Investig. Drugs. *9*, 379-395.

Pandey, A., Chawla, S., and Guchhait, P. (2015). Type-2 diabetes: current understanding and future perspectives. IUBMB life *67*, 506-513.

Pandol, S.J. (2010). Pancreatic embryology and development. San Rafael (CA): Morgan & Claypool Life Sciences.

Pheiffer, C., Jacobs, C., Patel, O., Ghoor, S., Muller, C., and Louw, J. (2016). Expression of UCP2 in Wistar rats varies according to age and the severity of obesity. J. Phys.Biochem. *72*, 25-32.

Piero, M.N., Nzaro, G.M., and Njagi, J.M. (2015). Diabetes mellitus – a devastating metabolic disorder. Asian J. Pharm. Biomed. Sci. *4*, 1-7.

Pópulo, H., Lopes, J.M., and Soares, P. (2012). The mTOR signalling pathway in human cancer. Int. J. Mol. Sci. *13*, 1886-1918.

Prats, C., Cadefau, J.A., Cusso, R., Qvortrup, K., Nielsen, J.N., Wojtaszewski, J.F., Hardie, D.G., Stewart, G., Hansen, B.F., and Ploug, T. (2005). Phosphorylation-dependent translocation of glycogen synthase to a novel structure during glycogen resynthesis. J. Biol. Chem. *280*, 23165-23172.

Prentki, M., Matschinsky, F.M., and Madiraju, S.R.M. (2013). Metabolic signaling in fuel-induced insulin secretion. Cell Metab. *18*, 162-185.

Rath, V.L., Ammirati, M., Danley, D.E., Ekstrom, J.L., Gibbs, E.M., Hynes, T.R., Mathiowetz, A.M., McPherson, R.K., Olson, T.V., Treadway, J.L., et al. (2000). Human liver glycogen phosphorylase inhibitors bind at a new allosteric site. Chem. Biol. *7*, 677-682.

Rhodes, C.J., White, M.F., Leahy, J.L., and Kahn, S.E. (2013). Direct autocrine action of insulin on beta-cells: does it make physiological sense? Diabetes *62*, 2157-2163.

Ritov, V.B., and Kelley, D.E. (2001). Hexokinase isozyme distribution in human skeletal muscle. Diabetes *50*, 1253-1262.

Roach, P.J., Depaoli-Roach, A.A., Hurley, T.D., and Tagliabracci, V.S. (2012). Glycogen and its metabolism: some new developments and old themes. Biochem. J. *441*, 763-787.

Ruiz-Ramírez, A., López-Acosta, O., Barrios-Maya, M.A., and El-Hafidi, M. (2016). Cell death and heart failure in obesity: role of uncoupling proteins. Oxid. Med. Cell. Longev. *2016*, 9340654.

Rybicka, K.K. (1996). Glycosomes--the organelles of glycogen metabolism. Tissue & cell *28*, 253-265.

Saltiel, A.R., and Kahn, C.R. (2001). Insulin signalling and the regulation of glucose and lipid metabolism. Nature *414*, 799-806.

Sarbassov, D.D., Guertin, D.A., Ali, S.M., and Sabatini, D.M. (2005). Phosphorylation and regulation of Akt/PKB by the rictor-mTOR complex. Science *307*, 1098-1101.

Schrauwen, P., and Hesselink, M. (2002). UCP2 and UCP3 in muscle controlling body metabolism. J. Exp. Biol. *205*, 2275-2285.

Shafiee, G., Mohajeri-Tehrani, M., Pajouhi, M., and Larijani, B. (2012). The importance of hypoglycemia in diabetic patients. J. Diabetes Metab. Disord. *11*, 17.

Shang, Y., Liu, Y., Du, L., Wang, Y., Cheng, X., Xiao, W., Wang, X., Jin, H., Yang, X., Liu, S., et al. (2009). Targeted expression of uncoupling protein 2 to mouse liver increases the susceptibility to lipopolysaccharide/galactosamine-induced acute liver injury. Hepatology *50*, 1204-1216.

Sharma, R., Raduly, Z., Miskei, M., and Fuxreiter, M. (2015). Fuzzy complexes: Specific binding without complete folding. FEBS Lett. *589*, 2533-2542.

Sharma, S., Leonard, J., Lee, S., Chapman, H.D., Leiter, E.H., and Montminy, M.R. (1996). Pancreatic islet expression of the homeobox factor STF-1 relies on an E-box motif that binds USF. J. Biol. Chem. *271*, 2294-2299.

Shearer, J., and Graham, T.E. (2002). New perspectives on the storage and organization of muscle glycogen. Can. J. Appl. Physiol. *27*, 179-203.

Sickmann, H.M., Walls, A.B., Schousboe, A., Bouman, S.D., and Waagepetersen, H.S. (2009). Functional significance of brain glycogen in sustaining glutamatergic neurotransmission. J. Neurochem. *109 Suppl 1*, 80-86.

Sivitz, W.I., and Yorek, M.A. (2010). Mitochondrial dysfunction in diabetes: from molecular mechanisms to functional significance and therapeutic opportunities. Antioxid. Redox Signal. *12*, 537-577.

Somsak, L., Bokor, E., Czifrak, K., Juhász, L., and Tóth, M. (2011). Carbohydrate derivatives and glycomimetic compounds in established and investigational therapies of type 2 diabetes mellitus. In Topics in the Prevention, Treatment and Complications of Type 2 Diabetes. M.B. Zimering, (Ed.) InTech.

Somsák, L., Czifrák, K., Tóth, M., Bokor, É., Chrysina, E.D., Alexacou, K.M., Hayes, J.M., Tiraidis, C., Lazoura, E., Leonidas, D.D., et al. (2008b). New inhibitors of glycogen phosphorylase as potential antidiabetic agents. Curr. Med. Chem. *15*, 2933-2983.

Somsák, L., Felföldi, N., Kónya, B., Hüse, C., Telepó, K., Bokor, E., and Czifrák, K. (2008a). Assessment of synthetic methods for the preparation of N-β-d-glucopyranosyl-N′-substituted ureas, -thioureas and related compounds. Carbohydr. Res. *343*, 2083-2093.

Somsák, L., Nagy, V., Hadady, Z., Docsa, T., and Gergely, P. (2003). Glucose analog inhibitors of glycogen phosphorylases as potential antidiabetic agents: Recent developments. Curr. Pharm. Des. *9*, 1177-1189.

Sorkin, A., and Fortian, A. (2015). Endocytosis and endosomal sorting of receptor tyrosine kinases. In Receptor Tyrosine Kinases: Structure, Functions and Role in Human Disease. L.D. Wheeler, and Y. Yarden, (Ed.) New York: Springer New York, pp. 133-161.

Stapleton, D., Nelson, C., Parsawar, K., McClain, D., Gilbert-Wilson, R., Barker, E., Rudd, B., Brown, K., Hendrix, W., O'Donnell, P., et al. (2010). Analysis of hepatic glycogen-associated proteins. Proteomics *10*, 2320-2329.

Stipanuk, M.H., and Caudill, M.A. (2013.). Biochemical, physiological, and molecular aspects of human nutrition. United States of America: Elsevier Saunders.

Tartier, L., Spenlehauer, C., Newman, H.C., Folkard, M., Prise, K.M., Michael, B.D., Menissier-de, M.J., and de, M.G. (2003). Local DNA damage by proton microbeam irradiation induces poly(ADP-ribose) synthesis in mammalian cells. Mutagenesis. *18*, 411-416.

Thorens, B., and Mueckler, M. (2010). Glucose transporters in the 21st Century. Am J Physiol Endocrinol. Metab. *298*, E141-145.

Torres, T.P., Sasaki, N., Donahue, E.P., Lacy, B., Printz, R.L., Cherrington, A.D., Treadway, J.L., and Shiota, M. (2011). Impact of a glycogen phosphorylase inhibitor and metformin on basal and glucagon-stimulated hepatic glucose flux in conscious dogs. J. Pharmacol. Exp. Ther. *337*, 610-620.

Treadway, J.L., Mendys, P., and Hoover, D.J. (2001). Glycogen phosphorylase inhibitors for treatment of type 2 diabetes mellitus. Expert. Opin. Investig. Drugs *10*, 439-454.

Weiss M, S.D., Philipson LH. (2014). Insulin biosynthesis, secretion, structure, and structure-activity relationships. South Dartmouth (MA): MDText.com, Inc.

Wiederkehr, A., and Wollheim, C.B. (2012). Mitochondrial signals drive insulin secretion in the pancreatic beta-cell. Mol. Cell. Endocrinol. *353*, 128-137.

Wilcox, G. (2005). Insulin and insulin resistance. Clin. Biochem. Rev. *26*, 19-39.

Yin, Y., Hua, H., Li, M., Liu, S., Kong, Q., Shao, T., Wang, J., Luo, Y., Wang, Q., Luo, T., et al. (2016). mTORC2 promotes type I insulin-like growth factor receptor and insulin receptor activation through the tyrosine kinase activity of mTOR. Cell. Res. *26*, 46-65.

Yuan, M., Pino, E., Wu, L., Kacergis, M., and Soukas, A.A. (2012). Identification of Akt-independent regulation of hepatic lipogenesis by mammalian target of rapamycin (mTOR) complex 2. J. Biol. Chem. *287*, 29579-29588.

Zahr, E., Molano, R.D., Pileggi, A., Ichii, H., Jose, S.S., Bocca, N., An, W., Gonzalez-Quintana, J., Fraker, C., Ricordi, C., et al. (2007). Rapamycin impairs in vivo proliferation of islet beta-cells. Transplantation *84*, 1576-1583.

Zhang, C.Y., Baffy, G., Perret, P., Krauss, S., Peroni, O., Grujic, D., Hagen, T., Vidal-Puig, A.J., Boss, O., Kim, Y.B., et al. (2001). Uncoupling protein-2 negatively regulates insulin secretion and is a major link between obesity, beta cell dysfunction, and type 2 diabetes. Cell *105*, 745-755.

Zhang, Y., Xu, D., Huang, H., Chen, S., Wang, L., Zhu, L., Jiang, X., Ruan, X., Luo, X., Cao, P., et al. (2014). Regulation of glucose homeostasis and lipid metabolism by PPP1R3G-mediated hepatic glycogenesis. J. Mol. Endocrinol. *28*, 116-126.

Zhou, M., Xu, A., Tam, P.K., Lam, K.S., Huang, B., Liang, Y., Lee, I.K., Wu, D., and Wang, Y. (2012). Upregulation of UCP2 by adiponectin: the involvement of mitochondrial superoxide and hnRNP K. PLoS One *7*, e32349.

Zoncu, R., Efeyan, A., and Sabatini, D.M. (2011). MTOR: From growth signal integration to cancer, diabetes and ageing. Nat. Rev. Mol. Cell Biol. *12*, 21-35.

PUBLICATION LIST (approved by the Kenézy Life Science Library)

UNIVERSITY OF DEBRECEN
UNIVERSITY AND NATIONAL LIBRARY

Registry number: DEENK/115/2017.PL
Subject: PhD Publikációs Lista

Candidate: Lilla Nagy
Neptun ID: JLM2H9
Doctoral School: Doctoral School of Molecular Medicine
MTMT ID: 10037938

List of publications related to the dissertation

1. **Nagy, L.**, Márton, J., Vida, A., Kis, G., Bokor, É., Kun, S., Gönczi, M., Docsa, T., Tóth, A., Antal, M., Gergely, P., Csóka, B., Pacher, P., Somsák, L., Bai, P.: Glycogen phosphorylase inhibition improves [béta]-cell function.
Br. J. Pharmacol. [Epub ahead of print], 2017.
IF: 5.259 (2015)

2. **Nagy, L.**, Docsa, T., Szántó, M., Brunyánszki, A., Hegedűs, C., Márton, J., Kónya, B., Virág, L., Somsák, L., Gergely, P., Bai, P.: Glycogen Phosphorylase Inhibitor N-(3,5-Dimethyl-Benzoyl)-N'-(β-D-Glucopyranosyl)Urea Improves Glucose Tolerance under Normoglycemic and Diabetic Conditions and Rearranges Hepatic Metabolism.
PLoS One. 8 (7), e69420-, 2013.
DOI: http://dx.doi.org/10.1371/journal.pone.0069420
IF: 3.534

List of other publications

3. Abdul-Rahman, O., Kristóf, E., Doan-Xuan, Q. M., Vida, A., **Nagy, L.**, Horváth, A., Simon, J., Maros, T. M., Szentkirályi, I., Palotás, L., Debreceni, T., Csizmadia, P., Szerafin, T., Fodor, T., Szántó, M., Tóth, A., Kiss, B. K., Bacsó, Z., Bai, P.: AMP-Activated Kinase (AMPK) Activation by AICAR in Human White Adipocytes Derived from Pericardial White Adipose Tissue Stem Cells Induces a Partial Beige-Like Phenotype.
PLoS One. 11 (6), e0157644, 2016.
DOI: http://dx.doi.org/10.1371/journal.pone.0157644
IF: 3.057 (2015)

4. Fodor, T., Szántó, M., Abdul-Rahman, O., **Nagy, L.**, Dér, Á., Kiss, B. K., Bai, P.: Combined Treatment of MCF-7 Cells with AICAR and Methotrexate, Arrests Cell Cycle and Reverses Warburg Metabolism through AMP-Activated Protein Kinase (AMPK) and FOXO1.
PLoS One. 11 (2), 1-16, 2016.
DOI: http://dx.doi.org/10.1371/journal.pone.0150232
IF: 3.057 (2015)

5. Bai, P., **Nagy, L.**, Fodor, T., Liaudet, L., Pacher, P.: Poly(ADP-ribose) polymerases as modulators of mitochondrial activity.
Trends Endocrinol. Metab. 26 (2), 75-83, 2015.
DOI: http://dx.doi.org/10.1016/j.tem.2014.11.003
IF: 8.964

6. Szántó, M., Brunyánszki, A., Márton, J., Vámosi, G., **Nagy, L.**, Fodor, T., Kiss, B. K., Virág, L., Gergely, P., Bai, P.: Deletion of PARP-2 induces hepatic cholesterol accumulation and decrease in HDL levels.
Biochim. Biophys. Acta-Mol. Basis Dis. 1842 (4), 594-602, 2014.
DOI: http://dx.doi.org/10.1016/j.bbadis.2013.12.006
IF: 4.882

7. Szántó, M., Brunyánszki, A., Kiss, B. K., **Nagy, L.**, Gergely, P., Virág, L., Bai, P.: Poly(ADP-ribose) polymerase-2: emerging transcriptional roles of a DNA-repair protein.
Cell. Mol. Life Sci. 69 (24), 4079-4092, 2012.
DOI: http://dx.doi.org/10.1007/s00018-012-1003-8
IF: 5.615

Total IF of journals (all publications): 34,368
Total IF of journals (publications related to the dissertation): 8,793

The Candidate's publication data submitted to the iDEa Tudóstér have been validated by DEENK on the basis of Web of Science, Scopus and Journal Citation Report (Impact Factor) databases.

27 April, 2017

9. KEYWORDS

glycogen, glycogen phosphorylase, glycogen phosphorylase inhibitors, Type 2 diabetes mellitus, mitochondria, UCP2, AKT2, mTORC2, pancreatic β cell, PDX1, insulin, insulin receptor, insulin receptor signaling.

glikogén, glikogén foszforiláz, glikogén foszforiláz gátlószerek, 2. típusú cukorbetegség mitokondrium, UCP2, AKT2, mTORC2, hasnyálmirigy β-sejtek, PDX1, inzulin, inzulin receptor, inzulin receptor jelátvitel.

The work was supported by the GINOP- 2.3.2-15-2016-00006 project. The project is co-financed by the European Union and the European Regional Development Fund.

10. ACKNOWLEDGEMENT

I wish to thank Dr. Péter Bay my supervisor and head of our laboratory for helping and guiding my work, and giving all the support for my work during my Ph.D. study.

I would like to thank Prof. László Virág, head of Department of Medical Chemistry and Prof. Pál Gergely for giving me the possibility to work at the Department.

I am grateful to Dr. Tibor Docsa for his help in several *in vivo* experiments and in enzyme kinetic measurements.

I would like to thank Prof. Attila Tóth for his help in Ca^{2+}-oscillation measurements.

I am thankful to Dr. András Vida for performing the *in silico* screening for glycogen-binding proteins and the sequence alignment for PDX1 promoter.

I am much obliged to Prof. Miklós Antal and Gréta Kis for performing electron microscopy measurements, furthermore, to Mónika Gönczi for her help and support.

I am grateful to Prof. László Somsák for making my research possible by providing the chemical compounds.

I am thankful to Somsák group, namely Bálint Kónya, Éva Bokor, Sándor Kun and Veronika Nagy for providing the glucose analog GP inhibitors.

Many thanks to all the staff of the Department of Medical Chemistry, especially our group: Judit Márton, Tamás Fodor, Dr. Edit Mikó, Tünde Kovács for their scientific and personal support.

I greatly appreciate the excellent technical assistance of Mrs. Ella Kovács D., Mrs. Erzsébet Herbály and László Finta.

I would like to thank to my family and friends for encouragement and support.

11. APPENDIX

The thesis is based on the following publications:

Nagy L, Docsa T, Szántó M, Brunyánszki A, Hegedűs C, Márton J, Kónya B, Virág L, Somsák L, Gergely P, Bai P.: Glycogen phosphorylase inhibitor N-(3,5-dimethyl-Benzoyl)-N'-(β-D-glucopyranosyl)urea improves glucose tolerance under normoglycemic and diabetic conditions and rearranges hepatic metabolism. PLoS One 2013 Jul 25;8(7):e69420. doi: 10.1371/journal.pone.0069420.

IF: 3.534

Nagy L, Márton J, Vida A, Kis G, Bokor É, Kun S, Gönczi M, Docsa T, Tóth A, Antal M, Gergely P, Csóka B, Pacher P, Somsák L, Bai P.: Glycogen phosphorylase inhibition improves β cell function. British Journal of Pharmacology 2017. Apr 13. doi: 10.1111/bph.13819.

IF: 5.259 (2015)